

THE APPLICATION OF GEOSTATISTICAL ORE RESERVE EVALUATION
METHODS IN ARCHAEOAN GOLD DEPOSITS: A CASE STUDY OF THE
WOODBINE DEPOSIT, AGNES MINE IN THE BARBERTON AREA.

Andrew John Brooker

A project report submitted to the Faculty of Engineering, University of the Witwatersrand,
Johannesburg, in partial fulfilment of the requirements for the degree of Master of Science
in Engineering.

Johannesburg, 1991.

DECLARATION:

I declare that this project report is my own, unaided work. It is being submitted for the degree of Master of Science in Engineering in the University of the Witwatersrand, Johannesburg. It has not been submitted before for any degree or examination in any other University.

A. J. Brooker.

(Andrew John Brooker)

Third day of December 1991

ABSTRACT:

The object of this project report is to examine how geostatistical methods can be applied to ore reserve evaluations in the Archaean gold deposits of the Barberton area, supported by a case study of the Woodbine deposit. Essentially there were two main problems identified when trying to evaluate an Archaean gold deposit; firstly, the presence of extreme values within the sampling data and secondly, the absence of a clear geological contacts between which the occurrence of gold is limited.

In examining the first of these problems, a number of geostatistical evaluation methods were examined in the light of their influence on extreme values within the sampling data. Three methods were examined in this project report. The second of the two problems is that of estimating the total gold content (grammes) within a block of ore when the gold mineralisation occurs over a width that is greater than the expected mining width. The approach adopted was to optimise the sampling data to various likely mining widths, thereby creating a number of data sets, one for each optimised stope width. The kriging of the optimised data allowed for the development of a Grade-Stope Width model for each "block", whereby the actual stope values could be compared to the block estimates generated by various geostatistical methods under consideration. This concept of a Grade-Stope Width model in a "wide reef" has important ramifications to Block Factor calculations.

For my wife Julie, whose patience I have sorely tried.

For my daughter Victoria, whose "wide-eyed" innocence I adore.

And for my son Alexander, whose sense of mischief I love.

"Gasp! How did you know it was your Birthday tomorrow Daddy?

It was meant to be a surprise!".

Victoria Virginia Brooker; 13 September 1990 (aged 4).

ACKNOWLEDGEMENTS:

Few ideas or technological advances develop in a vacuum, or are the product of one person working in isolation. The ideas presented in this project report are no exception and are the culmination of numerous discussions. It is for this reason that I would like to go beyond the usual acknowledgements to a Company and their typists, and mention those people who gave freely of their experience and advice.

I wish to extend my thanks to all the geologists at Eastern Transvaal Consolidated Mines for their patience when answering numerous questions about the gold deposits in the Barberton area; especially to Mr. E. du Plessis and Mr. W.D. Scott, whose knowledge of the Woodbine Deposit has been invaluable. Also at Eastern Transvaal Consolidated Mines, I would also like to thank Mr. F. Chadwick and his Survey/Sampling Department for the use of their sampling data, without which of course, no such evaluation would be possible.

At Anglovaal Head Office I would like to thank Mrs. N. Moodley for the many drafts of this project report and Dr. F. Camisani, Mr. L. Carter and Mrs. G. Knox of the Valuation Department for their advice as my ideas were being formulated and taking shape. Finally, I would like to thank the management of Anglovaal Ltd. and Eastern Transvaal Consolidated Mines for the opportunity of undertaking a project such as this, for their permission to publish the results and their generous financial support.

A.J. Brooker

CONTENTS		Page
	DECLARATION	ii
	ABSTRACT	iii
	DEDICATION	iv
	ACKNOWLEDGEMENTS	v
	CONTENTS	vi
	LIST OF FIGURES	ix
	LIST OF TABLES	xix
1	INTRODUCTION	1
1.1	An Outline of the Problem	1
1.2	Geographic and Historic Background	2
1.3	Previous Statistical and Geostatistical Studies in the Archaean Gold Deposits of Barberton	5
1.4	Scope and Organisation of this Work	7
2	GEOLOGY	11
2.1	Introduction	11
2.2	General Geology of the Barberton Mountain Land	11
2.3	Geology and Structure of the Moodies Hills	13
2.4	The Genesis of Gold Mineralisation in the Woodbine Deposit	18
2.5	The Geological Model and the Evaluation	21
3	ANALYSIS OF THE SAMPLING DATA	23
3.1	Introduction	23
3.2	Optimisation of the Development Sampling Data	23
3.3	An Examination of the Development Data	25
3.4	Identification of "Outliers"	28
3.5	The Treatment of "Outliers"	32
3.5.1	Case (a)	32
3.5.2	Case (b)	32
3.5.3	Case (c)	36
3.6	A Statistical Analysis of the Development Data	38
3.7	A Statistical Analysis of the Stope Data	40

CONTENTS	Page
4 SEMIVARIOGRAM MODELS AND CROSS VALIDATION EXERCISES	43
4.1 Introduction	43
4.2 Semivariograms and Cross Validation Exercises Based on Development Data	44
4.2.1 Semivariogram Models Generated from Development Data	45
4.2.2 Cross Validation Exercises Generated from Development Data	47
4.3 Cross Validation of the Stope Data using the Semivariograms Generated from Development Data	49
4.4 Semivariograms and Cross Validation Exercises of the Actual Stope Values	52
5 KRIGING OF "BLOCK" ESTIMATES AND ACTUAL VALUES	54
5.1 Introduction	54
5.2 The Evaluation of the "Block" Estimates for the Stopped Areas from Development Data	54
5.2.1 The Optimised Stope Widths	55
5.2.2 The Kriging Exercises for Case (a)	55
5.2.3 The Kriging Exercises for Case (b)	57
5.2.4 The Kriging Exercises for Case (c)	57
5.3 The Kriging of Actual Values	58
5.4 A Comparison Between the Block Estimates and the Actual Values	58
5.4.1 Actual Values v's Case (a) Block Estimates [(d) v's (a)]	61
5.4.2 Actual Values v's Case (b) Block Estimates [(d) v's (b)]	62
5.4.3 Actual Values v's Case (c) Block Estimates [(d) v's (c)]	62
5.5 Summary	63
6 THE BLOCK FACTOR CALCULATIONS IN "WIDE REEFS"	74
6.1 Introduction	74
6.2 The Block Factor	74
6.3 The Block Factor and Wide Reefs	76

CONTENTS	Page
7 CONCLUSIONS	79
APPENDICES	
APPENDIX A Statistics on the 120cm Optimisation of the Woodbine Data	81
APPENDIX B Statistics on the 150cm Optimisation of the Woodbine Data	86
APPENDIX C Statistics on the 200cm Optimisation of the Woodbine Data	91
APPENDIX D Statistics on the Woodbine Slope Data	96
APPENDIX E Semivariogram Models Generated for the Evaluation	107
APPENDIX F The Error Statistics from the Cross Validation Exercises	122
APPENDIX G Grade-Slope Width Graphs for Case (a)	136
APPENDIX H Grade-Slope Width Graphs for Case (b)	143
APPENDIX I Grade-Slope Width Graphs for Case (c)	150
BIBLIOGRAPHY	157

LIST OF FIGURES

Figure	Page
1.1 A simplified map of the Barberton greenstone belt showing the main regional structural trends as well as the positions of some of the gold occurrences, indicated by the small open circles	3
1.2 A near vertical projection, on the plane of the reef, of the stope areas between 24 and 26 level Woodbine Deposit	9
2.1 A Geological map showing the distribution of the three groups of rocks making up the stratigraphy of the Barberton greenstone belt	12
2.2 Summarized geological map of the Moodies Hills	14
2.3 Schematic cross section through part of the Agnes Gold Mine, in the vicinity of the Woodbine Shaft, showing the near vertical orientation of the stratigraphy	14
2.4 Geological map of the Barberton greenstone belt, showing the inferred emplacement ages of the various units	15
2.5 A typical geological map of the Woodbine Reef	20
3.1 Probability plot from the 120cm optimisation, cmg/t values	27
3.2 Probability plot of the 120cm optimised stope widths	27
3.3 Probability plot from the 120cm optimisation, $\ln(\text{cmg/t})$	29
3.4 Probability plot from the 120cm optimisation, $\ln(\text{cmg/t} + \beta)$	29

Figure	Page
3.5 Probability plot from the 120cm optimisation, ln(cmg/t) less the lower outliers	34
3.6 Probability plot from the 120cm optimisation, ln(cmg/t) less all outliers	34
3.7 Probability plot from the 120cm optimisation, ln(cmg/t+ β) less all outliers	35
3.8 Probability plot from the 120cm optimisation, transformed values	35
A1 Probability plot of the 120cm optimisation, cmg/t values	82
A2 Probability plot of the 120cm optimisation, ln(cmg/t)	82
A3 Probability plot of the 120cm optimisation, ln(cmg/t+35)	83
A4 Probability plot of the 120cm optimisation, ln(cmg/t) less low outliers	83
A5 Probability plot of the 120cm optimisation, ln(cmg/t) less a l outliers	84
A6 Probability plot of the 120cm optimisation, ln(cmg/t+45) less all outliers	84
A7 Probability plot of the 120cm optimisation, transformed values	85
A8 Probability plot of the 120cm optimised stope widths	85
B1 Probability plot of the 150cm optimisation, cmg/t values	87
B2 Probability plot of the 150cm optimisation, ln(cmg/t)	87

Figure	Page
B3 Probability plot of the 150cm optimisation, $\ln(\text{cmg}/t+45)$	88
B4 Probability plot of the 150cm optimisation, $\ln(\text{cmg}/t)$ less low outliers	88
B5 Probability plot of the 150cm optimisation, $\ln(\text{cmg}/t)$ less all outliers	89
B6 Probability plot of the 150cm optimisation, $\ln(\text{cmg}/t+60)$ less all outliers	89
B7 Probability plot of the 150cm optimisation, transformed values	90
B8 Probability plot of the 150cm optimised stope widths	90
C1 Probability plot of the 200cm optimisation, cmg/t values	92
C2 Probability plot of the 200cm optimisation, $\ln(\text{cmg}/t)$	92
C3 Probability plot of the 200cm optimisation, $\ln(\text{cmg}/t+55)$	93
C4 Probability plot of the 200cm optimisation, $\ln(\text{cmg}/t)$ less low outliers	93
C5 Probability plot of the 200cm optimisation, $\ln(\text{cmg}/t)$ less all outliers	94
C6 Probability plot of the 200cm optimisation, $\ln(\text{cmg}/t+75)$ less all outliers	94
C7 Probability plot of the 200cm optimisation, transformed values	95
C8 Probability plot of the 200cm optimised stope widths	95

Figure	Page
D1 Probability plot of the stope data, cmg/t values	97
D2 Probability plot of the stope data, $\ln(\text{cmg/t})$	97
D3 Probability plot of the stope data, $\ln(\text{cmg/t})$ less all outliers	98
D4 Probability plot of the stope data, $\ln(\text{cmg/t} + \beta)$ less all outliers	98
D5 Probability plot of the stope widths	99
D6 Probability plot of the stope data optimised to 120cm, cmg/t values	99
D7 Probability plot of the stope data optimised to 120cm, $\ln(\text{cmg/t})$	100
D8 Probability plot of the stope data optimised to 120cm, $\ln(\text{cmg/t})$ less the outlier	100
D9 Probability plot of the stope data optimised to 120cm, $\ln(\text{cmg/t} + \beta)$ less all outliers	101
D10 Probability plot of the stope widths optimised to 120cm	101
D11 Probability plot of the stope data optimised to 150cm, cmg/t values	102
D12 Probability plot of the stope data optimised to 150cm, $\ln(\text{cmg/t})$	102
D13 Probability plot of the stope data optimised to 150cm, $\ln(\text{cmg/t})$ less the outlier	103
D14 Probability plot of the stope data optimised to 150cm, $\ln(\text{cmg/t} + \beta)$ less all outliers	103

Figure	Page
D15 Probability plot of the stope widths optimised to 150cm	104
D16 Probability plot of the stope data optimised to 200cm, cmg/t values	104
D17 Probability plot of the stope data optimised to 200cm, $\ln(\text{cmg/t})$	105
D18 Probability plot of the stope data optimised to 200cm, $\ln(\text{cmg/t})$ less the outlier	105
D19 Probability plot of the stope data optimised to 200cm, $\ln(\text{cmg/t} + \beta)$ less all outliers	106
D20 Probability plot of the stope widths optimised to 200cm	106
E1 Semivariogram for the $\ln(\text{cmg/t} + \beta)$ values (120cm optimisation), of all Development Data	108
E2 Semivariogram for the $\ln(\text{cmg/t} + \beta)$ values (150cm optimisation), of all Development Data	109
E3 Semivariogram for the $\ln(\text{cmg/t} + \beta)$ values (200cm optimisation), of all Development Data	110
E4 Semivariogram for the $\ln(\text{cmg/t} + \beta)$ values (120cm optimisation), less all outliers	111
E5 Semivariogram for the $\ln(\text{cmg/t} + \beta)$ values (150cm optimisation), less all outliers	112
E6 Semivariogram for the $\ln(\text{cmg/t} + \beta)$ values (200cm optimisation), less all outliers	113
E7 Semivariogram for the indicators (high values of all optimisations)	114
E8 Semivariogram for the indicators (low values of all optimisations)	115

Figure	Page
E0 Semivariogram for the transformed values (applicable to all optimisations)	116
E10 Semivariogram of the optimised slope widths (120cm)	117
E11 Semivariogram of the optimised slope widths (150cm)	118
E12 Semivariogram of the optimised slope widths (200cm)	119
E13 Semivariogram of the actual slope $\ln(\text{cmg/t})$ values	120
E14 Semivariogram of the actual slope widths	121
F1 Error statistics from case (a), 120cm optimisation, cross validation of only development data	123
F2 Error statistics from case (a), 150cm optimisation, cross validation of only development data	123
F3 Error statistics from case (a), 200cm optimisation, cross validation of only development data	124
F4 Error statistics from case (b), 120cm optimisation, cross validation of only development data	124
F5 Error statistics from case (b), 150cm optimisation, cross validation of only development data	125
F6 Error statistics from case (b), 200cm optimisation, cross validation of only development data	125

Figure	Page
F7 Error statistics from case (c), 120cm optimisation, cross validation of only development data	126
F8 Error statistics from case (c), 150cm optimisation, cross validation of only development data	126
F9 Error statistics from case (c), 200cm optimisation, cross validation of only development data	127
F10 Error statistics from slope widths optimised to 120cm, cross validation of only development data	127
F11 Error statistics from slope widths optimised to 150cm, cross validation of only development data	128
F12 Error statistics from slope widths optimised to 200cm, cross validation of only development data	128
F13 Error statistics from case (a), 120cm optimisation, cross validation of only slope data	129
F14 Error statistics from case (a), 150cm optimisation, cross validation of only slope data	129
F15 Error statistics from case (a), 200 cm optimisation, cross validation of only slope data	130
F16 Error statistics from case (b), 120cm optimisation, cross validation of only slope data	130
F17 Error statistics from case (b), 150cm optimisation, cross validation of only slope data	131
F18 Error statistics from case (b), 200cm optimisation, cross validation of only slope data	131
F19 Error statistics from case (c), 120cm optimisation, cross validation of only slope data	132

Figure	Page
F20 Error statistics from case (c), 150cm optimisation, cross validation of only slope data	132
F21 Error statistics from case (c), 200cm optimisation, cross validation of only slope data	133
F22 Error statistics from slope widths optimised to 120cm, cross validation of only slope data	133
F23 Error statistics from slope widths optimised to 150cm, cross validation of only slope data	134
F24 Error statistics from slope widths optimised to 200cm, cross validation of only slope data	134
F25 Error statistics from actual slope value (cmg/t) cross validation	135
F26 Error statistics from actual slope width (cm) cross validation	135
G1 Estimated and actual grades in case (a) for block 25 W1	137
G2 Estimated and actual grades in case (a) for block 25 E2	137
G3 Estimated and actual grades in case (a) for block 25 E7A	138
G4 Estimated and actual grades in case (a) for block 25 E7B	138
G5 Estimated and actual grades in case (a) for block 25 E9A	139
G6 Estimated and actual grades in case (a) for block 25 E9B	139
G7 Estimated and actual grades in case (a) for block 25 E10	140

Figure		Page
G8	Estimated and actual grades in case (a) for block 26 E6	140
G9	Estimated and actual grades in case (a) for block 26 E7A	141
G10	Estimated and actual grades in case (a) for block 26 E7B	141
G11	Estimated and actual grades in case (a) for block 26 E9	142
H1	Estimated and actual grades in case (b) for block 25 W1	144
H2	Estimated and actual grades in case (b) for block 25 E2	144
H3	Estimated and actual grades in case (b) for block 25 E7A	145
H4	Estimated and actual grades in case (b) for block 25 E7B	145
H5	Estimated and actual grades in case (b) for block 25 E9A	146
H6	Estimated and actual grades in case (b) for block 25 E9B	146
H7	Estimated and actual grades in case (b) for block 25 E10	147
H8	Estimated and actual grades in case (b) for block 26 E6	147
H9	Estimated and actual grades in case (b) for block 26 E7A	148
H10	Estimated and actual grades in case (b) for block 26 E7B	148

Figure	Page
H11 Estimated and actual grades in case (b) for block 26 E9	149
I1 Estimated and actual grades in case (c) for block 25 W1	151
I2 Estimated and actual grades in case (c) for block 25 E2	151
I3 Estimated and actual grades in case (c) for block 25 E7A	152
I4 Estimated and actual grades in case (c) for block 25 E7B	152
I5 Estimated and actual grades in case (c) for block 25 E9A	153
I6 Estimated and actual grades in case (c) for block 25 E9B	153
I7 Estimated and actual grades in case (c) for block 25 E10	154
I8 Estimated and actual grades in case (c) for block 25 E6	154
I9 Estimated and actual grades in case (c) for block 25 E7A	155
I10 Estimated and actual grades in case (c) for block 26 E7B	155
I11 Estimated and actual grades in case (c) for block 26 E9	156

LIST OF TABLES	Page
Table	
2.1 Summary of the Stratigraphic column of the Moodies Group in the Eureka Syncline (after Anhaeusser, 1969) and the Moodies Hills (after Daneel, 1987)	15
3.1 The development data from the three optimised data sets	25
3.2 A summary of the statistics for the three optimised data sets	39
3.3 A statistical analysis of the Woodbine stope data	41
4.1 Summary of the cross validation exercises generated from development data	48
4.2 Summary of the cross validation exercises generated from stope data	51
5.1 Woodbine block estimates, all development data optimised to 120cm	64
5.2 Woodbine block estimates, all development data optimised to 150cm	65
5.3 Woodbine block estimates, all development data optimised to 200cm	66
5.4 Woodbine block estimates, development data less "outliers" optimised to 120cm	67
5.5 Woodbine block estimates, development data less "outliers" optimised to 150cm	68
5.6 Woodbine block estimates, development data less "outliers" optimised to 200cm	69
5.7 Woodbine block estimates, all development data transformed and optimised to 120cm	70
5.8 Woodbine block estimates, all development data transformed and optimised to 150cm	71

Table	Page
5.9 Woodbine block estimates, all development data transformed and optimised to 200cm	72
5.10 Comparison between block estimates and actual values	73

CHAPTER 1.

INTRODUCTION:

1.1 An Outline of the Problem:

The successful application of geostatistical methods to the evaluation of ore reserves in the Witwatersrand gold mines is widely documented. Yet, in South Africa at least, the application of these methods to the evaluation of Archaean gold deposits has met with limited success. This lack of success can, in part, be attributed to the fact that each Archaean gold deposit is relatively small in size, has its own unique geological and geostatistical characteristics and that the gold mineralisation is often very irregular.

The object of this project report is to examine how geostatistical methods can be applied to ore reserve evaluations in the Archaean gold deposits of the Barberton area. These methods were applied to a case study on the Woodbine deposit at Agnes Mine, which is presently owned by Eastern Transvaal Consolidated Mines Ltd., and is situated about eleven kilometers to the southwest of Barberton.

Essentially there are two main problems encountered when trying to evaluate an Archaean gold deposit; namely:

- (a) The presence of extreme values (or "outliers") within the sampling data.
- (b) The ore body frequently has no clear geological contacts between which the occurrence of gold is limited.

The first problem, that of extreme values, tends to form a very positively skewed population distribution. The occurrence of such extreme values can cause serious problems when trying to generate a meaningful semivariogram model for the evaluation of any given deposit. Further, when evaluating a deposit using lognormal kriging, the presence of a few extreme values within the sampling data will cause the variance of the transformed values to be overstated. This has very serious implications when retransforming the kriged estimators back into natural values as an overstated variance will result in the *overvaluation* of any given point or ore reserve block.

In the evaluation of precious metals, the cmg/t value is a measure of the specific mineral content per unit of area. Therefore the second problem causes some difficulty when evaluating a deposit where the mineralisation occurs over a width that is greater than the expected mining width. *Thus, at any given point a change in the stoping width will cause the cmg/t value, associated with that point, to change.* This has two implications; firstly, when evaluating an area or ore reserve block the cmg/t value, and therefore the total contents of that area, is not fixed and is *dependent* upon the estimated stoping width. Secondly; where the *estimated* stoping width (or block width) differs from the *actual* width at which the stope was later mined, comparisons between the actual value (cmg/t) realised and the estimated value (cmg/t) will lead to erroneous Block Factors. A realistic comparison will require the block width and actual stope width to be equal when comparing values (cmg/t) and determining Block Factors.

1.2 Geographic and Historical Background:

The Barberton Mountain Land is a vaguely triangular shaped area of rugged topography in

the Lowveld of the Eastern Transvaal and is adjacent to the northwestern border of Swaziland (see Figure 1.1). The Barberton greenstone belt, that forms part of the mountainous terrain, is comprised of a wide variety of volcanic, igneous and sedimentary rock types that are surrounded and intruded by granitic rocks of divergent textures, compositions and ages. (Anhaeusser, 1986).

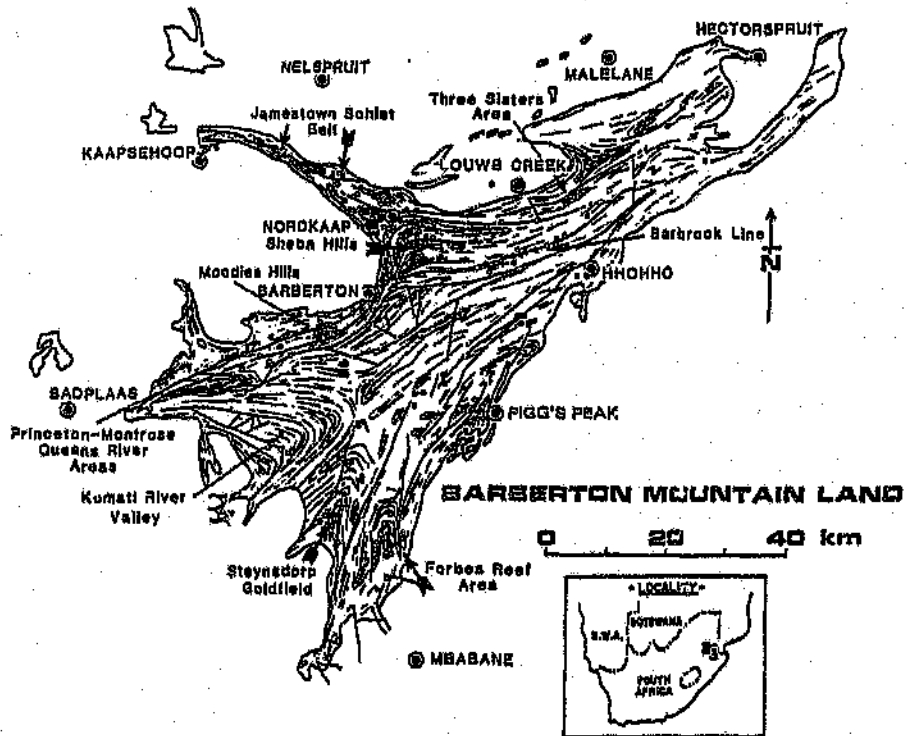


Figure 1.1: A simplified map of the Barberton greenstone belt showing the main regional structural trends as well as the positions of some of the gold occurrences, indicated by the small open circles (after Anhaeusser 1986).

Gold has been mined in the Barberton "fountain Land for over a century, with the first occurrences of gold being recorded in Swaziland in 1872. However, mining operations started with the working of alluvial deposits between Popinyana Creek and Figgs Peak in 1881 and in the Jamestown schist belt in 1882 (see Figure 1.1). Also in 1882 Auguste Robert (French Bob) discovered the Pioneer Reef, the first payable reef deposit, located in the Moodies Hills. Further exploration in the Moodies Hills during the early 1880's led to the discovery a host of other reefs of which the Woodbine Reef was one (Daneel, 1987). The discovery of further reefs within the Barberton area, such as the Barber Reef in 1884 and Edwin Bray's Golden Quarry in 1885, started a spectacular gold rush. However, these discoveries were soon eclipsed by the discovery of the Witwatersrand Goldfield in 1886.

Nevertheless, the Barberton Goldfield has been a small and consistent producer of gold over the last century. The output for the period 1884 to 1983 is approximately 251 553 kg (or 8 087 429 oz.) of gold and 8 875 kg (285 331 oz.) of silver. Of the gold produced, the majority (over 70 percent) has come from the four currently operating mines; namely, Sheba and Fairview Mines in the Sheba Hills, New Consort Mine in the Jamestown schist belt and Agnes Mine in the Moodies Hills. The remaining 30 percent of the gold mined coming from some 350 other gold occurrences, that were only small workings or short-lived prospects (Anhaeusser, 1986).

The Woodbine deposit, situated in the Moodies Hills, was discovered shortly after the discovery of the Pioneer Reef, along with a host of other deposits such as the Ivy Reef, Ivy Reef Extension, Snowden, Highlands and Lesiers Reef (later renamed the Giles Reef). The mining of these reefs was started in the early to middle 1880's by numerous prospectors and miners. However, the high royalties demanded by the owner of the surface and mineral

rights had driven away the smaller workers from the area by 1886 when the Moodies Gold Mining Syndicate was formed. However, by 1898 the Syndicate was experiencing financial difficulties and ceased operations during the Boer War (Daneel, 1987).

In 1908 Agnes Mine was started by Mr. A.J. Knuckey and worked the Agnes, Ivy and Woodbine Reefs until 1915. In 1915 all the smaller properties were absorbed into the newly created Agnes Gold Mining Company under the ownership of Mr. W.R. Rowe and Mr. O.W.W. Gibson. Operations have continued to this day, but ownership of Agnes Mine passed to Eastern Transvaal Consolidated Mines Ltd. on the 1st October 1949 (Daneel, 1987). Currently, Agnes mine is mining three reefs; namely, the Woodbine, Giles and Princeton Reefs.

1.3 Previous Statistical and Geostatistical Studies in the Archaean Gold Deposits of Barberton

Prior to 1977, the method used to evaluate an Archaean gold deposit in the Barberton area was to demarcate an ore reserve block and take the arithmetic average of the peripheral samples. Variations upon this basic theme may have been undertaken, whereby "trends" within an ore reserve block were noted and certain peripheral samples weighted by an area of influence. Indeed, even today the routine mine valuations are frequently undertaken in this manner.

In 1977 an experiment was conducted at Agnes Mine to determine if regression techniques could be applied to the Woodbine and Giles Reefs. The experiment was reviewed by Dr. D.G. Krige, who commented that there was a good correlation between the block values and

the current sampling values for the Giles deposit, yet the Woodbine deposit did not display any such correlation (Internal Report, Anglovaal 1977). This experiment, according to the Records Department of Anglovaal Limited, was the first attempt to introduce statistically based mine evaluation techniques to the Archaean gold deposits of the Barberton area.

The first application of geostatistics in evaluating Archaean gold deposits of the Barberton area was undertaken by Dr. E.J. Magri and Mrs. G. Knox in 1984, when both the Woodbine and Giles Reefs were evaluated (Internal Report, Anglovaal 1984). The 1984 evaluation was followed by numerous other geostatistical mine evaluations in the other Archaean gold deposits of the Barberton area.

Of the previous geostatistical evaluations, the problem of *extreme values* was documented. Some evaluations would label these values as "population outliers" and remove them from the data set, whilst others would leave the data sets intact. The former causes concern, to the pure statistician, in that the samples discarded may be truly representative samples from within that population. However, the latter has serious implications for any mine evaluation, whereby a small number of "outlier" values are allowed to inflate the overall population variance to an unrealistically high level. When dealing with transformed values (natural logarithms) this is especially problematic as the level of the sill for a semivariogram has an influence on the backtransformation process of logarithmic values back into natural values. The second problem, that of no clear geological contacts between which the occurrence of gold is limited, has not been documented or accounted for in previous geostatistical evaluations.

1.4 Scope and Organisation of this Work:

The field of investigation undertaken, in this project report, has been limited to the application of geostatistical methods in evaluating the ore reserves of Archaean gold deposits in the Barberton Mountain Land. A further limitation is that the sampling data, used in the case study of the Woodbine deposit, has been restricted to the 24 to 26 level development and 25 and 26 level stopes. This was found to be necessary as the data above 24 level was over fifteen years old and was not readily available. It also served to limit the amount of data to be physically collected.

There are, essentially, two problems encountered when evaluating an Archaean gold deposit, as stated in Section 1.1 above. In examining the first of these problems, there are a number of geostatistical evaluation methods that can be used to deal with extreme values (or "outliers") within the sampling data. Three such methods will be examined in this project report; namely:

Case (a): To leave the data sets intact and accept the extreme values as being part of the overall population and, thereby agreeing in principle, that the volatile semivariogram created is indicative of the nature of the ore body.

Case (b): To use "indicators" to isolate the effects of the extreme values, thus effectively treating them as a separate population, and yielding a more stable semivariogram for the remaining data.

Case (c): To examine the comparatively new "Rank Related Uniform Transform"

procedure, whereby the cmg/t values are replaced by a value equal to their relative rank within the data set. This approach is not influenced by "outliers" as such.

The second of the two problems encountered is that of estimating the total gold content (grammes) within a block of ore when the gold mineralisation occurs over a width that is greater than the expected mining width. The approach adopted was to optimise the sampling data to various likely mining widths, thereby creating a number of data sets, one for each optimised width. Therefore, at any given sample point, a number of values (cmg/t) were obtained for various widths. As the cmg/t value is a direct measure of the gold content per unit area, one could estimate the total gold content (grammes) for a range of likely mining widths, for any given sample point.

To determine the total gold content (grammes) for an ore reserve block, for any given mining width, it was necessary to generate a separate semivariogram model for each optimised width and to krigé each data set separately. This would yield a number of different values and variances for any given block of ore, *dependent* upon the optimised stopes width. Thus a Grade-Stopes Width model could then be created for each block of ore to determine the grade (g/t) for any given likely mining width.

The case study of the Woodbine deposit illustrates the practical aspects of applying the various geostatistical methods and serves as an empirical means of gauging the effectiveness of one method compared to another. For this comparison, eleven stoped-out areas, between 24 and 26 level, were demarcated or "blocked" as if the ore were still "in situ," then evaluated geostatistically using only the development sampling data. The stoped-out areas used in the evaluation were as follows:

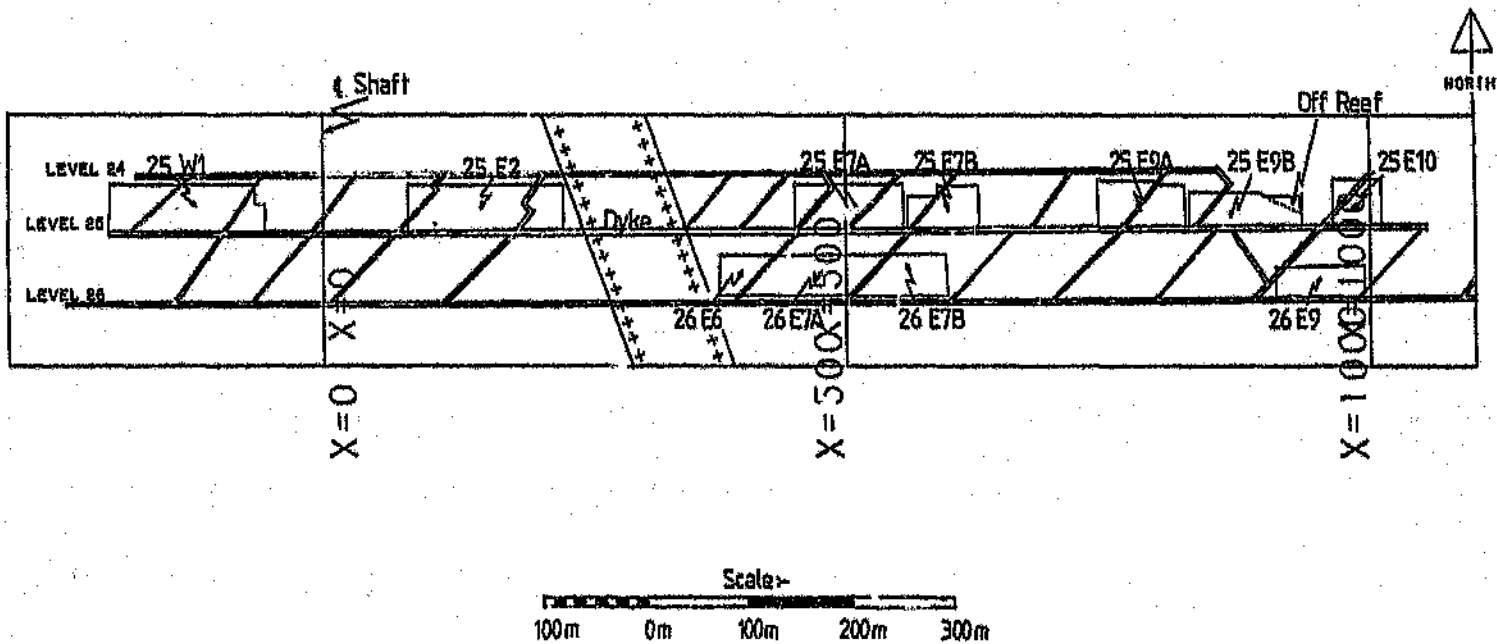


Figure 1.2: A near vertical projection, on the plane of the reef, of the stoped areas between 24 and 26 level Woodbine Deposit.

25 W1	26 E6
25 E2	26 E7A
25 E7A	26 E7B
25 E7B	26 E9
25 E9A	
25 E9B	
25 E10	

A portion of the 25 E9B stope was taken to be "off reef" as its stope sampling indicated that there was reef in foot or hanging. This "off reef" portion was not included in the evaluation exercise (see Figure 1.2). The resulting "block estimates" were then compared to the stope sampling values that were actually obtained within the stoped-out areas or "blocks."

The project report is organised into a number of chapters that are arranged into a logical sequence of steps, as one would undertake in any evaluation. The following chapter will outline the geological setting of the region and specifically the Woodbine deposit, in an attempt to understand the factors that influence the occurrences of gold. This is followed by a number of chapters that elaborate upon the evaluation methods used; detailing the collection and manipulation of the data, the creation and cross validation of the semivariograms and the evaluation of the "blocks" by the various geostatistical methods outlined above. A final chapter will summarise and conclude the project report.

CHAPTER 2.**GEOLOGY:****2.1 Introduction:**

Before an evaluation of a mineral deposit is undertaken, it is advisable for the evaluator to develop an understanding of the geological processes and conditions that created the deposit. It is the evaluator's interpretation and understanding of the geological processes that will, to a certain degree, dictate the format in which the sampling data is captured and the manner in which the subsequent evaluation is undertaken. This chapter is intended to provide an overview of the regional geology of the Barberton Mountain Land, with particular emphasis on the Moodies Hills, and attempt to identify those factors that have influenced the gold mineralisation in the Woodbine deposit.

2.2 General Geology of the Barberton Mountain Land:

The Barberton greenstone belt is comprised of a wide variety of volcanic, igneous and sedimentary rock types, that are surrounded and intruded by a host of different granitic rock types. In the Eastern Transvaal and Swaziland the volcano-sedimentary assemblages of the Onverwacht, Fig Tree and Moodies groups constitute the Swaziland Supergroup (Anhaeusser, 1975). Figure 2.1 shows the distribution of the three groups of rocks making up the stratigraphy in the Barberton greenstone belt.

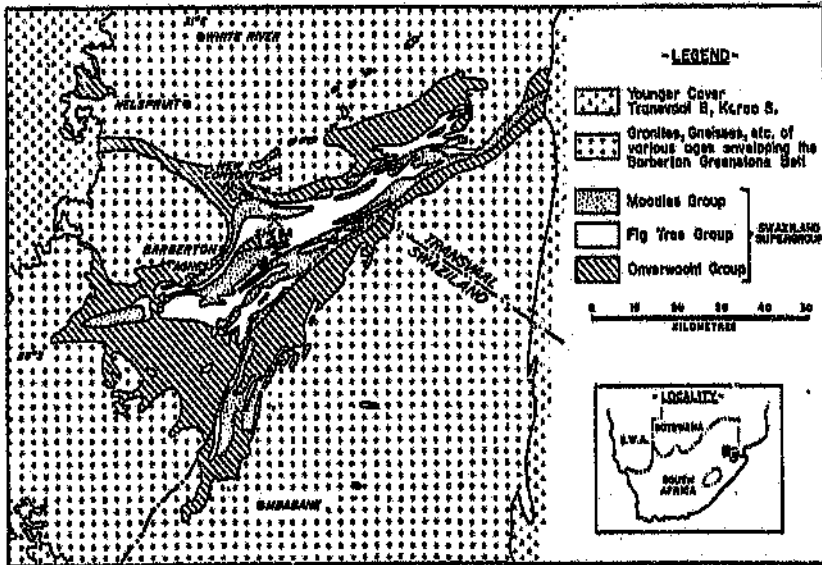


Figure 2.1: A Geological map showing the distribution of the three groups of rocks making up the stratigraphy of the Barberton greenstone belt, (after Wagener, 1986).

The Onverwacht Group at the base of the succession constitutes an initial magmatic phase. The lower portion of the Onverwacht Group (or the Tjakastad Subgroup) is comprised of a suite of ultramafic and mafic flows approximately 7 530 metres thick. The lower portion of this Subgroup is frequently missing, having been assimilated by intrusions of tonalitic and trondhjemitic gneisses ranging in age from 2 700 to 3 500 Ma. A persistent sedimentary horizon, known as the Middle Marker, occurs at the top of the Tjakastad Subgroup and denotes a marked change in the character of the volcanic assemblages occurring in the upper portion (or the Geluk Subgroup) of the Onverwacht Group. The Geluk Subgroup consists of mafic and felsic flows, together with volcanoclastics and minor chemical sediments that are approximately 7 685 metres thick (Viljoen and Viljoen, 1969).

Overlying the Onverwacht succession is the sedimentary assemblage of the Fig Tree Group.

It is comprised mainly of argillaceous sediments, capped by trachytic flows and pyroclastics. The sediments of the Fig Tree Group are about 2 150 metres thick and are dominated by greywackes, shales and siliceous chemical precipitates, such as banded ferruginous chert and banded iron-formation.

The Moodies Group, which hosts the Woodbine deposit, is the youngest member of the Barberton Sequence and consists of shallow water arenaceous sediments that are approximately 3 140 metres thick in the area of the Eureka Syncline (Viljoen and Viljoen, 1969). The Group is subdivided into three formations; namely, the Clutha, Joe's Luck and Baviaanskop Formations. This Group consists of conglomerates, quartzites, sub-greywackes, sandstones and shales, together with minor volcanic horizons, jaspilites and banded iron-formations (Anhaeusser, 1986).

2.3 Geology and Structure of the Moodies Hills:

The three Groups in the Barberton Sequence all have surface outcrops in the general area of the Moodies Hills, although due to certain structural events, the sequence has been disrupted (see Figures 2.2 and 2.3). The Woodbine deposit is situated in the Moodies Group and it is the geology and structure of this Group that will be examined in this section.

As stated in Chapter 2.2 above, the Moodies Group consists of three Formations and in the Moodies Hills area comprises sixteen lithostratigraphic units, as opposed to twelve in the Eureka Syncline area. These have been tabulated in Table 2.1, showing their possible correlation with the three formations of the Moodies Group as defined by Anhaeusser in 1975 (Daneel, 1987). Although these lithologies have been subjected to regional low grade metamorphism, they are referred to by their sedimentary names.

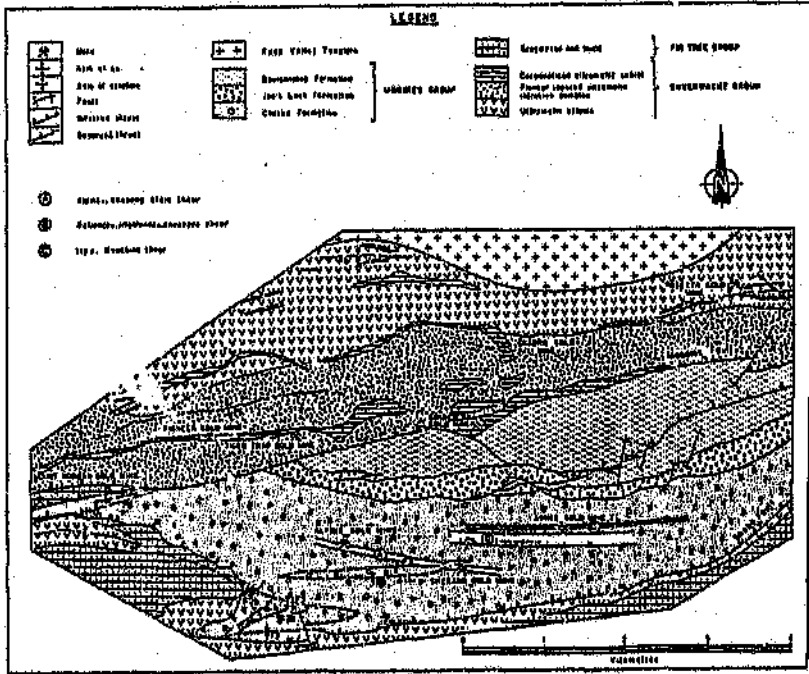


Figure 2.2: Simplified geological map of the Moodies Hills (after Daneel 1987).

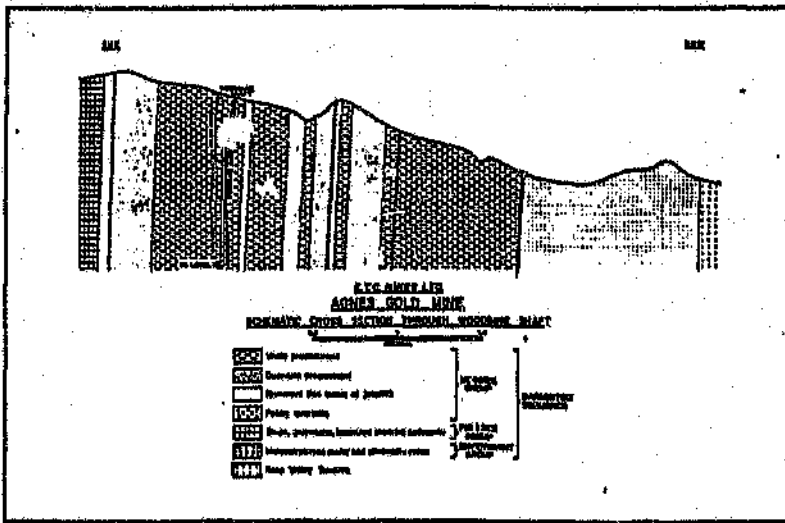


Figure 2.3: Schematic cross section through part of the Agnes Gold Mine, in the vicinity of the Woodbine Shaft, showing the near vertical orientation of the stratigraphy (after Wagener, 1986).

Table 2.1 Summary of the Stratigraphic Column of the Moodies Group in the Eureka Syncline (after Anhaeusser, 1969) and the Moodies Hills (after Daneel, 1987).

EURKA SYNCLINE (ANHAEUSSER, 1969)			MOODIES HILLS (DANEEL, 1987)	
UNIT NAME	SYMBOL	FORMATION NAME	UNIT NAME	SYMBOL
Upper shale Upper quartzite	MdS3 MdQ3	Bavlaanskop	Upper shale Upper conglomerate Upper arkose	MdS3 MdC3 MdA3
Middle shale Second jaspilite Second lava horizon Middle quartzite	MdS2 MdI2 MdL2 MdQ2	Joe's Luck	Second jaspilite Felsic tuff Amygdaloidal lava Middle quartzite Middle arkose	MdI2 MdL MdL MdQ2 MdA2
First jaspilite First lava horizon Lower shale Lower quartzite Calcareous quartzite Basal conglomerate	MdI MdL1 MdS1 MdQ1 MdCq MdB	Clutha	Lower siltstone Lower shale Main jaspilite Lower shale Lower siltstone Lower arkose Gritty arkose Basal conglomerate	MdS1b MdS1b MdI1 MdS1a MdS1a MdA1 MdGA MdC1

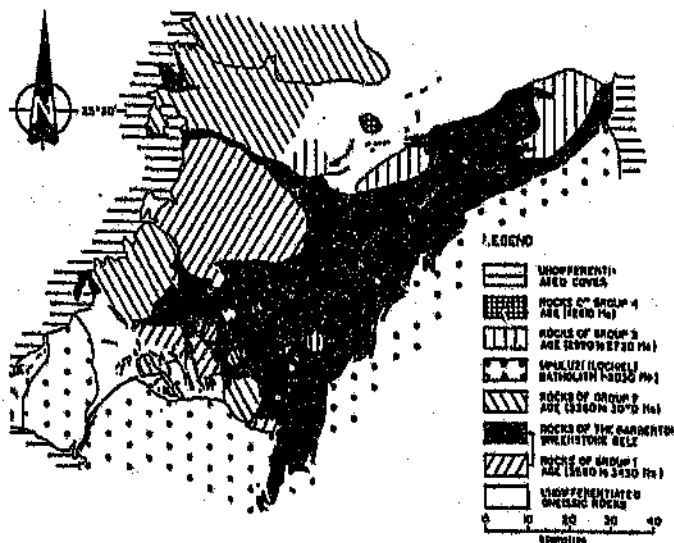


Figure 2.4: Geological map of the Barberton greenstone belt, showing the inferred emplacement ages of the various units (after Barton, 1983).

The numerous occurrences of gold mineralisation in the Moodies Group are all confined to the upper portion of the lower arkose unit (MdA1), the lower siltstone and lower shale units (MdS1a and MdS1b) and tend to be confined to three distinct shear zones, as shown in Figure 2.2. One such occurrence of gold mineralisation is the Woodbine deposit of Agnes Mine on the Ivy-Woodbine shear (Daneel, 1987).

Much of the tectonic activity that created the present structure of the Moodies Hills is the result of three major periods of magmatic activity that created the various granitic rock types that surrounded the Barberton greenstone belt. The formation of the Mpageni Pluton some 25 kilometres to the east of Nolspruit was a fourth and relatively minor period of activity. The dates attributed to the formation of certain plutons can vary widely, depending on the source of reference used. However, for the purpose of this paper, the sequence and dates of the magmatic events will be accepted as those given by Barton (1983) graphically shown in Figure 2.4.

Regional mapping by Daneel (1987), indicated that the Moodies Hills have been subjected to five major periods of deformation. The first period would appear to be prior to the deposition of the Moodies Group sediments, as rounded fragments (or clasts) of the Fig Tree Group, Onverwacht Group and granites were noted within the basal conglomerate of the Moodies Group (MdC1) by Anhaeusser (1969), Wuth (1980) and Daneel (1987). This would suggest the deformation and denudation of the pre-Moodies strata before the formation of the Moodies Group sediments.

The diapiric emplacement of the Kaap Valley Tonalite appears to have occurred after the deposition of the Moodies Group sediments and to be the cause of the second period of deformation. Daneel (1987) gives evidence for the existence of four thrust sheets within the

Moodies Hills, thrusting towards the south, that were created at this time. He suggested that the younger thrust sheets were thrust over the older sheets causing the thrust surface and the sheets of the earlier thrusts to be deformed. The thrust faults or the boundaries of shear zones tended to be sub-parallel to the strata, particularly along a contact between lithologies of high competency contrast. These thrust faults can be explained by the rise of the diapir causing an upward arching of the Barberton Sequence, and gravity sliding or gravitational collapse giving rise to compressional forces necessary for thrust faulting to occur. Figures 2.2 and 2.3 show the unconformable relationship between the Moodies, Fig Tree and Onverwacht Groups along the Moodies and Sheba Faults.

The final emplacement of the Kaap Valley Tonalite and the intrusion of the Nelspruit Granite resulted in the third period of deformation. These events resulted in the Moodies Hills area being subjected to compression from the north-northwest. Daneel (1987) believed that this period of deformation could have been responsible for the steep dips and in some places overturning of the stratigraphy and structures. Anhaeusser (1969) attributes the regional low grade metamorphism and a gold mineralisation event to this phase of deformation. Evidence for this in the Moodies Hills, and the Woodbine deposit itself, comes from the fact that diabase dykes cut across zones of gold mineralisation, indicating that the gold mineralisation occurred before the dyke intrusion. The age of these dykes is believed to be post third period deformation as these dykes have intruded through the steeply dipping and deformed Barberton sequence strata and the consolidated Kaap Valley Tonalite.

The fourth and fifth periods of deformation caused gentle folding and crenulations within the Moodies Hills. These periods of deformation were probably the result of lithostatic loading by younger cover rocks.

2.4 The Genesis of Gold Mineralisation in the Woodbine Deposit:

There is, essentially, only one school of thought regarding the genesis of the Woodbine deposit. It is believed that the gold was introduced into the host rocks after their formation and this mode of occurrence is referred to as the epigenetic model. However, during the early 1980's, and later with a paper printed in 1986, Wagener proposed a syngenetic model where the gold mineralisation is said to have occurred as the host rocks were deposited or formed.

Wagener (1986) considered that the syngenetic model for the deposition of gold gave the simplest explanation for the Woodbine deposit's strata bound character. He also viewed the stratigraphy as the dominant influence on the orientation of the ore body. The gold mineralisation possibly being of volcanogenic exhalative origin.

Pearton et al., (1984) and Daneel (1987) challenged Wagener's syngenetic model and the "strata bound character" of the Woodbine deposit. Pearton et al., (1984) showed that the occurrences of mineralisation in the Moodies Hills are restricted to those zones that have been subjected to both shearing and hydrothermal alteration. One such shear zone is the Ivy-Woodbine shear (see Figure 2.2) and rather than being "strata bound," the shear zone actually cuts across the strata at an angle of five degrees. Daneel (1987) proposed an epigenetic gold enrichment model controlled by the structural environment. The association of gold mineralisation with zones of shearing and hydrothermal alteration was also found to apply to the ultramafic schists of the Onverwacht Group to the north of Agnes Mine (Wuth, 1980). Wuth proposed that the gold mineralisation occurred as a result of the precipitation of hydrothermal solutions into suitable physio-chemical traps. The Mount Morgan, Pioneer, Tiger Trap, Golden Hill, Quadro and Rossette gold mines are all situated in the sheared and

altered ultramafic schists of the Onverwacht Group north of the Moodies Fault (see Figure 2.2).

In the process of gathering data for this project report, the matter regarding the origin of the Woodbine deposit was discussed with Mr. W.D. Scott and Mr. E. du Plessis, the Chief Geologist for Eastern Transvaal Consolidated Mines and Senior Geologist at Agnes Miae, respectively. It was clear, from their collective underground experience of the Woodbine deposit and the strong association of gold mineralisation with zones of shearing and hydrothermal alteration, that they favour the epigenetic model. Thus, for the purposes of this project report, an epigenetic model is proposed for the genesis of the Woodbine deposit.

The Ivy-Woodbine shear zone is characterised by intense, but locally inhomogeneous, shearing and deformation. Uneven movement along the shear zone caused localised dilation of the shear and it is thought that this may have created a low pressure region that attracted hydrothermal solutions, or at least facilitated the movement of such fluids, into and along the shear zone. The shear, itself, is sometimes defined by a single mylonite (up to 50 cm thick), or by numerous small sub-parallel shears creating a mineralised band up to three metres wide (see Figure 2.5).

Pearson et al., (1984) and Daneel (1987) proposed that the gold mineralisation accompanied the latter stages of hydrothermal alteration and is closely associated with pyrite, chalcopyrite and sphalerite. Daneel (1987) also regarded the hydrothermal alteration process as a rock preparation phase, prior to mineralisation. The alteration process involved the development of siderite, the destruction of chlorite (that was iron rich) and dolomite, and the bleaching of red jasper bands (where present). The alteration front, or "halo" about the mineralised zone, may be sharp or diffuse over a few metres with complete or only partial alteration. This suggests the potential presence of two populations in the mineralisation (see later discussion).

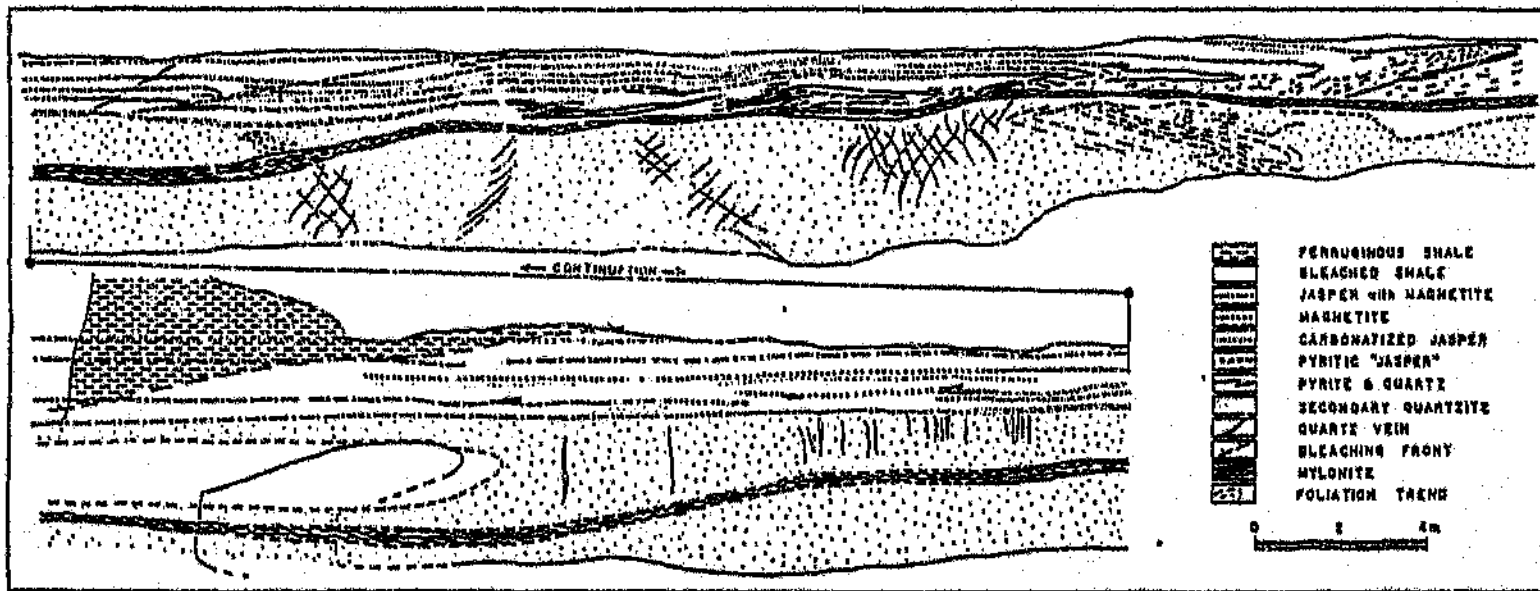


Figure 2.5: A typical geological map of the Woodbine Reef, (after Pearton, et al., 1984).

The development of sulphide minerals within the iron rich host rocks is common to all three mineralised shear zones in the Moodies Hills. The Ivy-Woodbine shear zone occurs within laminated ferruginous shales with minor interbedded jaspilites and contains the best development of sulphide mineralisation. For the purpose of this project report, it is assumed that the gold precipitated out of solution as a result of a fluid to wall rock interaction, probably in some form of physio-chemical trap. The fluids containing the gold and sulphide minerals reacting with ferruginous zones, within the host rocks, thereby inducing the sulphides (and gold) to be deposited. The close association of sulphide minerals and gold in the Woodbine deposit was noted by Daneel (1987), amongst others.

2.5 The Geological Model and the Evaluation:

The geological model proposed above has a number of features that will influence an evaluation and these are:

- (a) That the mineralisation about the shear is not confined to any particular stratigraphic horizon, as happens with the sedimentary Witwatersrand Reefs. In the case of the Woodbine deposit, the mineralised width is frequently greater than the anticipated stope width.
- (b) The close association of pyrite and gold mineralisation means, for the Woodbine deposit, that one is usually able to visually identify high grade areas.

The first feature is dependent upon the ability of the hydrothermal fluids to penetrate the host rocks of the shear zone. Such features as the host rock's permeability, its chemical nature and the density of cross fracturing within any given area will have an influence on the cmg/t value, and probably the grade (g/t), at any given point. At Agnes Mine, work is being undertaken to determine the influence of specific geological structures on the grade

distribution of the Woodbine deposit. Unfortunately, this study was not complete at the time that this project report was written. Consequently, when areas of high gold concentrations are encountered, it is assumed that these geological features are the cause.

The second feature is important to the evaluation in that it enables the miner and geologist to visually identify areas of high gold concentrations. This feature also allows the mine evaluator to optimise the mineralised zone to a number of likely stoping widths, determining a cmg/t value for each width, in the knowledge that the mineralised zone is usually readily identifiable.

CHAPTER 3

ANALYSIS OF THE SAMPLING DATA:3.1 Introduction:

The object and scope of this project report, as stated in Chapter 1.4, is to examine the performance of various geostatistical evaluation methods in evaluating an Archaean gold deposit; namely the Woodbine deposit. Thus, the format in which the sampling data was collected had to be versatile enough so, that with a few modifications, it could be used for any of the geostatistical methods examined. Furthermore, in collecting the data, cognizance was taken of those evaluation problems likely to be encountered and the geological characteristics mentioned in Chapter Two. The sampling data available came from two primary sources; namely, the development sampling sheets for 24, 25, and 26 levels and the stope sampling sheets of eleven stoped-out areas between 24 and 26 level (see Figure 1.2).

3.2 Optimisation of the Development Sampling Data:

The problem of the ore body having no clear geological contact, between which the occurrence of gold mineralisation is limited, was dealt with by optimising the development data to three minimum widths. Such an exercise could be justified in the Woodbine deposit, because of the close association between the development of sulphide mineralisation and gold values. This association, usually, allowing the miner or geologist to visually identify the mineralised zone.

Each individual development sample section was examined and a cmg/t value calculated for three *minimum* stope widths, namely 120cm, 150cm and 200cm. At the time that the sampling data was optimised, a stope width of a 120cm was considered to be a practical minimum mining width due to the size of scraper that was being employed in the Woodbine deposit. Thus 120cm was chosen as one of the optimised minimum stope widths. The optimised widths of 150cm and 200cm were chosen as being representative, by degrees, of stoping widths where mining controls were lax. In examining each individual development sample, the optimised width was allowed to open and close at a rate of one metre per five metres along strike when determining the optimised value (cmg/t) and width. Where values warranted it, the optimised stope width was allowed to open up beyond the minimum stope width and a value of 4.0 g/t was used as a "cut off" grade for such decisions, as being the currently accepted mineable grade.

The number of development samples collected for each optimised width differs slightly; the 120cm, 150cm and 200cm optimisation exercises having 2183, 2181 and 2178 sample points, respectively. These differences are due to the fact that the Woodbine deposit is near vertical, with the development samples being taken in the hangingwall of the drives or raises, and occasionally full reef exposures were obscured by ventilation pipes. Where the full reef exposure was obscured, a partial sample section was cut. However, the reduced sample width meant that, at those locations, an optimised value for certain widths could not be determined.

3.3 An Examination of the Development Data:

The optimisation exercise generated three data sets, one for each of the optimised widths. Various statistics were determined for each of the data sets. Probability plots drawn from these data sets, giving the basic statistics, can be seen in Appendixes A, B and C for the 120cm, 150cm and 200cm optimisations, respectively. Figures A1, B1 and C1 yielding information regarding the cmg/t values, whilst Figures A8, B8 and C8 giving information about the optimised widths. The basic statistics have been summarized and tabulated below:

Table 3.1: The Development Data from the Three Optimised Data Sets.

Statistic	OPTIMISED WIDTH		
	120cm	150cm	200cm
Arithmetic Mean (cmg/t) :	685	709	744
Std. Deviation (cmg/t) :	1942	1942	1946
Skewness :	19.31	19.31	19.25
No. of Samples :	2183	2181	2178
Median (cmg/t) :	405	440	477
Minimum (cmg/t) :	1	1	1
Maximum (cmg/t) :	52834	52844	52879
Average Optimised Width (cm):	131	156	201
Average grade (g/t) :	5.23	4.54	3.70

From Table 1, it is clear that all of the data sets are very positively skewed and have wide ranges of values. Figure 3.1 has been drawn from the 120cm optimised data and illustrates the degree of skewness that is present in the Woodbine data. Indeed, of the 2183 samples optimised to a 120cm, only 319 have a value greater than 1000 cmg/t. Yet those same 319 samples, only 14.6% of the total number of samples, account for approximately 52% of the arithmetic mean value. Clearly, the few extreme values present within the data sets are cause for concern when reviewing the statistics given above.

Where the mineralised channel of a reef is wider than the expected stope width, as with the Woodbine deposit, the cmg/t value for any given point is *not fixed* and is dependent upon the width at which it was optimised. This is not only true "for any given point," it also holds for block estimates as well. Thus, when determining block estimates, both the cmg/t value and optimised width must be determined from each of the optimised data sets. In this manner a Grade Stope Width model can be developed for any given ore reserve block (see Chapters 5 and 6). Figure 3.2 illustrates the statistical characteristics of the optimised stop widths. It should be noted that the majority of development samples (some 70%) could not justify an optimised stope width of greater than 120cm and consequently the widths are not normally distributed. This fact has certain ramifications when generating the semivariograms to be used in estimating the various optimised widths, as explained in the next chapter.

When a data set is positively skewed it is, in South Africa at least, common practice to take the natural logarithms of the cmg/t values and examine the lognormal model. The results of this exercise have been shown graphically in Figures A2, B2 and C2 in Appendixes A, B

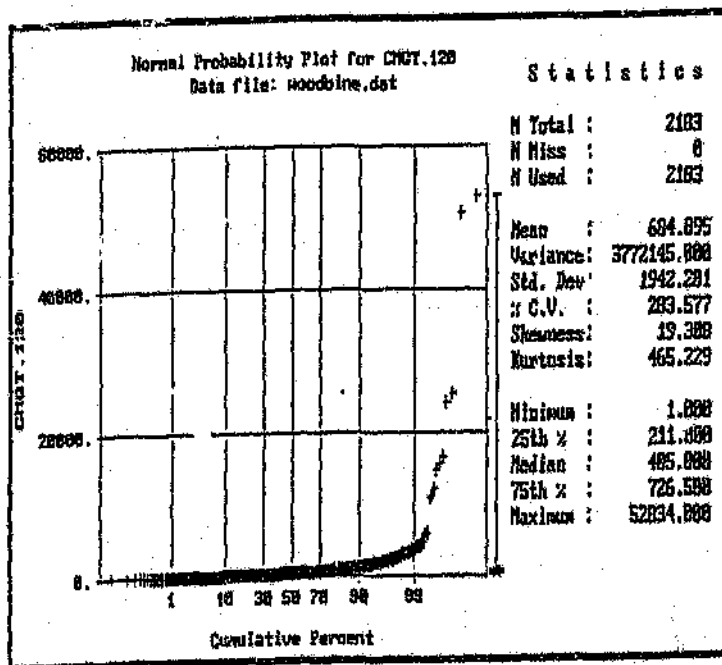


Figure 3.1 : Probability Plot from the 120cm Optimisation, cmg/t Values.

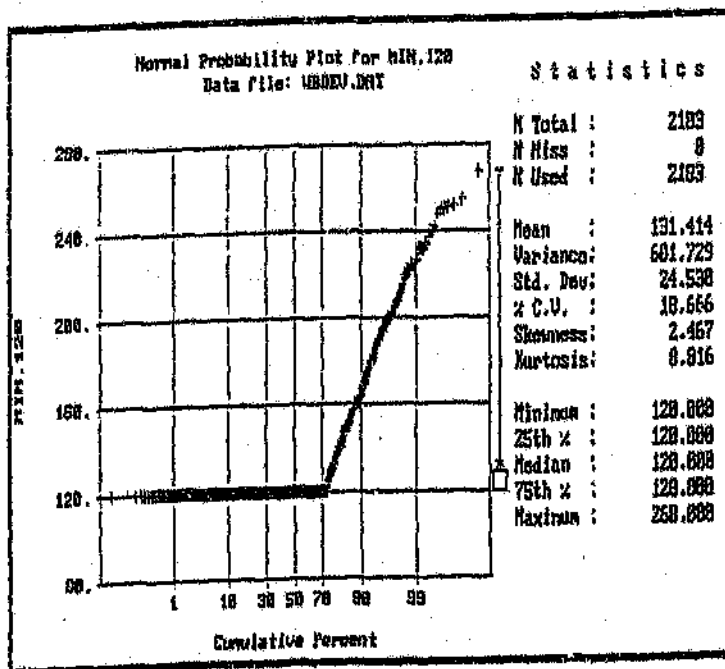


Figure 3.2 : Probability Plot of the 120cm Optimised Stop Widths.

and C, respectively. The Woodbine data shows the characteristics of having a three-parameter lognormal distribution, but has two significant departures from it. Figure 3.3 has been drawn from the 120cm optimised data to demonstrate these characteristics. The majority of the Woodbine data has the essential features of a three-parameter lognormal distribution, with the $\ln(\text{cmg/t})$ values plotting as a straight line and the characteristic downturn of the lower tail requiring a Beta (β) additive constant to correct it. However, a small proportion of the Woodbine data do depart from this model in the upper and lower value ranges (see A and B in Figure 3.3). These departures from the "model" may be viewed as "outliers", which are discussed in Chapter 3.4 below.

In examining the geostatistical methods outlined in Cases (a) of Chapter 1.4, the data values (cmg/t) will be transformed into natural logarithms before any study is undertaken, as the Woodbine data closely approximates a three-parameter lognormal distribution. Case (b) differs from the others, in that two types of data transformation will need to be undertaken. Indicator transforms will be performed on all of the data, using the upper and lower "outliers" as cut-off values. Then the data, less the "outliers", shall be transformed into natural logarithms before any analysis. The data values (cmg/t), for Case (c), will be transformed into rank related values.

3.4 The Identification of "Outliers":

Essentially there are three sources of sampling data inconsistency; namely, an extreme value from the same population, a value from another population and lastly, a value resulting from

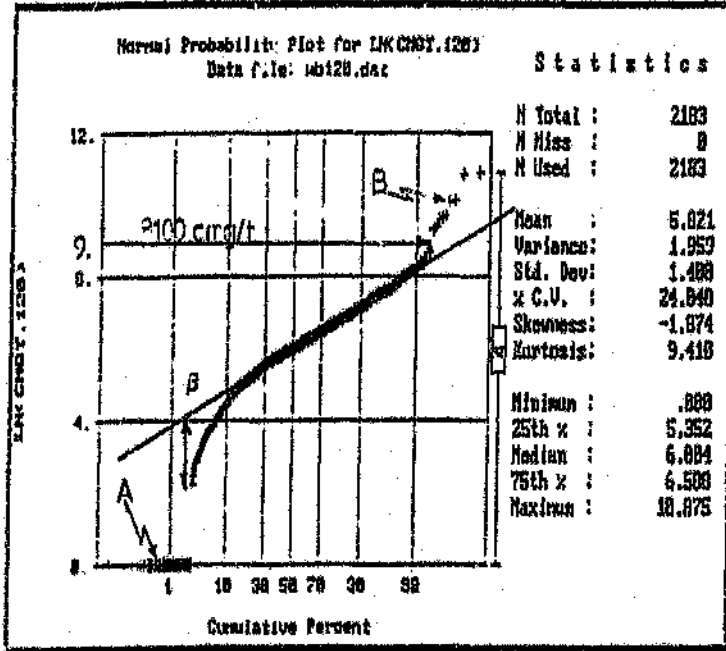


Figure 3.3 : Probability Plot from the 120cm Optimisation, In (cmg/t).

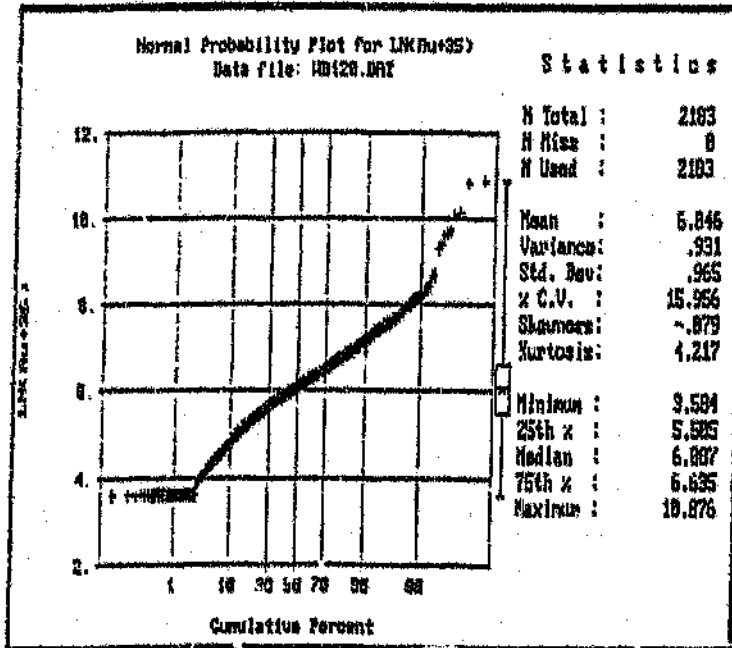


Figure 3.4 : Probability Plot from the 120cm Optimisation, In (cmg/t + β)

an error in assaying or sampling. Though not strictly correct, these data inconsistencies will be referred to as "outliers" for the purpose of this present report.

The lower valued "outliers" (see A in Figure 3.3) can be the result of off reef development. However, before the development sampling data was captured, the data was reviewed by the author and the geologists at Agnes Mine. It is therefore assumed that the data captured is on reef. Another reason for the existence of samples valued at 1 cmg/t is the result of a historic assay cut off, where an assay of 0.4 g/t was recorded as "trace". Consequently, there could be a number of sample sections that recorded only "trace" values and thus have a value of 1 cmg/t. However, more recently, this assay cut off improved to 0.1 g/t and this maybe the reason why there are no "trace" values on 26 level or in the stope data.

The removal of the lower valued "outliers" can be justified as they are, probably, the product of an assay cut off (or an assay "error"). Furthermore, to leave such values intact within a data set, when examining lognormal statistics, is to overstate the variance of the logarithmic values. As the mean value (μ) of a three-parameter lognormal variate is related to the geometric mean (m) and the natural logarithmic variance of the values (σ_v^2), where:

$$\mu = m[\exp(\sigma_v^2/2)]^{1/2} \dots\dots\dots(1)$$

When the logarithmic value of the geometric mean is approximately six (as with the Woodbine data), a value of 1 cmg/t has a similar influence on the variance of the natural logarithms, as a value of approximately 160 000 cmg/t. The inclusion of the lower valued

"outliers" could, therefore, result in an over valuation of the mean value (μ) and is naturally of some concern to the Mine Evaluator.

The cause of the higher valued "outliers" (see B in Figure 3.3), is less easy to define; they can simply be the "unlikely" occurrence of extremely rare values, but are part of the same population as the rest of the sample data. Alternatively, they may be the result of some samples being drawn from another population; for example, samples intersecting fractures filled by quartz veins carrying visible gold and of a completely different geological origin to the deposit as a whole. As stated in Chapter Two, work is being undertaken at Agnes Mine to determine the influence of specific geological structures on the grade distribution of the Woodbine deposit. However, this work was incomplete at the time that this project report was written and so it was not possible to define the higher values as population "outliers" on geological grounds.

Unfortunately, testing for "outliers" on a purely statistical basis is unsatisfactory as the theory regarding the detection of "multiple outliers" is both complex and inconclusive. From a practical view point, however, the higher "outliers" are identifiable by the fact that they have departed from the lognormal line. It is this criteria that will be used to define the higher "outliers" and a value of 8100 cmg/t is used as an upper cut-off (see Figure 3.3). This cut off applies to *all* three of the optimised data sets and not just the 120cm optimisation. This fairly arbitrary decision was taken for consistency.

3.5 The Treatment of "Outliers":

The manner in which the "outliers" are dealt with is dependent upon the geostatistical method to be examined. As outlined in Chapter 1.4, three geostatistical methods are examined in this project report and were put forward as Case (a), (b) and (c).

3.5.1 Case (a):

In this Case the data set was left intact and the "outliers", and their effects upon the variance of the natural logarithms and the semivariogram model, being accepted as indicative of the character of the Woodbine deposit. Though the lognormal statistics of the data do not truly conform to the three-parameter lognormal model, a Beta constant (β) was applied to the data to reduce the degree of skewness to a minimum; see Figures A3, B3 and C3 in Appendixes A, B and C. The Beta constants applied were +35, +45 and +55 mg/t for the 120cm, 150cm and 200cm optimisations, respectively.

Figure 3.4 illustrates the degree to which the data from the 120cm optimisation can approach the three-parameter lognormal model with the application of a Beta constant to reduce the skewness of the population distribution. The upper and lower "outliers" clearly being problematic in their departure from the lognormal model. However, such data sets could, and do, arise where the Mine Evaluator is unwilling to remove such "outlier" values.

3.5.2 Case (b):

Case (b) allows for the removal of "outliers" from the data sets and to treat them as a

separate population by using "Indicators", rather than cutting the "outliers" completely. In this case two Indicator data sets were formed, one for the low "outliers" and another for the high "outliers". The basic concept is to be able to estimate any given point or ore reserve block using the development data, without the influence of the "outliers". Then, by separating the problematic data into different classes, giving the "outlier" data point a value of "1" and all other data points a value of "0", one can determine the probability of the "outlier" data influencing any given point or ore reserve block.

Figures 3.5, 3.6 and 3.7 have been drawn from the 120cm optimisation to illustrate the progressive stages of removing the "outlier" data and adding a Beta constant to normalize the remaining data, so that it conforms to the three-parameter lognormal model. In Figure 3.5 the lower "outliers" have been removed and thereby emphasizing the division between the majority of the Woodbine data and the higher "outliers". Figure 3.6 graphically illustrates how the Woodbine data conforms to the three-parameter lognormal model, once all the "outliers" have been removed. Figure 3.7 shows the 120cm optimised data made lognormal, requiring a small Beta constant of +45 cmg/t. The other optimisations of a 150cm and 200cm requiring a +60 cmg/t and +75 cmg/t Beta constant, respectively. The adjustments made to the 120cm, 150cm and 200cm optimisations can be found in Appendixes A, B and C, respectively (see Figures A4, 5 and 6, B4, 5 and 6 and C4, 5 and 6).

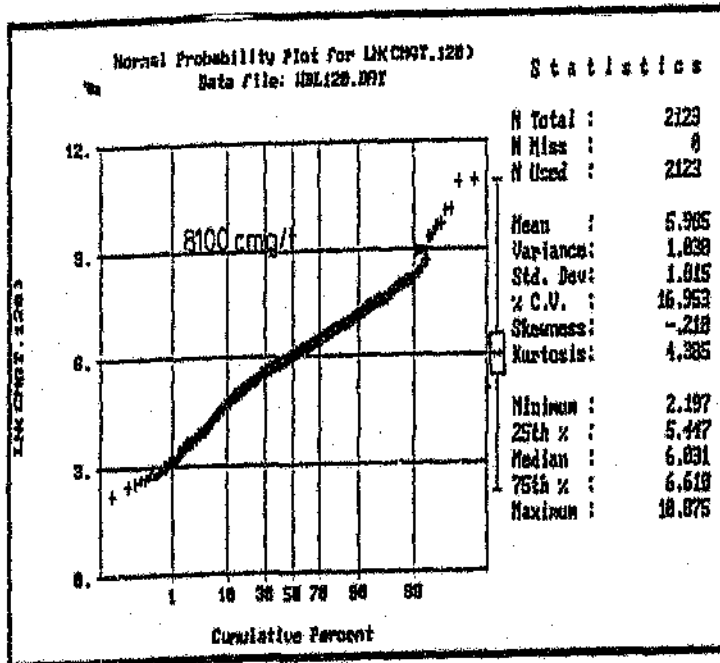


Figure 3.5 : Probability Plot from the 120cm Optimisation, ln (cmg/t) less the lower Outliers.

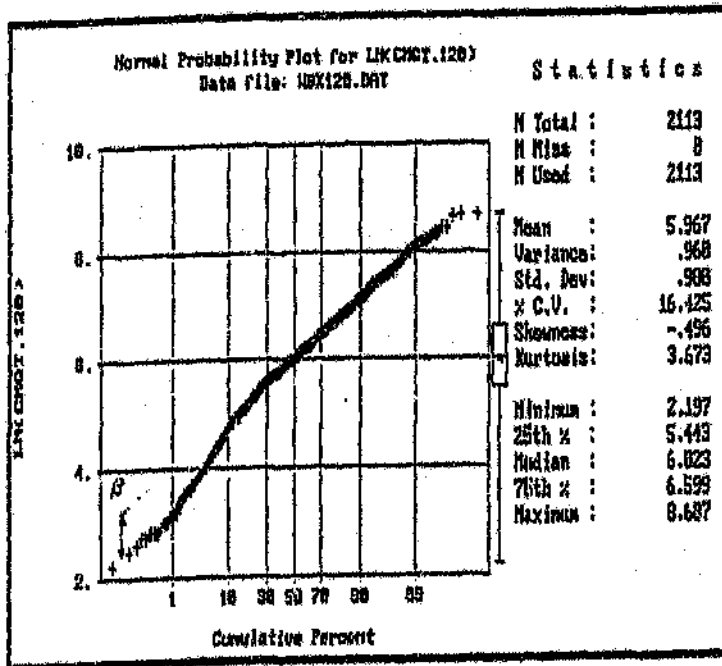


Figure 3.6 : Probability Plot from the 120cm Optimisation, ln (cmg/t) less all Outliers.

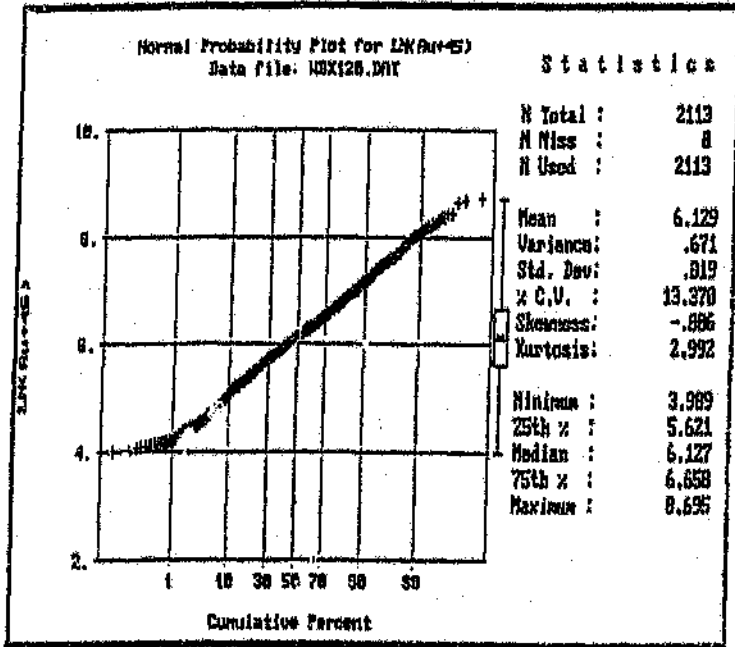


Figure 3.7 : Probability Plot from the 120cm Optimisation, ln (cmg/t + β) less all Outliers.

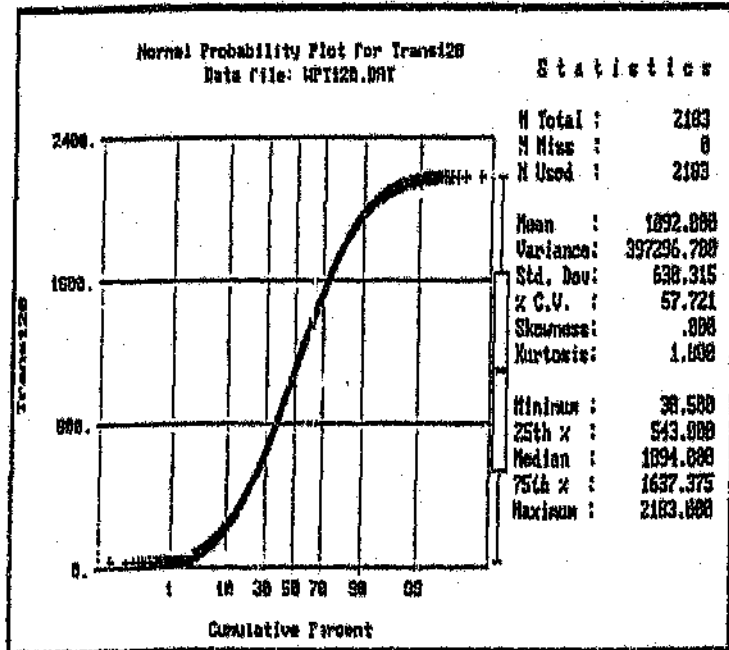


Figure 3.8 : Probability Plot from the 120cm Optimisation, Transformed Values.

Therefore, for Case (b), the estimated value (cmg/t) for any given point or ore reserve block is determined using the following relationship:

$$V = (1-p-q).v_m + p.v_l + q.v_h \dots \dots \dots (2)$$

where:

- V = Point or Block Estimate (cmg/t)
- v_m = Estimated value, less all "outliers" (cmg/t)
- v_l = Arithmetic average of the lower "outliers" (cmg/t)
- v_h = Arithmetic average of the higher "outliers" (cmg/t)
- p = Probability of influence of lower "outliers"
- q = Probability of influence of higher "outliers"

The use of arithmetic averages for defining the influence of the "outliers" on an estimated value, may seem crude; however it should be remembered that due to sparsity of "outlier" data, local estimates cannot be made. The values for "p" and "q" are derived from the kriging results of any given point or area, using the Indicator data sets.

5.5.3 Case (c):

The third and final case, examines the effectiveness of transforming the Woodbine data (cmg/t) into its dimensionless rank related form. The transformation process involves giving the actual cmg/t value a value equal to its ranking within the data set. For example, in the 120cm optimisation, the highest value equals 52834 cmg/t and therefore receives a ranking of 2183, as there are only 2183 data points. The second highest value in the data set

receiving a ranking of 2182 and so on.

Where two or more cmg/t values are equal, then the transformation process is slightly more complex. There are two methods of dealing with this problem; the first is to take the equal cmg/t values and give their rank ("n-#") at random. Thus, if there are three cmg/t values, all of equal value, then their ranking "n", "n-1" and "n-2" are determined at random. In this manner, one ensures that each cmg/t value receives a unique rank related value. However, the disadvantage of this method lies in the fact that equal values must be given a unique rank. In a sizeable, positively skewed data sets there is the very real likelihood of numerous sample points being of equal value. Thus, in applying this method of determining the rank of equal values, the rank given becomes a function of random selection, rather than it being based on the actual cmg/t value.

The alternative approach is to take the equal cmg/t values and apply the average value of their ranks ("n-#") to all of those cmg/t values. For example, three equal cmg/t values that would have had ranks of "n", "n-1" and "n-2" are all given one rank value equal to "n-1". The most significant advantage of this method, compared to the first, is that the rank applied to each *different* cmg/t value is unique and the allocation of a particular rank to a sample location is not a function of random selection. It is for these reasons that the second method is the one used in this project report.

The advantage of such a rank related transform is that the influence of "outliers" are essentially negated. Thus there is no need to treat the "outliers", as defined above, any

differently that the rest of the data. If one examines Figure 3.8, drawn from the 120cm optimisation, one can see that though the degree of skewness of the transformed values is equal to zero, the probability plot shows the data departing from a straight line, indicating that the data is not normally distributed.

3.6 A Statistical Analyses of the Development Data:

In determining the statistics, given in Table 3.2 below, the natural cmg/t values for the first two Cases were calculated using formula (1), above. For the third Case, statistics cannot be carried out directly on the transformed values, the statistics will be those of the natural values given in Chapter 3.3 above. If one were to undertake any sort of statistical analysis of the transformed values, the median and mean values would be the same and upon conversion back into natural cmg/t values they will also yield the same cmg/t value. Yet, with a positively skewed data set, the median and mean values are not the same.

Table 3.2: A Summary of the Statistics for the Three Optimised Data Sets.

	Beta	Median	Variance	Mean
	(cmg/t)	(cmg/t)	(log)	(cmg/t)
Case (a): includes all data.				
120cm Optimisation	+35	405	0.931	638
150cm Optimisation	+45	440	0.837	660
200cm Optimisation	+55	477	0.774	693
Case (b): less all "outliers".				
120cm Optimisation	+45	413	0.671	597
150cm Optimisation	+60	452	0.593	621
200cm Optimisation	+75	488	0.544	656
Case (c):				
120cm Optimisation	---	405	---	685
150cm Optimisation	---	440	---	709
200cm Optimisation	---	477	---	744

If one compares Table 3.1 to Table 3.2, it can be seen that the use of logarithms, in Case (a), to determine the mean value has caused a "smoothing" of the higher "outliers" thus yielding a slightly lower mean value. Any comparisons made for Cases (b) would not be valid as the "outliers" have been removed from the data before any calculations were made. The most noteworthy comparison that can be drawn from the two Tables, is the degree to which the mean value for Case (c) differs from the arithmetic mean, given in Table 3.1, and the means determined for Cases (a) and (b) in Table 3.2. The reasons for this discrepancy have been discussed in Section 3.5.3, above.

3.7 A Statistical Analysis of the Stope Data:

The stope data was taken from the original stope sampling sheets at Agnes Mine. A total of 714 samples were collected from the eleven stoped-out areas and their positions coordinated. Each sample was examined and optimised to 120cm, 150cm and 200cm. As the development samples were optimised to three widths, it was necessary to examine the stope samples in the same light so that a series of cross validation exercises could be undertaken to check the validity of the semivariogram models derived from the optimised development data. The actual stope width and cmg/t value, realised at that width, were also noted for later comparisons between the various "block" estimates and the "actual" value and width at which any given stope was mined at. The statistics, regarding the stope data, can be found in Appendix D.

The stope data set had only one extreme value of 13799 cmg/t (see Figure D1, D6, D1 and D16 in Appendix D). This outlier was removed from the data set when determining the "actual" stope values in Chapter Five. To leave such an "outlier" in a data set would distort the mean and variance of the three-parameter lognormal statistics. Furthermore to leave such a value in place would also adversely influence the semivariogram used to kriged the actual block values. However the "outlier" was left intact for the cross validation exercises of Chapter Four for reasons that will be explained in that Chapter.

The stope data has been summarized and tabulated below, in Table 3.3. It is interesting to note that the cmg/t values generated by the optimisation model and "actual" cmg/t values do

differ slightly. The average cmg/t value for the actual stope widths, with a width of only 179cm, is a fraction greater than the average cmg/t value determined for the 200cm optimisation. This is a product of the optimisation process, where there is always a minimum optimised stope width restriction in place when collecting the data. When collecting the actual stope data, there is no such restriction. The result being that where, for any given point, the minimum optimised stope width is greater than that of the actual stope width, the difference is given a zero grade. Thus, in this case, the cmg/t value is the same for the actual stope width as the optimised width. However, when the actual stope width is greater than a particular minimum stope width, then the optimised cmg/t value is frequently less than the "actual" value. Thus, on *average*, the statistics for the actual stope data result in a larger cmg/t value over a smaller stope width, when compared to the statistics from the optimised data.

Table 3.3: A Statistical Analysis of the Woodbine Stope Data.

	Beta (cmg/t)	Variance (log)	Mean (cmg/t)	Width (cm)	Samples (No.)
Optimised to 120cm	+ 5	0.715	654	132	713
Optimised to 150cm	+ 10	0.662	677	156	713
Optimised to 200cm	+ 25	0.617	706	202	713
Actual Values	+ 30	0.610	721	179	713

From this simple tabulation it is reasonable to assume that the stope data and development data have been drawn from the same population; compare Table 3.2 with Table 3.3. With the stope data, one would be expect to have a higher mean and lower variance as it is assumed that the stopes were mined selectively according to some or other paylimit. Indeed, given this, the statistics compare favourably.

CHAPTER 4**SEMIVARIOGRAM MODELS AND CROSS VALIDATION EXERCISES:****4.1 Introduction:**

The objective of this Chapter is to define and examine the spatial statistics of the variables within the Woodbine sampling data, by way of a semivariogram for each variable. As there is an element of subjectivity inherent in the modeling of a semivariogram, the validity of each semivariogram model chosen is determined by way of a cross validation exercise.

In evaluating any given area within a gold mine, the Mine Evaluator usually has at his disposal a combination of both development and stope sampling data with which to generate the necessary semivariograms used in estimating the value (cmg/t) and stope width (cm). However, for the purposes of this project report, an extreme case is taken whereby it is initially assumed that the only source of data available is the development sampling data between 24 and 26 levels (see Figure 1.2), as would perhaps be the case when mining operations start in a new area. From this assumption, a semivariogram model is then generated for each variable and then cross validated, using the same development data, to ensure the validity of the model chosen. Yet this test only supports the notion that the semivariogram model reproduces the development data correctly. It does not define how this fit might differ from the "true" semivariogram model which fits the entire area between 24 and 26 level, once stoped.

The ultimate "test" for a semivariogram, as a predictive tool, is for it to be able to accurately forecast the values to be found at an unsampled point or area. By cross validating only the optimised stope data with the semivariograms generated by solely development data, it is possible to determine if the spatial statistics of the stope data conform to those of the development sampling.

The actual stope data are used in Chapter Five to determine the value (cmg/t) and width at which each stope, or "block", was mined at. In this manner one will be able to examine the Grade-Stope Width model of each "block", so as to compare the various geostatistical evaluation methods with the "actual" values realised and determine if the development sampling data yields sufficient information to be able to accurately predict the gold content of any given block.

4.2 Semivariograms and Cross Validation Exercises Based on Development Data:

In each of the geostatistical methods examined, Case (a), (b) or (c), the data was optimised to three minimum widths. As a result, it was necessary to generate a different semivariogram for each optimisation for the cmg/t values and widths. For all of the semivariograms, a lag of four metres, with a tolerance of two metres, yielded the most stable graphs. Due to the spatial distribution of the development data along drives, raises and winzes, only omnidirectional semivariograms were modelled for these exercises (see Appendix E).

4.2.1 Semivariogram Models Generated from Development Data:

The semivariogram models determined for the $\ln(\text{cmg/t} + \beta)$ values in Case (a), where no "outliers" are removed from the data set, are graphically illustrated in Figures E1, E2 and E3 of Appendix E for the 120cm, 150cm and 200cm optimisations, respectively. All three semivariograms have two structures and have a Nugget Effect of approximately thirty percent of the semivariogram Sill. Visually, the model chosen fits the data very well.

However, it must be remembered that in lognormal geostatistics the level of the Sill influences the kriged estimate (z^*) of any give point or area. The kriged estimator (z^*) is defined by:

$$\log z^* = \sum a_i \log x_i + \frac{1}{2} \sum a_i (\sigma_{x_i}^2 - \sigma_{y_i}) + \frac{1}{2} \lambda \dots \dots \dots (3)$$

where:

z^* = kriged estimator of the untransformed true value,

y = actual value of ore block to be estimated,

x_i = values of data,

a_i = kriging weights for the transformed values x_i ,

$\sigma_{x_i}^2$ = the population variance of the transformed values,

σ_{y_i} = covariance between transformed values y and x_i , (calculated from semi-variogram)

λ = la Grange multiplier.

Therefore, the fact that the "outliers", both high and low, have caused an increase in the population variance ($\sigma_{x_i}^2$) is likely to result in an overvaluation of any kriged estimate. Thus, the kriged estimates of the various "blocks", generated in Case (a), must be viewed with some caution in light of the formula given above.

The semivariogram models determined for the $\ln(\text{cmg}/t + \beta)$ values in Case (b), where all "outliers" are removed from the data set, are graphically illustrated in Figures E4, E5 and E6 of Appendix E for the 120cm, 150cm and 200cm optimisations, respectively. Again, it can be seen that the three semivariograms have two structures and have a Nugget Effect of approximately thirty percent of the semivariogram Sill and the model chosen, visually, fits the data well. Also, in Case (b), it was necessary to generate semivariogram models from the high and low indicators (see Figures E7 and E8, in Appendix E, respectively). Both the high and low "outliers" have very short ranges of influence and the semivariogram models can be viewed as pure Nugget Effect.

The formula given in (3) above also applies to Case (b). However, the removal of all "outliers" has reduced the population variance (σ_x^2) and the Sill of the semivariogram. Thus, the basis of examining Case (b) is that the use of indicators, to model the characteristics of the "outliers", will generate better "block" estimates.

The semivariogram model determined for the cmg/t values in Case (c), where the values have been subject to a Rank Related Uniform Transform, is graphically illustrated in Figure E9 of Appendix E. One model was chosen for all three optimisations, as any variation in the transformed values is a result of the number of data points, rather than the actual cmg/t values. The 120cm, 150cm and 200cm optimisations contained 2183, 2181 and 2178 data points, respectively, and therefore the population variances and semivariogram graphs of the three optimisations were almost identical. The similarities between the semivariogram graphs, for the different optimisations, are also due to the fact that the different optimisations

did not greatly effect the ranks of the individual samples. The semivariogram has two structures and a Nugget Effect of approximately thirty percent of the semivariogram Sill.

The semivariogram models determined for the optimised slope width values are graphically illustrated in Figures E10, E11 and E12 of Appendix E. Upon examination of these Figures, it would appear that the range of influence decreases as the optimised width increases; which is exactly the opposite of what one would expect. However, the variability of the optimised width decreases as the width of the optimisation increases. Thus the sill of the semivariogram model decreases, indicating uniformity of the variable. For example, the 200cm optimised slope width has a Sill (and population variance) of only 31cm^2 and therefore a standard error of plus or minus $\pm 5.6\text{cm}$.

4.2.2 Cross Validation Exercises Generated from Development Data:

Each of the semivariograms generated from development data, with the exception of the indicator semivariograms, were cross validated against that same data, so as to confirm the validity of the models fitted to the data. The cross validation process involves the removal of a single sample (T), whereby a value (T*) and standard error (σ_e) for that point is estimated from the surrounding samples. An error statistic is determined for that point, thus:

$$\text{Error Statistic} = (T - T^*)/\sigma_e \dots\dots\dots(4)$$

This process is repeated for all samples, creating a set of error statistics. If the semivariogram model reproduces the data accurately, then the error statistics will have a

mean of zero and a standard deviation of one. The error statistics of these exercises have been shown graphically in Appendix F, (Figures F1 to F12) and summarized in Table 4.1 below:

Table 4.1: Summary of the Cross Validation Exercises from Development Data.

	<u>Mean</u>	<u>Standard Deviation</u>
Case (a): includes all data.		
120cm Optimisation	0.001	1.022
150cm Optimisation	0.001	1.015
200cm Optimisation	0.001	1.011
Case (b): less all "outliers".		
120cm Optimisation	-.001	1.002
150cm Optimisation	-.001	0.999
200cm Optimisation	-.001	0.993
Case (c):		
120cm Optimisation	0.001	1.026
150cm Optimisation	0.001	1.024
200cm Optimisation	0.000	1.019
Optimised Slope Widths:		
Minimum 120cm	-.001	0.880
Minimum 150cm	-.001	0.927
Minimum 200cm	-.000	1.051

The degree to which the error statistics from the cross validation exercises can depart from the "ideal", before indicating that a semivariogram model does not "fit" the data, is as subjective as the model fitting process itself. The literature on cross validation procedures provides little guidance as to the level of tolerance about the "ideal" that is acceptable. However, if one examines Table 4.1, it is clear that none of the semivariograms produce any bias, as mean values of the error statistics all approximate zero.

The standard deviation of the error statistics, for Cases (a), (b) and (c), all approach one. The cross validation of the optimised stope widths did produce standard deviations that departed from the "ideal" of one. However, it should be remembered that this data is not normally distributed due to the data having a minimum value enforced when the data was captured. Consequently, the standard deviation of these error statistics have departed from zero. As the mean of these error statistics is close to zero, indicating no bias, the optimised stope width semivariogram models were left unaltered for the kriging exercises of the next Chapter.

4.3 Cross Validation of the Stope Data using the Semivariograms Generated from Development Data:

As stated above, the ultimate "test" in justifying a semivariogram's validity as a predictive tool, is for it to be able to accurately forecast the values to be found at an unsampled point or area. The semivariograms found in Appendix E, were derived solely from optimised development data and therefore no account was taken of the stope data in their generation.

By cross validating only the stope data with the semivariograms generated, it is possible to predict a value at a location that was actually sampled, yet not used in determining the semivariogram model. Effectively, an unsampled point as far the semivariogram model is concerned. There are 714 stope values, of which one could be classified as an "outlier". The single "outlier" has been left in the stope data sets, as this exercise is designed to see if the semivariograms, found in Appendix E, can accurately forecast all of the values to be found within the stopes. If the error statistics conform to the "ideal", then it can be said that the spatial statistics of the stope data conform to those of the development sampling.

To accommodate this exercise, the stope data was optimised to the same three widths as the development data, thereby allowing a direct comparison to be made between the cross validation of the development data and that of the optimised stope data, for any given optimisation. The error statistics of the cross validation exercises for the stope data have been shown graphically in Appendix F, (Figures F13 to F24) and summarized in Table 4.2 below. It is clear that none of the semivariograms caused a bias in the error statistics, as the mean values all approximate zero. However, the standard deviation of the error statistics, for Cases (a), (b) and (c), are all less than the "ideal" of one. This would suggest that the "actual" errors are less than the "theoretical" errors.

Table 4.2: Summary of the Cross Validation Exercises Generated from Slope Data:

	<u>Mean</u>	<u>Standard Deviation</u>
Case (a): Semivariograms.		
120cm Optimisation	-.001	0.764
150cm Optimisation	-.001	0.776
200cm Optimisation	-.001	0.800
Case (b): Semivariograms.		
120cm Optimisation	-.001	0.834
150cm Optimisation	-.001	0.848
200cm Optimisation	-.002	0.858
Case (c): Semivariograms.		
120cm Optimisation	-.002	0.839
150cm Optimisation	-.002	0.842
200cm Optimisation	-.002	0.841
Slope Width Semivariograms:		
Minimum 120cm	-.004	1.001
Minimum 150cm	-.002	1.096
Minimum 200cm	-.001	1.477

If one examines formula (4), above, there are two reasons why this should occur. The first is that the $(T-T^*)$ comparison was better than anticipated, or secondly, the standard error (σ_e) , generated by the semivariogram model was too pessimistic for the optimised slope data sets. The latter is unlikely if one examines how well the semivariogram model fits the graphs

in all cases. However, the most likely reason for the error statistics departing from the ideal is that the stope data is less variable due to the selectivity applied to the mining of certain districts based on the use of pay limits. Therefore the $(T-T^*)$ comparisons were uncharacteristically small, in comparison to the deposit as a whole.

The cross validation of the 200cm optimised stope widths did produce a standard deviation that departed from the "ideal" of one. Again, it should be remembered that the optimised stope widths are not normally distributed due to the data having a minimum value enforced when the data was captured. Consequently, the standard deviation of these error statistics have departed from zero.

In both cases, stope value (cmg/t) and width, the mean of these error statistics is close to zero, indicating no bias. Therefore, the optimised development semivariogram models were left unaltered for the kriging exercises of the next Chapter.

4.4 Semivariograms and Cross Validation Exercises of the Actual Stope Values:

The semivariograms and cross validation exercises examined above, used optimised data sets. For the next chapter, the actual widths at which the stopes were mined at and the cmg/t values realised at those widths must be examined. The eleven stoped out areas are to be evaluated using the development data, for each of the three Cases, as if the ore was still "in situ" and the results then compared to the actual values at which a given stope was mined at.

The semivariogram models generated by the actual stope data, cmg/t values and stope widths, can be found in Appendix E, (see Figure E13 and E14). The semivariogram modeling the actual cmg/t values has been transformed into natural logarithms after a Beta constant was added, as described in Chapter Three. One "outlier" was removed from the data before modeling the semivariogram. The semivariogram of the actual widths can be seen in Figure E14. It is interesting to note that the Sill is of a lower level than any of the semivariograms generated in Cases (a) and (b), and may explain the poor cross validation error statistics of Section 4.3 above.

The cross validation exercises undertaken on the actual stope data can be found in Appendix F (see Figures F25 and F26). The error statistics for both semivariogram models (cmg/t value and widths) conform to the "ideal" of a mean of zero and a standard deviation approaching one.

CHAPTER 5

KRIGING OF "BLOCK" ESTIMATES AND ACTUAL VALUES:**5.1 Introduction:**

The purpose of this Chapter is to examine the performance of various geostatistical evaluation methods, outlined as Cases (a), (b) and (c) in Chapter One, and to determine how these kriged estimates of the Woodbine Ore Reserves compare with the actual values encountered when the "blocks" have been mined and sampled. Eleven stoped areas between 24 and 26 level were chosen for the evaluation and comparison exercises, as their stope sampling sheets were readily available (see Figure 1.2).

Each stoped-out area, referred to as simply a "block," will be subjected to a number of evaluations and comparisons. In examining the performance of the various geostatistical evaluation methods, the development sampling data will be used to determine the "block" estimates of the stoped areas. The stope sampling data being used to determine the "actual" value (cmg/t) and width at which each stope was mined at. In this manner one will be able to compare the various geostatistical evaluation methods. These comparisons will be shown in tabular form and graphically.

5.2 The Evaluation of "Block" Estimates for the Stoped Areas from Development Data:

The evaluation exercises will be undertaken to determine a block estimate for its cmg/t

value, stope width and variance for each of the optimisations. This process being repeated for each of the Cases (a), (b), (c), and the actual stope values. A portion of the 25 E9B stope was taken to be "off reef" as its stope sampling indicated that there was reef in foot or hanging. This "off reef" portion was not included in the evaluation exercise, (see Figure 1.2).

5.2.1 The Optimised Stope Widths:

The block estimates for the optimised stope widths were determined using ordinary kriging and the semivariogram models determined in the previous Chapter. Only the development data were used, thus forecasting the stope width to be mined, as if the reef were still "in situ". This exercise yielded three estimated block widths for each stoped-out area. The estimated stope widths, for each "block", will remain constant irrespective of the Case under investigation. The results of the kriging exercise for the optimised stope widths have been tabulated in Tables 5.1, 5.4 and 5.7 for the 120cm optimisation, in Tables 5.2, 5.5 and 5.8 for the 150cm optimisation, and in Tables 5.3, 5.6 and 5.9 for the 200cm optimisation.

5.2.2 The Kriging Exercises for Case (a):

The evaluation of the eleven "blocks" under consideration used all of the optimised development data, as defined by Case (a). Each of the three optimisations were kriged separately, using ordinary kriging. This exercise yielded three estimated block values (cmg/t) dependent upon the optimised stope width. Thus for any given block one can forecast the estimated block value (g/t) for any given "likely" stope width. Once an area has been stoped, the actual block values can then be readily compared to the block estimates to gauge

how well the optimised development data modeled what was actually found within the block. The results of this exercise were tabulated in Tables 5.1 to 5.3.

These tables go further than simply stating the estimated cmg/t, stope width and variance; they also give an upper and lower confidence limit. For this exercise a 80% central confidence limit was used assuming a normal distribution for errors. Essentially, this means that there is a 1 in 10 chance of the "actual" value, of the given block, being greater than the upper confidence limit and a 1 in 10 chance of the "actual" value being less than the lower confidence limit.

The results tabulated in Tables 5.1 to 5.3 have also been shown graphically in Appendix G. Each Figure shows the stope width along the horizontal axis and the grade (g/t) along the vertical axis. The central line on each graph joins the three estimated block values for the optimised stope widths of 120cm, 150cm and 200cm (EST.MEAN). So as to gauge the range of values that the actual values can take, each diagram has plotted on it the upper 90% confidence limit (EST.UL90) and the lower 90% confidence limit (EST.LL90). These Figures constitute a Grade-Stope Width model, by which the estimated block grade can be determined for any "likely" mining widths, ranging from approximately 100cm to 230cm. Given that there are eleven stopes are being evaluated, there is the probability, and thus the expectation, that at least one of the block's actual stope value will exceed the upper 90% confidence limit and at least one of the block's actual stope value will exceed the lower 90% confidence limit.

5.2.3 The Kriging Exercises for Case (b):

In the evaluation of the eleven "blocks" under consideration, as defined by Case (b), each of the three optimisations were kriged separately, as were the low and high Indicators. In a similar manner to Chapter 5.2.1 above, this yielded three actual block values (cmg/t) dependent upon it's optimised stope widths. The only difference being, the necessity of adjusting the Mean cmg/t value (\bar{y}_m) by the indicator probabilities " p^*_{vl} " and " q^*_{vh} ", (see the formula given on Tables 5.4 to 5.6). The results of the Case (b) kriging have been tabulated in Tables 5.4 to 5.6 and the Grade-Stope Width models have been shown graphically in Appendix H.

5.2.4 The Kriging Exercises for Case (c):

The process of determining a block value, using the Rank Related Uniform Transform is not as straight forward as with the other two Cases. In Cases (a) and (b) it was possible to krig any given block, directly, using the log transformed point samples. Then, using formula (3) in Chapter Four, to convert the transformed estimates (z^*) back into natural values.

However, in using the Rank Related Uniform Transform process, it is necessary to create a grid of points over the entire area to be evaluated. For the area of the Woodbine deposit, a grid of 5 metres by 5 metres was superimposed over the eleven "blocks" to be evaluated. Taking the transformed data values and using ordinary kriging, each point of the grid was evaluated separately. With this process completed, the point estimates were then converted back into natural values by linear interpolation amongst the original data. To determine an estimated value for each "block", the natural values of those grid points that fell within the block boundary were averaged.

This exercise was conducted for each of the optimisations, the results of which have been tabulated in Tables 5.7 to 5.9 and the Grade-Stop Width models have been shown graphically in Appendix I. Given that the "block" estimates were determined on a point basis, no confidence limits were determined for the "block" estimates in this exercise.

5.3 The Kriging of the Actual Values:

As each of the eleven "blocks" under consideration has been stoped-out and was sampled at regular intervals, it was possible to determine an average width at which the stopes was mined and a cmg/t value realised at that width by simply averaging the stopes samples. These results were used for the purpose of gauging, empirically, how the various geostatistical methods performed in evaluating the stoped-out areas of the Woodbine deposit. The results of this exercise can be found on Table 5.10 and on all of the Figures in Appendixes G, H and I.

5.4 A Comparison Between the Block Estimates and the Actual Values:

For Cases (a) and (b), the block estimates compare very favourably with the actual values, (see Appendixes G, H and Table 5.10). There are, however, two exceptions to this; the Stopes 25 E9A and 25 E9B were overvaluated and undervaluated, respectively, when compared to the actual values. In these cases the stopes values encountered within the block were noticeably different from those found in the development along the block's periphery. Statistically, two such occurrences were to be expected.

However, there may be a number of *contributing factors* to the poor estimation of the 25 E9A and 25 E9B stopes. From the 25 E9B stope to the end of 25 level's development, the only development sampling data available was at an interval of five metres instead of the usual two metres. This fact alone could account for the "actual" values being significantly different from block estimate. The 25 E9A peripheral development sampling contained two high "outlier" values and one was in the centrally located raica. This has probably given the "q" factor an unrealistically high weighting. Furthermore, the 25 E9B stope has only a limited amount of development above it on 24 level and these values were suspiciously low. Given the values obtained in the 25 E9B stope, it *may be* an indication that the eastern portion of the 24 level development was outside of the main shear zone.

The performance of Case (c) is very disappointing, in that it seriously undervalues most of the "blocks". It is believed, that in kriging the grid points with the transformed data, the point estimates have been "smoothed" too much. The Archaean gold deposits tend to behave very erratically and have a wide range of values, and hence ranked values, within any defined area. There is no uniform change in value distribution between areas of high or low grade. For this reason, the kriged estimate of any given point will tend towards the *mean rank* value of the sampling data within the range of influence of the semivariogram used. Thus, the value will tend, upon back transformation, towards the median value of the positively skewed data set.

This notion, that the Case (c) values are tending towards the median value of the data sets, is further reinforced upon examination of Tables 5.7 to 5.9. The average estimated value of

the eleven stoped areas, for Case (c) is 460 cmg/t, 493 cmg/t and 531 cmg/t for the 120cm, 150cm and 200cm optimisations respectively. The stope data had median values of 442 cmg/t, 471 cmg/t and 503 cmg/t for the same optimisations (see Appendix D). If one compares these results to the mean values for the stopes data of 654 cmg/t, 677 cmg/t and 706 cmg/t, or to the evaluations of Cases (a) and (b), then it is clear that the Rank Related Uniform Transform process has seriously undervalued the deposit as a whole.

Furthermore, the median *and* mean values of the deposit as a whole are only slightly less than that of the stopes data for any given optimisation (see Table 3.1 and 3.3 above). Thus, it is unlikely that the "selectivity" applied, by mining only certain "blocks" within the Woodbine deposit, has caused a serious bias. Or one that would account for the consistent undervaluation of all stoped areas (see Table 5.10).

For any comparison to be made between Grade-Stopes Width models and the actual values realised once the blocks were mined, one of the two variables (stope width or grade) must be fixed. As explained above, the cmg/t value of any block is influenced by its stope width. Thus, the stope width was kept constant to allow grade comparisons to be made and the width chosen was that at which each "block" was *actually mined* at. The block estimates and the actual values were calculated from the grade-stope width models by using linear interpolation.

Two methods of comparison were used; firstly the percentage difference between each of the calculated g/t values and secondly the difference in grade. A cumulative comparison was

made of all the stopes on 25 level, 26 level and the total of the two levels. These latter three comparisons were based on the total tonnages and contents produced per level or both levels. These values were then tabulated in Table 5.10.

5.4.1 Actual Values v's Case (a) Block Estimates [(a)/(d) v's (a)]:

If one compares the percentage differences of the Case (a) block estimates and the actual values [(a)/(d)], then one notices that the block estimates tend, with two exceptions, to be within a range of approximately plus or minus 14% of the actual values. The two exceptions are the 25 E9A and 25 E9B stopes. As explained above, the development values found on the periphery of this block were noticeably different from those values found in the stope as indicated by the stope sampling.

When this comparison is put in terms of g/t, then the block estimates tend to be within a range of approximately plus or minus 0.59 g/t of the block values. This excludes the 25 E9A and 25 E9B stopes.

However for the whole of the 25 level, the block estimates have overvalued the actual value by some 8.9% (or 0.36 g/t). A similar comparison for the 26 level shows that the block estimates have undervalued the actual value by some 4.9% (or 0.18 g/t). Yet for the two levels combined the block estimates have undervalued the actual value by only 5.2% (or 0.20 g/t).

5.4.2 Actual Values v's Case (b) Block Estimates [(d) v's (b)]:

The comparison of the percentage differences for Case (b) block estimates and the actual values [(b)/(d)], yields similar results to those of Section 5.3.1 where all but two of the block estimates fall within a range of approximately plus or minus 16% of the actual values. In terms of grade, the block estimates tend to be within a range of approximately plus or minus 0.63 g/t of the block values. This excludes the 25 E9A and 25 E9B stopes.

In terms of how the block estimates compare to actual values on a level by level basis; the block estimates have overvaluated the actual value by some 5.1% (or 0.21 g/t) on 25 level and undervaluated by 0.3% (or 0.01 g/t) on 26 level. However, for the two levels combined the block estimates have undervaluated the actual value by only 3.6% (or 0.14 g/t).

5.4.3 Actual Values v's Case (c) Block Estimates [(d) v's (c)]:

The final comparison, that of Case (c) against the actual values, is disappointing. Though the Rank Related Uniform Transform process negates the need to worry about "outliers", it fails to accurately evaluate any given "block". The percentage differences of the Case (c) block estimates and the actual values [(c)/(d)] tend to fall within a range of approximately minus 5% to minus 39% of the actual values. This includes the two stopes that caused problems in Sections 5.3.1 and 5.3.2 above. In terms of grade, then the block estimates have tended to undervalue the "blocks" by between 0.09 g/t and 1.68 g/t.

This trend of undervaluing is seen clearly on a level by level basis. The block estimates have undervaluated the actual value by some 26.7% (or 1.09 g/t) on 25 level and

undervalued by 29.5% (or 1.07 g/t) on 26 level. For the two levels combined the block estimates have undervalued the actual value by 27.4% (or 1.08 g/t).

5.5 Summary:

From an examination of Table 5.10, one can determine that Cases (a) and (b) yielded some very useful results when determining "block" estimates. Case (b) yielding marginally better results when viewed on a level by level basis or as a whole. Statistically, the expected number of departures from the Grade-Stope Width model, "actual" values falling outside of the confidence limits, were realised. Thus, for these two Cases the method of evaluation and the concept of a Grade-Stope Width model seems appropriate. However, the method of evaluation used in Case (c) proved to be inappropriate and the block estimates consistently undervalued the stoped areas. Furthermore, the method used to obtain these estimates did not allow for confidence limits to be determined for their Grade-Stope Width estimates.

TABLE 5.1: WOODS BINE BLOCK ESTIMATES, ALL DEVELOPMENT DATA OPTIMISED TO 120cm.
 (Beta Constant used = +35 mg/t.)

BLOCK	MEAN CHG/T	LOG. VARIANCE	LOWER 90% LIMIT (CHG/T)	UPPER 90% LIMIT (CHG/T)	AVERAGE S.W. (cm)	TONS	GRADE (g/t)		
							MEAN	L.L. (90%)	U.L. (90%)
25 WJ	337	0.0658	224	465	123	22226	2.74	1.82	3.78
25 E2	737	0.0697	497	1011	134	23895	5.56	3.71	7.54
25 E7A	1129	0.0368	859	1426	149	18435	7.58	5.76	9.57
25 E7B	942	0.0480	766	1202	140	9777	6.73	5.04	8.59
25 E9A	1427	0.0544	1020	1884	157	14894	9.09	6.50	12.00
25 E9B	324	0.0521	226	434	128	10497	2.53	1.77	3.39
25 E10	518	0.0658	358	708	123	6756	4.21	2.85	5.76
25 LEVEL	750	---	534	992	136	106440	5.52	3.94	7.31
26 E4	577	0.0989	354	837	126	4544	4.58	2.81	6.64
26 E7A	452	0.0649	286	643	122	13865	3.70	2.35	5.27
26 E7B	466	0.0899	317	1370	147	12120	6.57	4.19	9.32
26 E9	356	0.0573	245	481	121	8044	2.94	2.02	3.98
26 LEVEL	588	---	376	831	129	39002	4.55	2.91	6.44

TABLE 5.2: MODOURINE BLOCK ESTIMATES, ALL DEVELOPMENT DATA OPTIMISED TO 150cm.
 (Beta Constant used = +45 cmg/t.)

BLOCK	MEAN CMG/T	LOG. VARIANCE	LOWER 90% LIMIT (CMG/T)	UPPER 90% LIMIT (CMG/T)	AVERAGE S.M. (%)	TONS	GRADE (g/t)		
							MEAN	L.L. (90%)	U.L. (90%)
25 W1	361	0.0595	243	494	151	27286	2.39	1.61	3.27
25 E2	750	0.0631	513	1018	156	27772	4.81	3.29	6.52
25 E7A	1143	0.0321	804	1426	164	20291	6.97	5.39	8.69
25 E7B	965	0.0355	734	1218	159	11104	6.07	4.62	7.66
25 E9A	1428	0.0488	1038	1863	170	16127	8.40	6.11	10.96
25 E9B	339	0.0470	239	450	154	12629	2.20	1.55	2.92
25 E10	557	0.0591	383	753	151	8294	3.69	2.54	4.99
25 LEVEL	767	---	555	1004	158	123502	4.87	3.52	6.37
26 E6	593	0.0897	371	850	153	6040	3.80	2.42	5.56
26 E7A	491	0.0754	310	689	152	12275	3.23	2.09	4.53
26 E7B	1014	0.0821	659	1422	165	13604	6.15	3.99	8.82
26 E9	377	0.0516	262	505	150	9971	2.51	1.75	3.37
26 LEVEL	622	---	406	670	155	46089	4.01	2.61	5.60

TABLE 5.3. WOODBINE BLOCK ESTIMATES, ALL DEVELOPMENT DATA OPTIMIZED TO 200ra.
 (Beta Constant used = +35 cpg/t.)

BLOCK	MEAN CNG/T	LOG. VARIANCE	LOWER 90% LIMIT (CNG/T)	UPPER 90% LIMIT (CNG/T)	AVERAGE S.W. 1cm	TONS	GRADE (g/t)		
							MEAN	L.L. (90%)	U.L. (90%)
25 W1	396	0.0538	271	536	200	36140	1.98	1.36	2.68
25 E2	777	0.0576	539	1045	200	35685	3.89	2.70	5.22
25 E7A	1169	0.0286	916	1444	201	24868	5.82	4.56	7.18
25 E7B	1000	0.0323	778	1252	201	14677	4.98	3.83	6.23
25 E9A	1450	0.0444	1075	1884	204	19353	7.15	5.27	9.23
25 E9B	368	0.0422	263	484	202	16566	1.82	1.30	2.40
25 E10	626	0.0541	437	838	200	10986	3.13	2.16	4.19
25 LEVEL	808	---	586	1037	201	157554	3.98	2.92	5.16
26 E6	625	0.0813	398	886	201	7935	3.11	1.98	4.41
26 E7A	525	0.0675	347	727	200	22730	2.63	1.73	3.64
26 E7B	1050	0.0747	760	1467	204	16819	5.19	3.43	7.19
26 F9	401	0.0469	282	533	200	13295	2.01	1.41	2.66
26 LEVEL	656	---	436	987	201	60779	3.26	2.17	4.51

TABLE 5.4: WOODSIDE BLOCK ESTIMATES, DEVELOPMENT DATA LESS "OUTLIERS" OPTIMISED TO 120cm.
 (Data Constant used = +45 cmg/t.)

BLOCK	MEAN	"p"	"q"	MEAN	LOG.	LOWER 90%	UPPER 90%	AVERAGE	TONS	GRADE (g/t)		
	CMG/T (vm)			CMG/T (v)	(VARIANCE)	LIMIT (CMG/T)	LIMIT (CMG/T)	S.W. (ca)		MEAN	L.L. (90%)	U.L. (90%)
25 H1	318	0.0359	0.0000	307	0.0477	214	409	123	22226	2.49	1.74	3.33
25 E2	747	0.0203	0.0000	732	0.0505	525	965	134	33855	3.46	3.90	7.20
25 E7A	1016	0.0000	0.0000	1016	0.0246	812	1236	149	18455	6.82	5.45	8.30
25 E7B	862	0.0000	0.0000	862	0.0286	675	1066	140	9777	6.17	4.82	7.61
25 E9A	1256	0.0332	0.0126	1493	0.0372	1134	1890	157	14694	9.51	7.22	12.03
25 E9B	313	0.0859	0.0000	286	0.0306	208	372	129	10497	2.24	1.63	2.91
25 E10	474	0.0000	0.0000	474	0.0459	339	624	123	6756	3.85	2.76	5.07
25 LEVEL	---	---	---	718	---	539	915	136	106440	5.29	3.97	6.74
26 E6	525	0.0000	0.0000	525	0.0701	347	720	126	4874	4.17	2.75	5.78
26 E7A	497	0.0973	0.0000	449	0.0571	308	607	122	13065	3.60	2.53	4.97
26 E7B	852	0.0461	0.0159	1176	0.0619	812	1576	147	12120	7.96	5.52	10.72
26 E9	357	0.0000	0.0000	357	0.0413	258	466	121	8844	2.95	2.14	3.85
26 LEVEL	---	---	---	856	---	440	886	129	39002	4.92	3.41	6.63

where: $V = (i-p-q).vm + p.vl + q.vh$

vl = 1 cmg/t

vh = 23375 cmg/t at 120cm Optimisation.

TABLE 1. ESTIMATES, DEVELOPMENT DATA LESS "OUTLIER" OPTIMISED TO 150cm.
 Used = +20 cmg/t.

PROD.	MEAN CMG/T (v)	"p"	"q"	MEAN CMG/T (v)	COV. VARIANCE	LOWER 90% LIMIT (CMG/T)	UPPER 90% LIMIT (CMG/T)	AVERAGE S.W. (cm)	TONS	GRADE (g/t)		
										MEAN	L.L. (90%)	U.L. (90%)
26 M	337	0.0359	0.0000	344	0.0394	247	451	151	27286	2.28	1.64	2.99
26 EL	772	0.0283	0.0000	756	0.0438	351	984	156	27772	4.85	3.53	6.31
26 E7A	1077	0.0000	0.0000	1027	0.0222	828	1241	164	20291	6.26	5.65	7.57
26 E7B	878	0.0000	0.0000	876	0.0240	695	1071	159	11184	5.51	4.37	6.74
26 E9A	267	0.0332	0.0128	1534	0.0308	1170	1868	170	16127	8.85	6.88	10.99
26 E9B	322	0.0559	0.0000	294	0.0326	217	380	154	12629	1.91	1.41	2.46
26 E1F	496	0.0000	0.0000	496	0.0411	360	646	151	8294	3.28	2.38	4.28
26 LEVEL	---	---	---	739	---	544	930	158	123582	4.69	3.58	6.90
26 E6	39	0.0000	0.0000	553	0.0601	376	757	153	6040	3.63	2.46	4.95
26 E7A	537	0.0973	0.0000	485	0.0481	342	645	152	17275	3.19	2.25	4.24
26 E7B	882	0.0464	0.0159	1199	0.0534	691	1508	165	13684	7.26	5.16	9.62
26 E9	360	0.0000	0.0000	360	0.0346	265	454	150	9971	2.40	1.77	3.09
26 LEVEL	---	---	---	661	---	468	877	153	46889	4.26	3.02	5.65

where: $V = (1-p-q) \cdot v_m + p \cdot v_l + q \cdot v_h$

$v_l = 1 \text{ cmg/t}$

$v_h = 23379 \text{ cmg/t at 150cm Optimisation.}$

TABLE 3.6: WOODBINE BLOCK ESTIMATES, DEVELOPMENT DATA LESS "OUTLIERS" OPTIMISED TO 200cm.
(Beta Constant used = +75 cmg/t.)

BLOCK	MEAN CHG/T (va)	"p"	"q"	MEAN CHG/T (v)	LOG. VARIANCE	LOWER 90% LIMIT (CHG/T)	UPPER 90% LIMIT (CHG/T)	AVERAGE S.W. (cm)	TONS	GRADE (g/t)		
										MEAN	L.L. (90%)	U.L. (90%)
25 W1	393	0.0359	0.0000	379	0.0366	275	494	200	36140	1.89	1.37	2.47
25 E2	883	0.0203	0.0000	787	0.0390	579	1016	290	35605	3.93	2.90	5.00
25 E7A	1056	0.0000	0.0000	1056	0.0197	861	1266	201	24868	5.25	4.20	6.30
25 E7B	922	0.0000	0.0000	922	0.0197	750	1107	201	14837	4.59	3.73	5.51
25 E9A	1302	0.0332	0.0126	1538	0.0285	1205	1899	204	19353	7.54	5.91	9.31
25 E9B	342	0.0059	0.0000	313	0.0300	231	402	202	16566	1.55	1.14	1.99
25 E10	554	0.0000	0.0000	554	0.0379	406	717	500	10984	2.77	2.03	3.59
25 LEVEL	---	---	---	772	---	596	965	201	157554	3.84	2.96	4.80
26 E4	590	0.0000	0.0000	590	0.0552	404	789	201	7935	2.94	2.01	3.98
26 E7A	872	0.0973	0.0000	516	0.0432	368	604	200	22730	2.58	1.84	3.40
26 E7B	908	0.0464	0.0159	1223	0.0489	879	1607	204	16619	6.00	4.31	7.88
26 E9	386	0.0000	0.0000	366	0.0320	286	496	200	13293	1.93	1.43	2.48
26 LEVEL	---	---	---	690	---	494	908	201	60779	3.43	2.46	4.51

where: $V = (1-p-q).va + p.vl + q.vh$

vl = 1 cmg/t

vh = 23403 cmg/t at 200cm Optimisation.

TABLE 5.7: HOOBINE BLOCK ESTIMATES, ALL DEVELOPMENT DATA TRANSFORMED AND OPTIMISED TO 100%.

BLOCK	NATURAL VALUES (MG/T)				S.W. (%)	AVERAGE TONS	GRADE (g/t)		
	MEAN	LOWER LIMIT	UPPER LIMIT	90%			MEAN	LL.90%	UL.90%
25 H1	273	---	---	---	128	22226	2.22	---	---
25 E2	357	---	---	---	134	23855	4.17	---	---
25 E7A	658	---	---	---	149	18435	4.26	---	---
25 E7B	397	---	---	---	140	9777	4.26	---	---
25 E9A	642	---	---	---	157	14854	4.12	---	---
25 E9B	266	---	---	---	129	10497	2.08	---	---
25 E10	339	---	---	---	123	6786	2.92	---	---
25 LEVEL	477	---	---	---	136	108440	3.81	---	---
26 E6	381	---	---	---	126	4974	3.02	---	---
26 E7A	381	---	---	---	122	13865	3.12	---	---
26 E7B	579	---	---	---	147	12128	3.94	---	---
26 E9	289	---	---	---	121	8344	3.39	---	---
26 LEVEL	415	---	---	---	129	35002	3.21	---	---

TABLE 5.61 WOODGING BLOCK ESTIMATES, ALL DEVELOPMENT DATA TRANSFORMED AND OPTIMISED TO 150cm.

BLOCK	NATURAL VALUES (CMS/T)				AVERAGE S.M. (CM)	TONS	GRADE (g/t)		
	MEAN	LOWER LIMIT	UPPER LIMIT	90% LIMIT			MEAN	LL. 90%	UL. 90%
25 W1	583	---	---	---	151	27286	2.01	---	---
25 W2	525	---	---	---	156	27722	3.8	---	---
25 W3	679	---	---	---	169	28291	4.1	---	---
25 W4	635	---	---	---	159	11164	3.99	---	---
25 W5A	579	---	---	---	170	16127	3.99	---	---
25 W5B	386	---	---	---	154	12629	1.85	---	---
25 W5C	391	---	---	---	151	8294	2.59	---	---
25 LEVEL	508	---	---	---	188	123502	3.23	---	---
26 E6	412	---	---	---	153	6840	2.69	---	---
26 E7A	412	---	---	---	152	17375	2.71	---	---
26 E7B	634	---	---	---	163	13664	3.89	---	---
26 E9	321	---	---	---	150	9971	2.14	---	---
26 LEVEL	453	---	---	---	155	46869	2.92	---	---

TABLE 5.9: MACHINE FLOCC ESTIMATES, ALL DEVELOPMENT DATA TRANSFORMED AND OPTIMISED TO 200cm.

BLOCK	NATURAL VALUES (LMS/T)				AVERAGE S.M. 1200	TONS	GRADE (g/l)		
	SEAN	LOWER LIMIT	UPPER LIMIT	90%			SEAN	LL.500	CL.500
25 M1	358	---	---	---	200	36190	1.49	---	---
25 E2	634	---	---	---	200	35505	3.17	---	---
25 E7A	725	---	---	---	201	24868	3.41	---	---
25 E7B	675	---	---	---	201	14037	3.35	---	---
25 E9A	724	---	---	---	204	19353	3.55	---	---
25 E9B	309	---	---	---	202	16566	1.83	---	---
25 E10	435	---	---	---	200	10986	2.18	---	---
25 LEVEL	547	---	---	---	201	137554	2.72	---	---
26 E6	445	---	---	---	201	7935	2.21	---	---
26 E7A	443	---	---	---	200	22739	2.72	---	---
26 E7B	681	---	---	---	204	16819	3.34	---	---
26 E9	351	---	---	---	200	13295	1.76	---	---
26 LEVEL	468	---	---	---	201	60779	2.43	---	---

TABLE 510

TABLE 10: COMPARISON BETWEEN BLOCK ESTIMATES AND ACTUAL VALUES.

BLOCK	ACTUAL VALUES		ESTIMATED VALUES (g/t)			TONE	DIFFERENCE (%)			DIFF. IN GRADE (g/t)		
	Grind	Mo(g/t)	Case (a)	Case (b)	Case (c)		(a)/(b)	(b)/(c)	(c)/(a)	(a)-(b)	(b)-(c)	(c)-(a)
25 WL	174	1.93	2.17	2.37	1.94	31405	12.6	7.5	-4.7	0.24	0.15	-0.09
25 E2	168	5.17	4.58	4.42	3.56	29356	-11.4	-10.6	-29.3	-0.59	-0.55	-1.52
25 E7A	204	5.19	5.74	5.19	3.57	25330	10.6	-0.1	-31.2	0.55	-0.30	-1.62
25 E7B	186	5.34	5.33	4.07	3.56	15926	1.7	-6.7	-32.0	0.09	-0.35	-1.68
25 E9A	184	4.52	7.82	8.24	3.79	17484	62.2	71.0	-21.4	3.06	3.42	-1.03
25 E9B	141	3.23	2.35	2.08	1.98	11555	-27.2	-36.3	-29.4	-0.88	-1.17	-1.27
25 E10	181	3.08	3.31	2.94	2.31	9431	7.5	-4.6	-25.0	0.23	-0.14	-0.77
25 LEVEL	174	4.08	4.45	4.19	2.00	137697	8.9	5.1	-26.7	0.36	0.21	-1.09
26 E6	167	4.32	2.61	3.38	2.52	6592	-10.2	-15.8	-37.2	-0.41	-0.65	-1.49
26 E7A	186	3.18	2.75	2.71	2.32	21321	-13.5	-14.9	-27.1	-0.43	-0.97	-0.86
26 E7B	229	4.86	4.89	5.66	3.18	18146	0.6	15.2	-34.5	0.03	0.74	-1.68
26 E9	164	2.32	2.34	2.24	2.01	10429	5.2	0.7	-9.7	0.12	0.02	-0.22
26 LEVEL	189	3.63	3.45	3.62	2.56	56988	-4.9	-0.3	-39.5	-0.18	-0.01	-1.07
TOTALS	179	3.95	4.12	4.09	2.67	194888	5.2	3.6	-27.4	0.20	0.14	-1.08

CHAPTER 6**THE BLOCK FACTOR CALCULATIONS IN "WIDE REEFS":****6.1 Introduction:**

A problem encountered in Chapter 5.4, that of comparing "actual" values and block estimates when the cmg/t value is dependent upon stope width, also has ramifications for Block Factor calculations. The term "wide reef" is used to denote a geological horizon of economic interest, where the mineralisation occurs over a width that is greater than the expected mining or stoping width, such as the Woodbine deposit. Therefore, the mineral content that can be expected from any given area, or ore reserve block, will be dependent upon the width at which the block was actually mined.

6.2 The Block Factor:

The block factor is one of the basic tools in gauging the accuracy of any Ore Reserve estimate and has been for many years. The term "block factor" needs to be defined clearly before continuing further. A block factor, as defined by the Institute of Mine Surveyors, is "the ratio, expressed as a percentage, which the specific mineral content of the ore broken from ore reserve blocks as indicated by the current sampling results bears to the content of this ore computed from block estimates." This may be also be expressed as:

$$BF = \frac{\text{Mineral content of ore broken, based on current sampling}}{\text{Mineral content of ore broken, based on block estimates}} * 100\%$$

In the precious metal mines the cmg/t value is a measure of the mineral content of ore per unit area. Thus, as a generalised case, the block factor may also be expressed as:

$$BF = \frac{\text{Av sampling cmg/t value of ore broken from blocks}}{\text{Av cmg/t value of that ore, based to block estimates}} * 100\%$$

The block factor may refer to a single ore reserve block, to a mine section, a reef horizon or to the mine as a whole. It is an expression of the relationship between the specific mineral content indicated by current sampling, against the estimated content as indicated by the block estimates. *It is important to note*, that from the above definition, it is clear that the "block factor" is measured in content per unit area and is *not* a comparison between the current sampling grade (g/t) and the block grade (g/t), as shown below:

$$BF = \frac{\text{Av sampling g/t value of ore broken from blocks at SW}}{\text{Av g/t value of that ore, based to block estimates at BW}} * 100\%$$

The reason for this is self evident, the block width and the current stoping width may not

necessarily be the same. For example, the same cmg/t value for both current sampling and block estimate (in other words, a Block Factor of 100%) would yield two different grades (g/t) if the stope width did not equal the block width.

6.3 The Block Factor and Wide Reefs:

Problems can arise in determining the block factor for a reef that has a width wider than the expected stope width, as can happen in the Archaean gold deposits or where an optimum cut is taken through a conglomerate package. Traditionally, each ore reserve block is delineated to fix the area of the block, then a *single block width* is determined to enable the block tons to be calculated. The block is then evaluated to determine a *single block value* (in either g/t or cmg/t), which is used to determine the block's total contents (grammes).

The use of a single block width is acceptable if one can assume that the full reef width is less than the anticipated stope width. Then the total specific mineral content of the broken ore as indicated by current sampling can be *directly* compared to the total contents of this ore as computed from block estimates. However if the full reef width is greater than the anticipated stope width, then the cmg/t value will vary depending on the block width chosen, thus the estimated "total specific mineral content" for the block will become a variable, dependent upon block width. *Therefore if the total contents of a block is not fixed, then the traditional Block Factor is not a valid means of gauging the accuracy of your block estimates.*

There are essentially two ways in which this problem can be dealt with; firstly to calculate the total specific mineral content of the broken ore as indicated by current sampling at the block width, irrespective of what the actual stope width was, so as to make the comparison valid. This has certain disadvantages in that the calculation has to be made separately from those necessary for the "flow of ore," that require actual stope widths for tonnage and content calculations. An alternative method is to generate a Grade-Stope Width model for each ore reserve block. Thus, for any given "actual" stope width, a block estimate or block value in μ/t for that stope width could be determined graphically or calculated, (using linear interpolation). This will allow for valid comparisons to be made between estimated block values (cmg/t) and "actual" values (cmg/t).

If one examines block 25 E2 in Tables 5.1, 5.2 and 5.3, a Case (a) evaluation would have yielded values of 737, 750 and 777 cmg/t at widths of 134, 156 and 200cm, respectively. A traditional evaluation would have given only one such value and width to the block. Therefore the results of any Block Factor calculations would be solely dependent upon the block width chosen by the Mine Evaluator when calculating the annual Ore Reserve. The "actual" value of 25 E2 was 853 cmg/t, which would have given a Block Factor ranging from 116% at 134cm to 110% at 200cm. A Block Factor calculation using the Grade-Stope Width model at the actual stope width of 165cm would have yielded a true Block Factor of 111%.

As the Block Factor is frequently used as a means of gauging the accuracy of the Ore Reserve, every effort should be made to ensure that the calculations are correct. Therefore,

In a wide reef, some form of Grade-Stop Width model is required when determining Block Factors.

CHAPTER 7

CONCLUSIONS:

The object of this project report was to examine how geostatistical methods can be applied to ore reserve evaluations in the Archaean gold deposits of the Barberton area. Essentially there were two main problems identified when trying to evaluate an Archaean gold deposit; namely:

- (a) The presence of extreme values (or "outliers") within the sampling data.
- (b) The ore body frequently has no clear geological contacts between which the occurrence of gold is limited.

In examining the first of these problems, there are a number of geostatistical evaluation methods that can be used to deal with extreme values (or "outliers") within the sampling data. Three such methods were examined in this project report; namely:

- Case (a): To leave the data sets intact and accept the extreme values as being part of the overall population and, thereby agreeing in principle, that the volatile semivariogram created is indicative of the nature of the ore body.
- Case (b): To use "Indicators," to isolate the effects of the extreme values, thus effectively treating them as a separate population, and yielding a more stable semivariogram for the remaining data.
- Case (c): To examine the comparatively new "Rank Related

Uniform Transform" procedure, as this approach is not influenced by "outliers" as such.

The second of the two problems encountered is that of estimating the total gold content (grammes) within a block of ore when the gold mineralisation occurs over a width that is greater than the expected mining width. The approach adopted was to optimise the sampling data to various likely mining widths, thereby creating a number of data sets, one for each optimised stope width.

The kriging of the optimised data allowed for the development of a Grade-Stop Width model for each "block", whereby the actual stope values could be compared to the block estimates generated by various geostatistical methods under consideration. This concept of a Grade-Stop Width model in a "wide reef" has important ramifications to Block Factor calculations.

From the comparisons made between the various geostatistical methods under consideration, one can determine that Cases (a) and (b) yielded some very useful results when determining "block" estimates. Case (b) yielded marginally better results when viewed on a level by level basis or as a whole. Statistically, the expected number of departures from the Grade-Stop Width model, "actual" values falling outside of the confidence limits, were realised. Thus, for these two Cases the method of evaluation and the concept of a Grade-Stop Width model seems appropriate. However, the method of evaluation used in Case (c) proved to be inadequate when dealing with the gold values of the Woodbine deposit.

APPENDIX A

Statistics on the 120cm Optimisation of the Woodbine Data

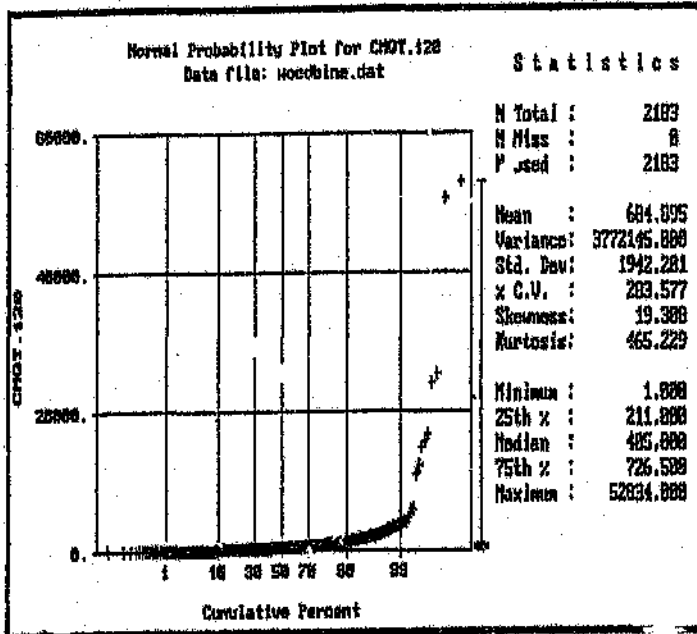


Figure A1: Probability Plot of the 120cm Optimisation, Cmg/t.

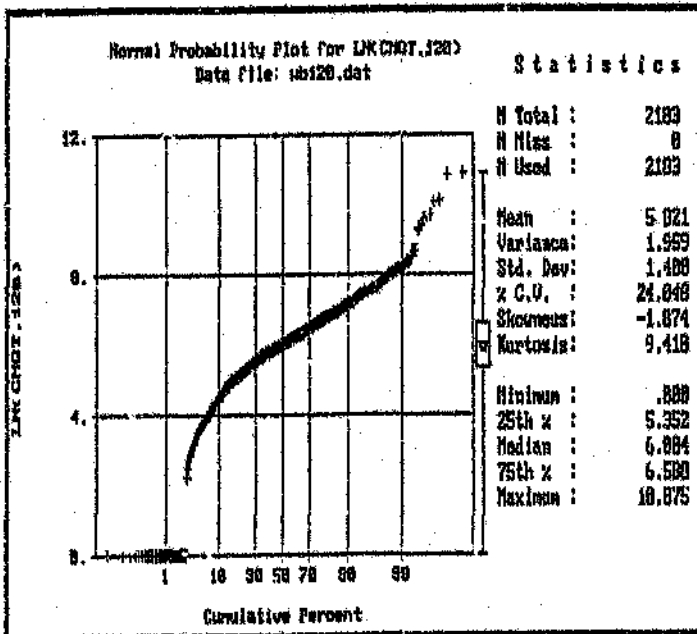


Figure A2: Probability Plot of the 120cm Optimisation, ln (cmg/t).

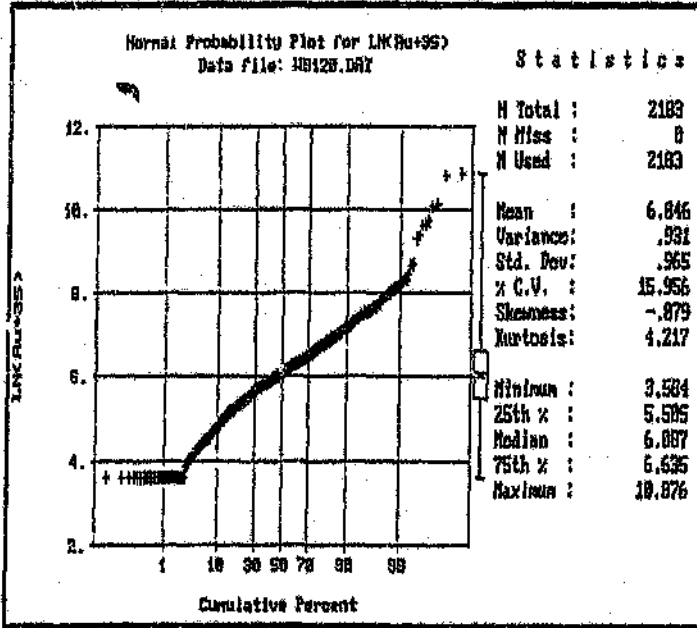


Figure A3: Probability Plot of the 120cm Optimisation, ln (cmg/t+35).

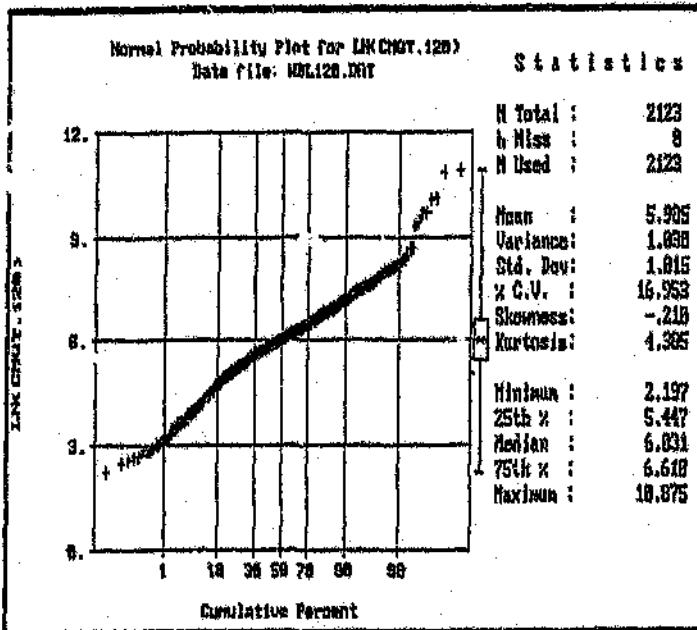


Figure A4: Probability Plot of the 120cm Optimisation, ln (cmg/t) less low Outliers.

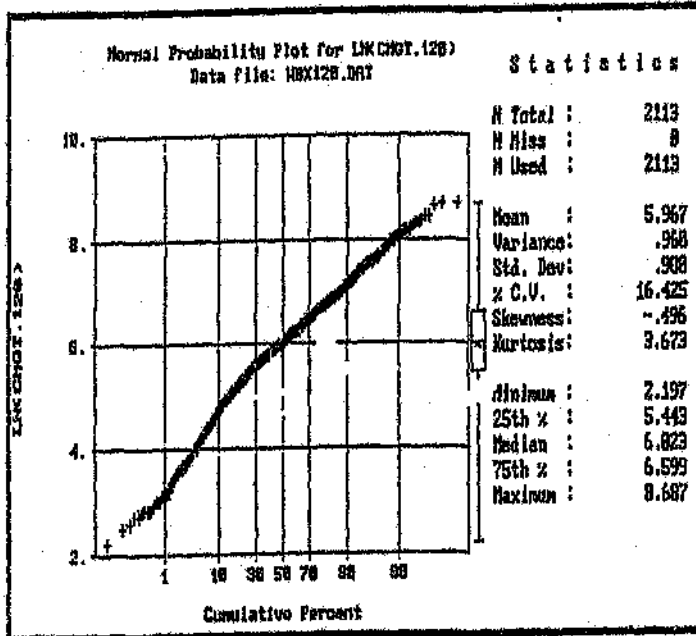


Figure A5: Probability Plot of the 120cm Optimisation, $\ln(\text{cmg/t})$ less all Outliers.

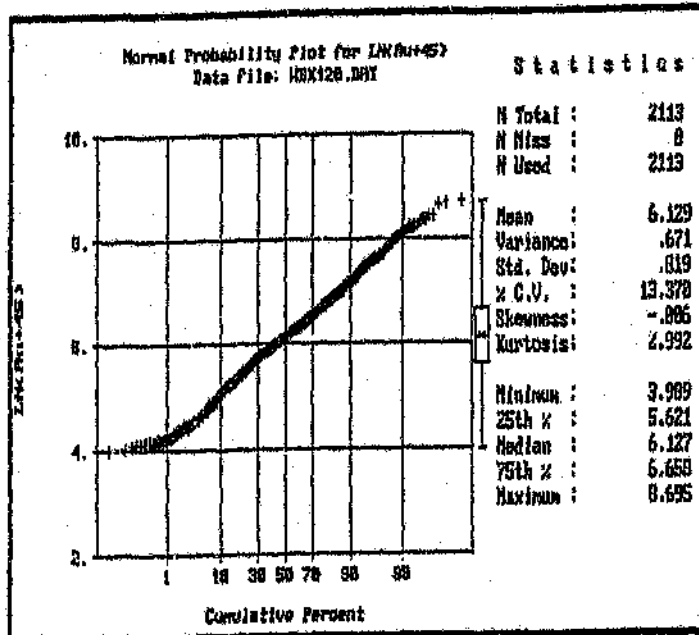


Figure A6: Probability Plot of the 120cm Optimisation, $\ln(\text{cmg/t} + 45)$ less all Outliers.

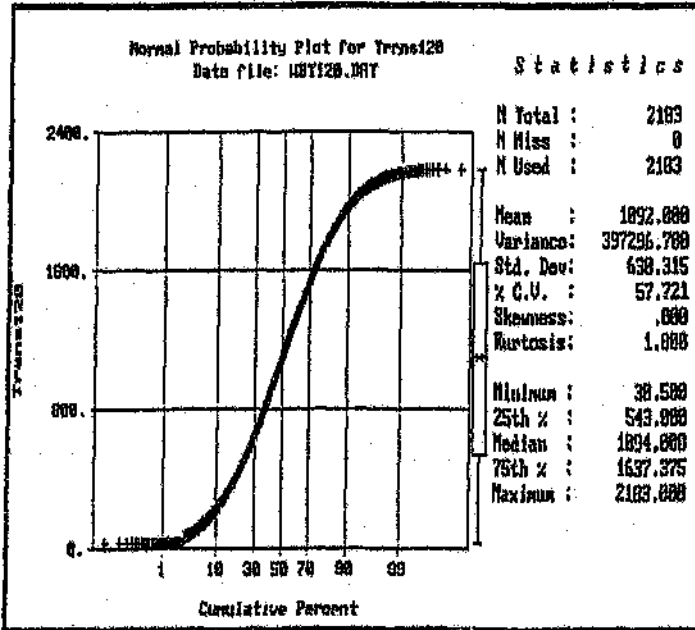


Figure A7: Probability Plot of the 120cm Optimisation, Transformed Values.

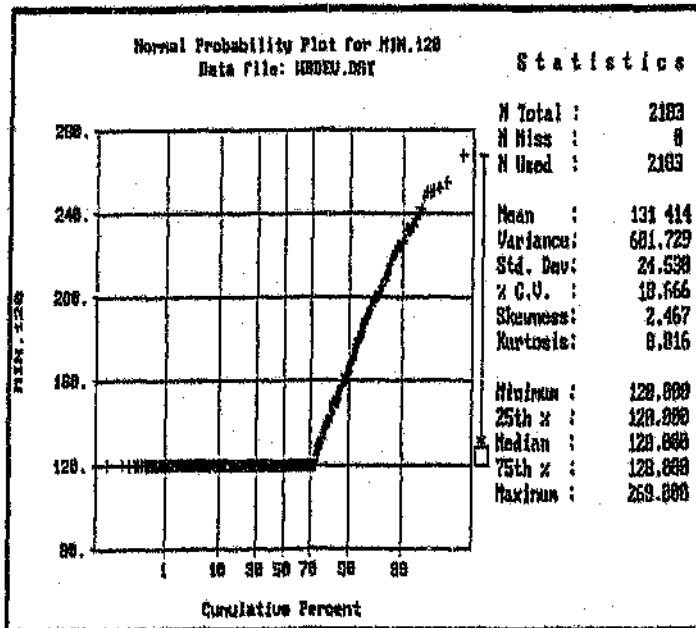


Figure A8: Probability Plot of the 120cm Optimised Slope Widths.

APPENDIX B

Statistics of the 150cm Optimisation of the Woodbine Data

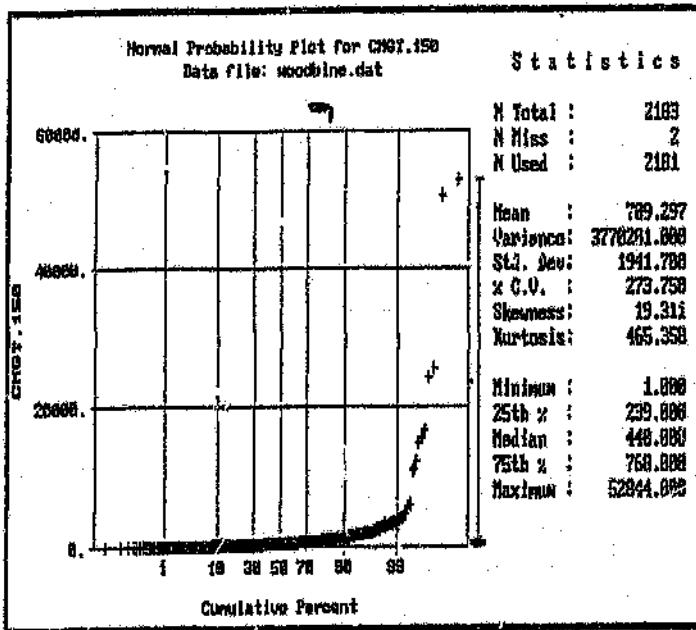


Figure B1: Probability Plot of the 150cm Optimisation, Cmg/t.

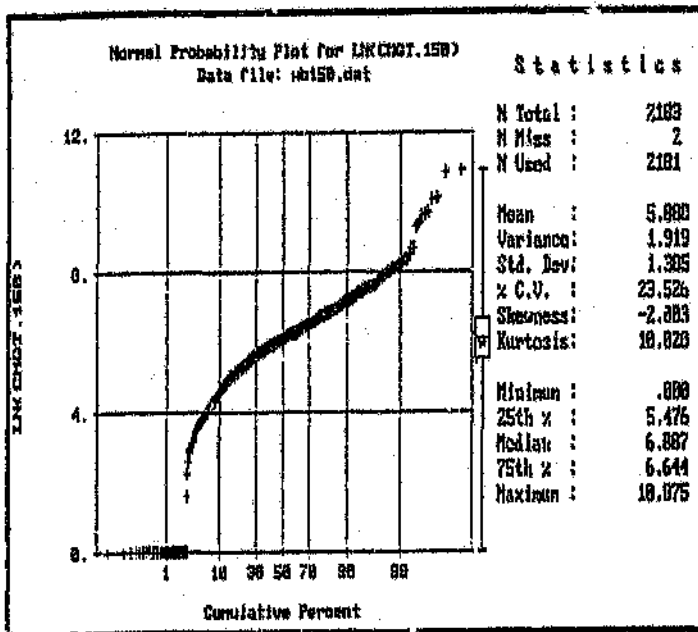


Figure B2: Probability Plot of the 150cm Optimisation, ln (cmg/t).

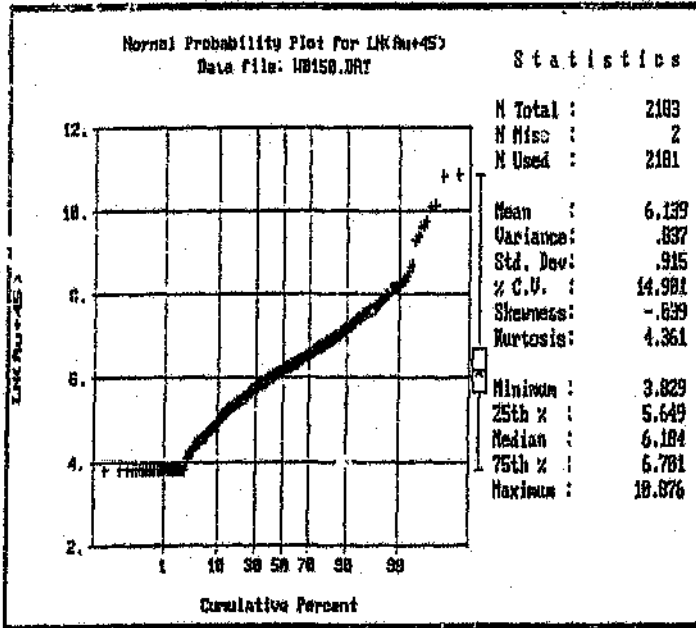


Figure B3: Probability Plot of the 150cm Optimisation, In (cmg/t+45).

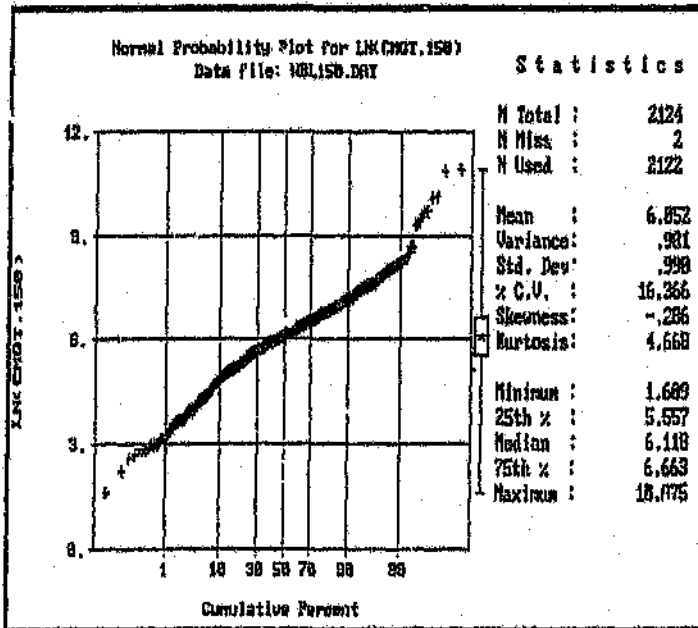


Figure B4: Probability Plot of the 150cm Optimisation, In (cmg/t) less low Outliers.

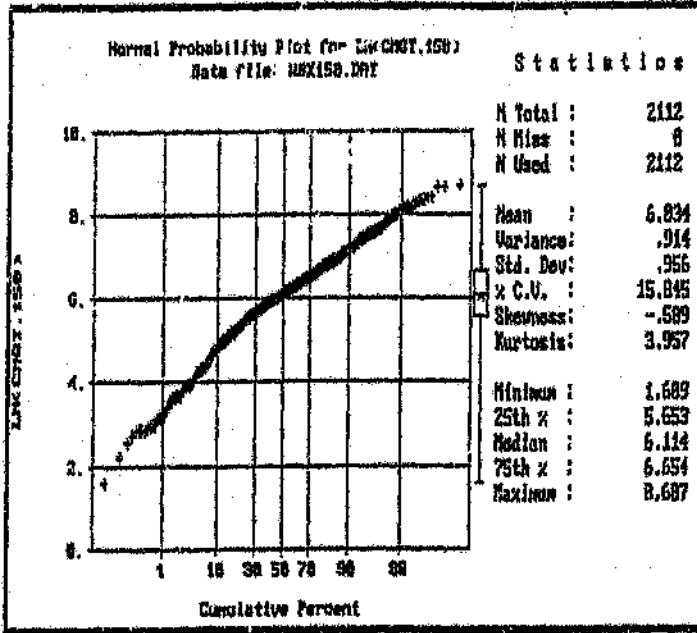


Figure B5: Probability Plot of the 150cm Optimization, In (cmg/t) less all outliers.

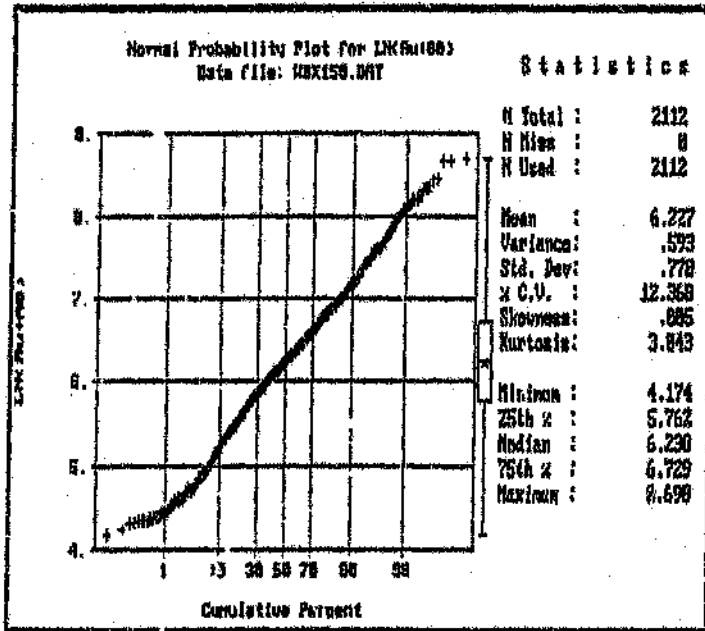


Figure B6: Probability Plot of the 150cm Optimization, In (cmg/t+60) less all Outliers.

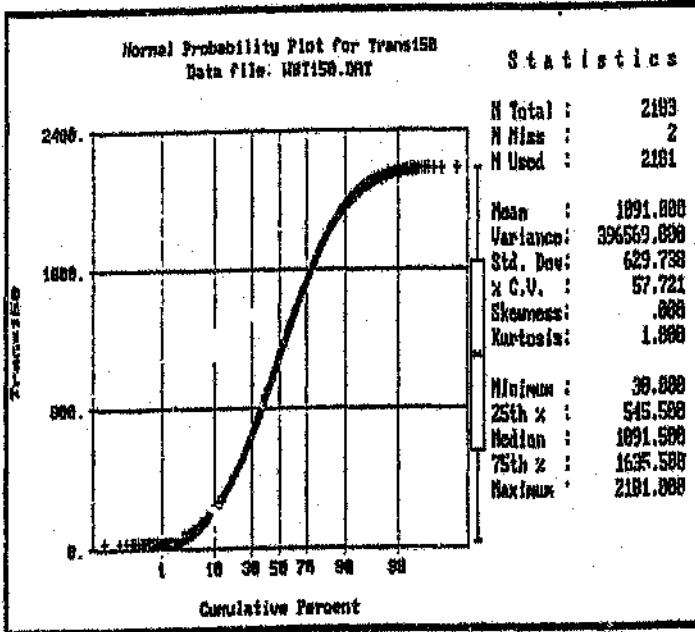


Figure B7: Probability Plot of the 150cm Optimisation, Transformed Values.

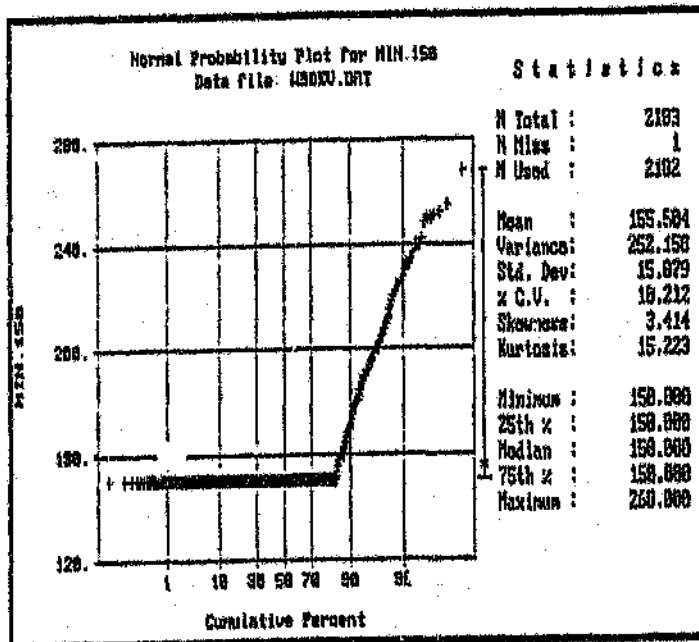


Figure B8: Probability Plot of the 150cm Optimised Stop Widths.

APPENDIX C

Statistics on the 200cm Optimisation of the Woodbine Data

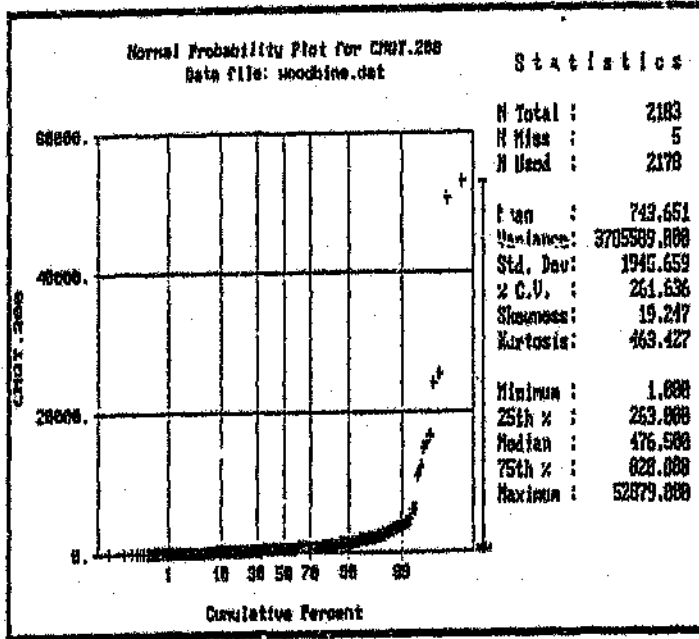


Figure C1: Probability Plot of the 200cm Optimisation, Cmg/t.

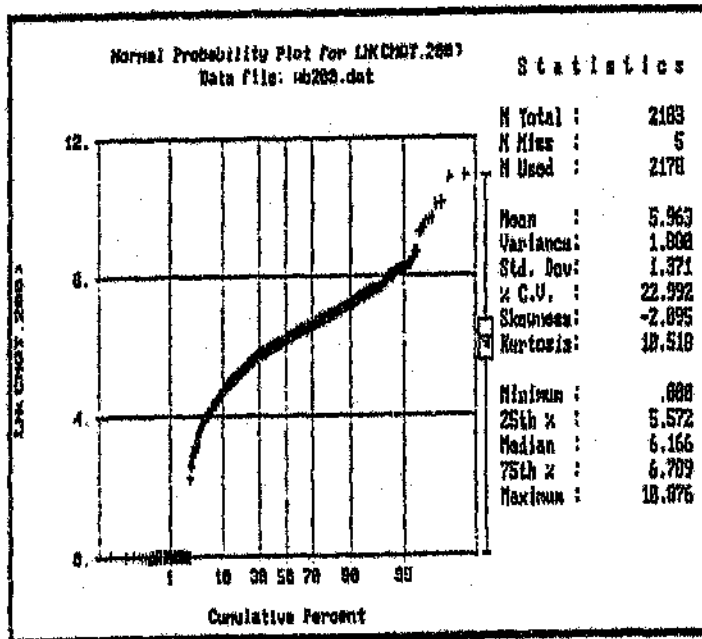


Figure C2: Probability Plot of the 200cm Optimisation, ln (cmg/t).

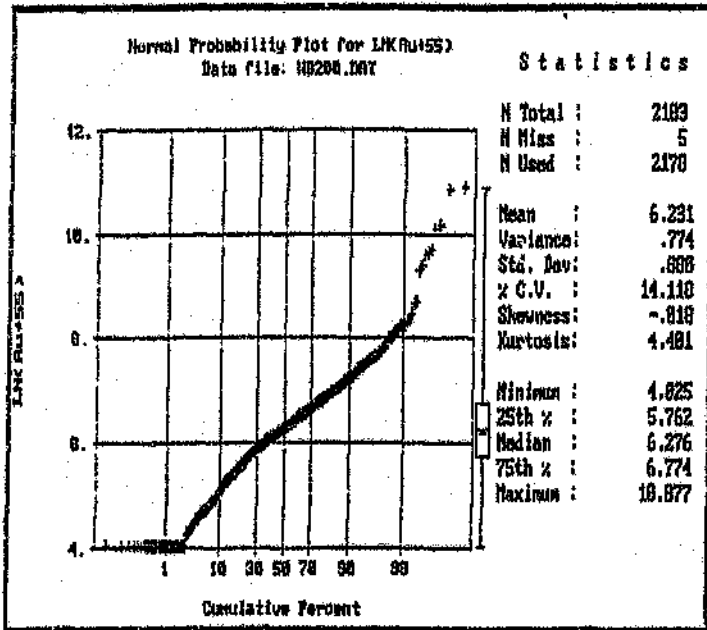


Figure C3: Probability Plot of the 200cm Optimisation, In (cmg/t+55).

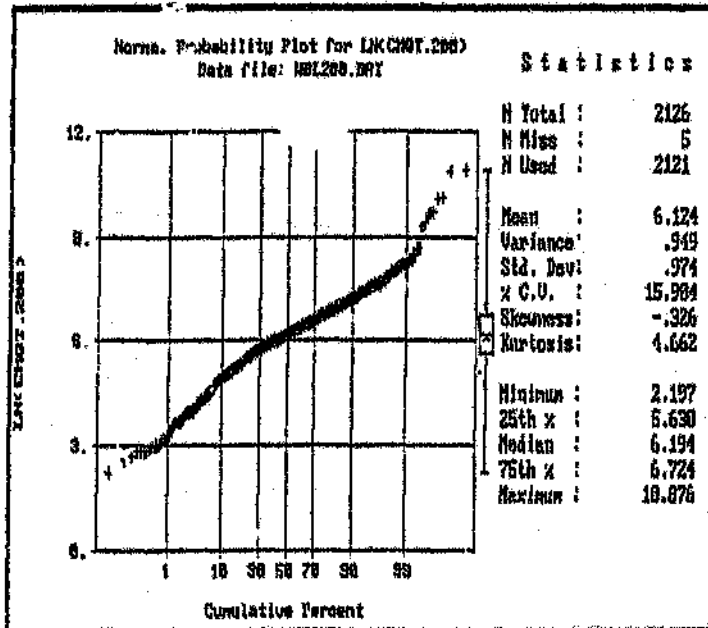


Figure C4: Probability Plot of the 200cm Optimisation, In (cmg/t) less low Outliers.

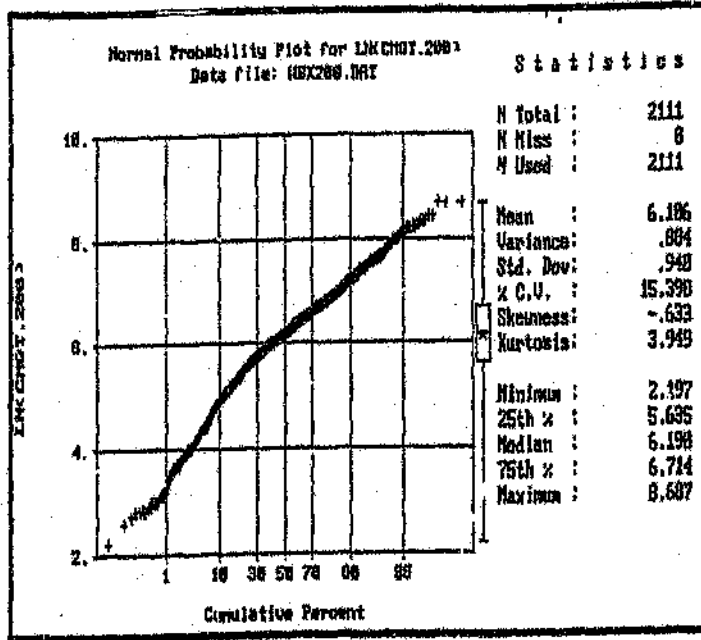


Figure C5: Probability Plot of the 200cm Optimisation, in (cmg/t) less all outliers.

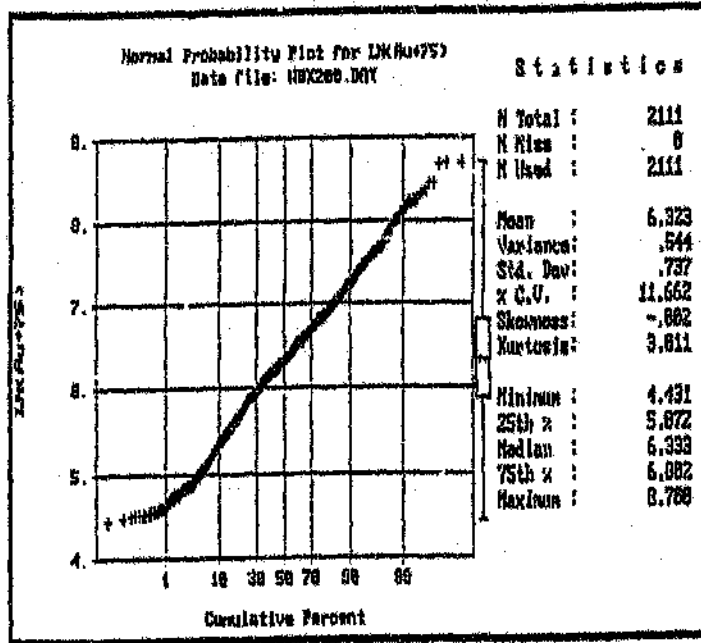


Figure C6: Probability Plot of the 200cm Optimisation, in (cmg/t+75) less all Outliers.

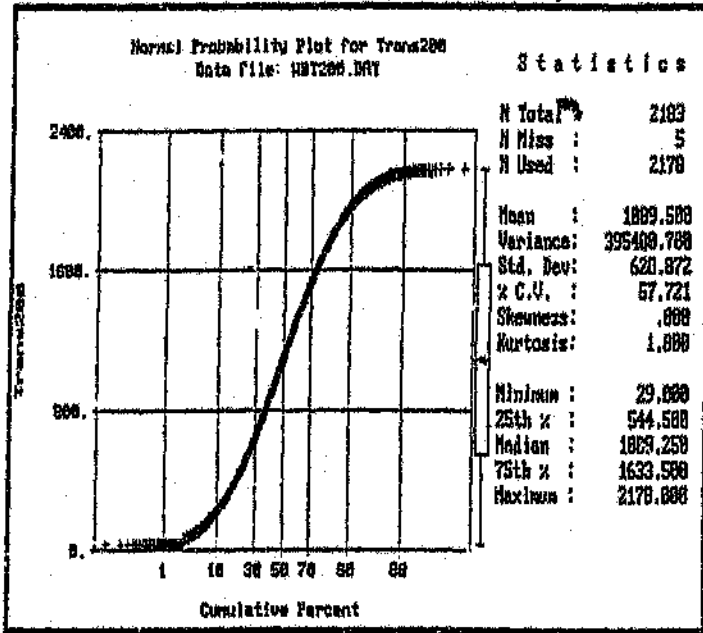


Figure C7: Probability Plot of the 200cm Optimisation, Transformed Values.

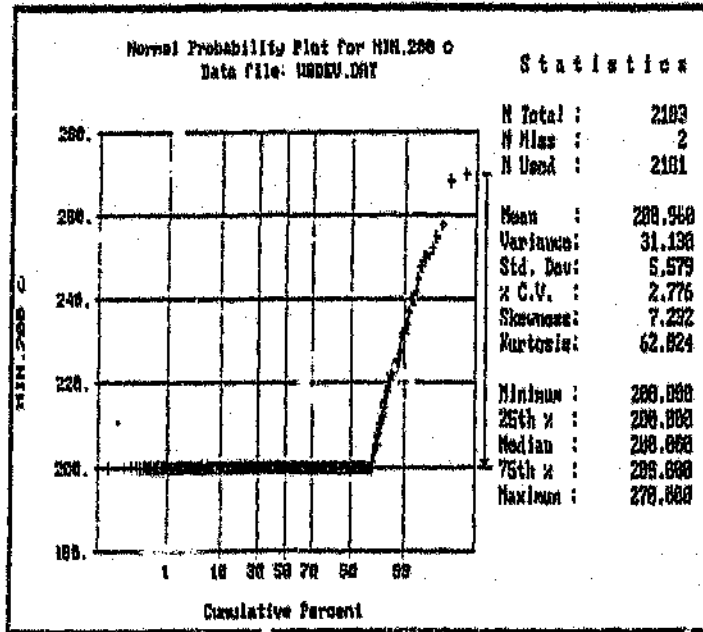


Figure C8: Probability Plot of the 200cm Optimized Slope Widths.

APPENDIX D

Statistics on the Woodbine Stope Data

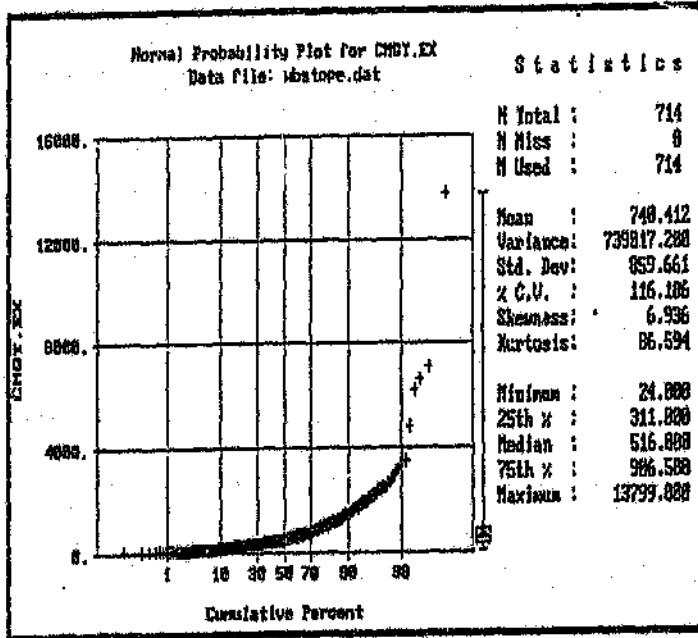


Figure D1: Probability Plot of the Slope Data, Cmg/t Values.

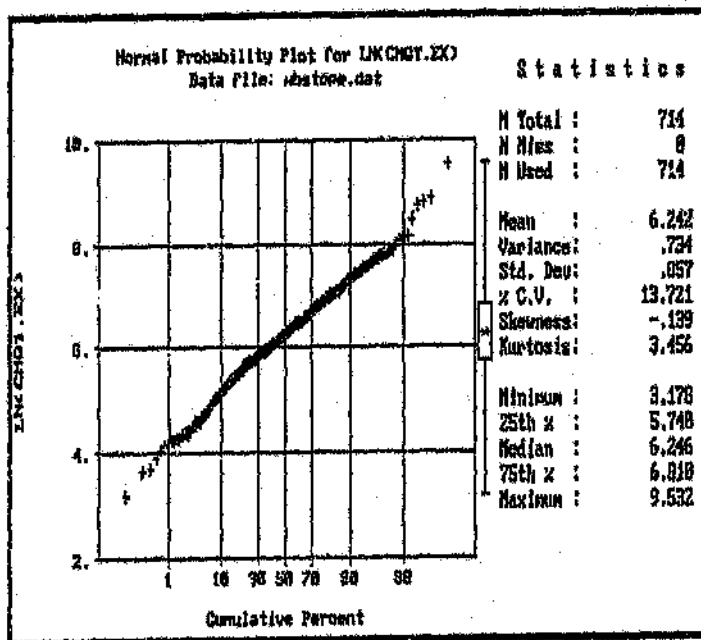


Figure D2: Probability Plot of the Slope Data, ln (cmg/t).

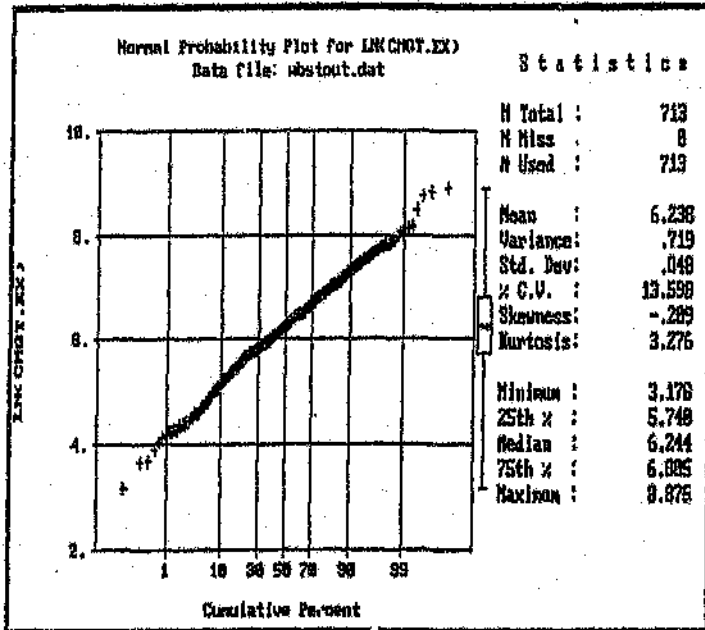
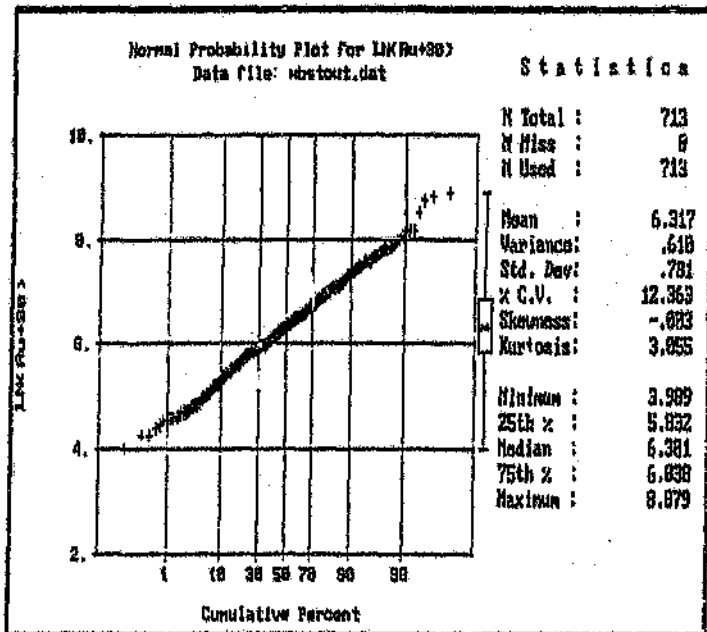


Figure D3: Probability Plot of the Stops Data, ln (cmg/t) less all Outliers.

Figure D4: Probability Plot of the Stops Data, ln (cmg/t + β) less all Outliers.

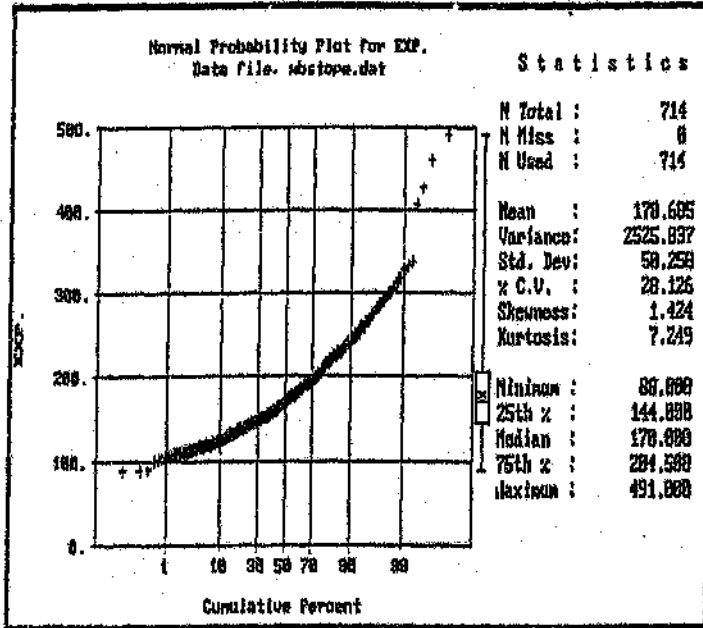


Figure D5: Probability Plot of the Slope Widths.

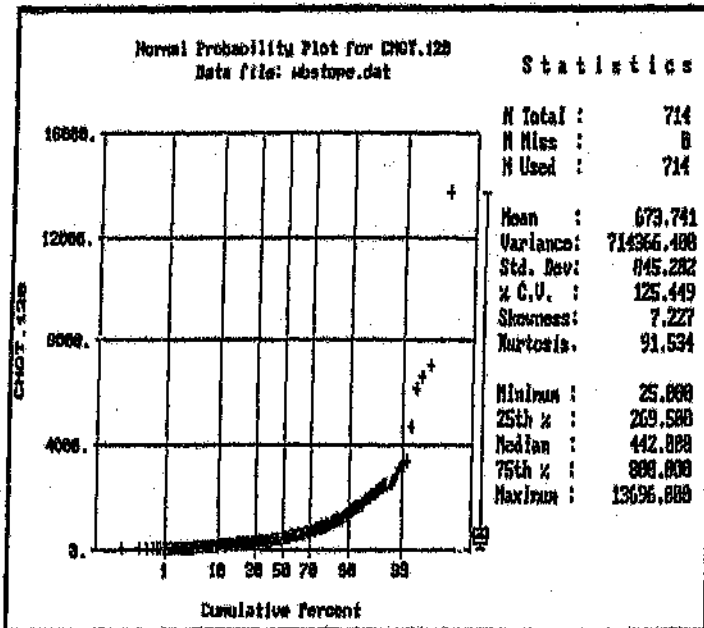


Figure D6: Probability Plot of the Slope Data Optimised to 120cm, Cmg/t Values.

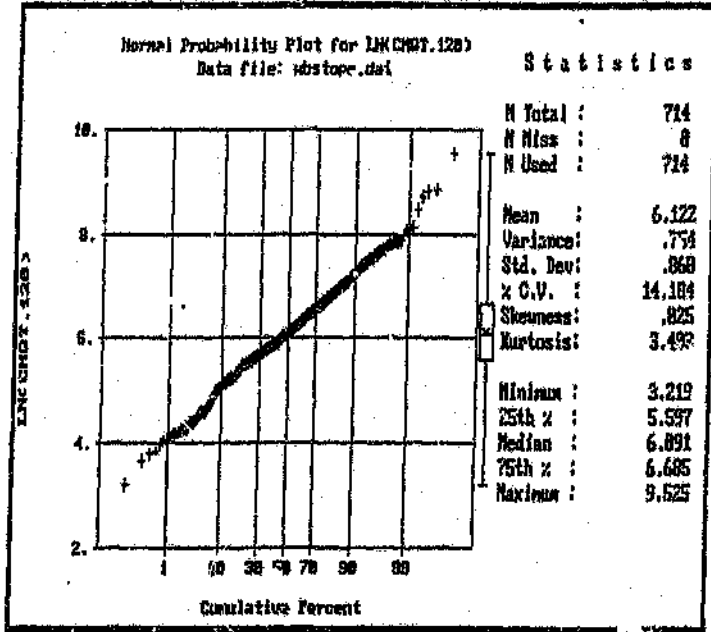


Figure D7: Probability Plot of the Stope Data Optimised to 120cm, In (cmg/t).

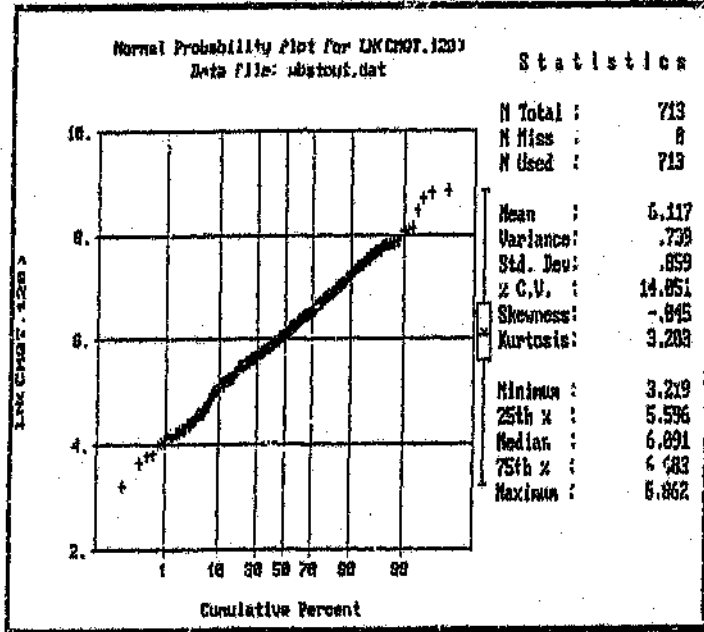


Figure D8: Probability Plot of the Stope Data Optimised to 120cm, In (cmg/t) less the Outlier.

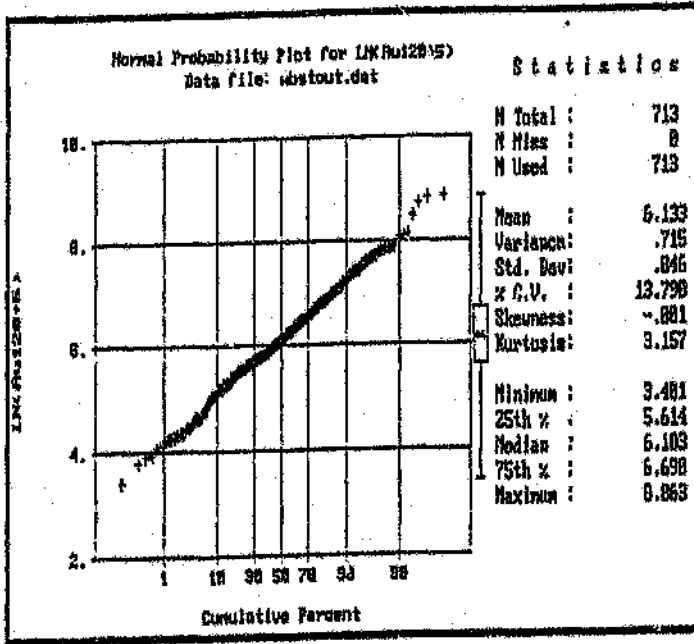


Figure D9: Probability Plot of the Stops Data Optimized to 120cm, in (mg/t+β) less the Outlier.

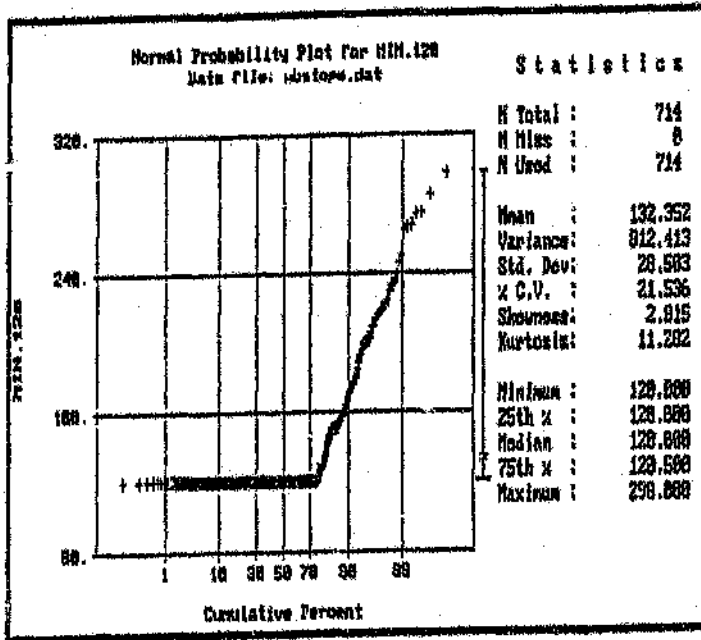


Figure D10: Probability Plot of the Stops Widths Optimized to 120cm.

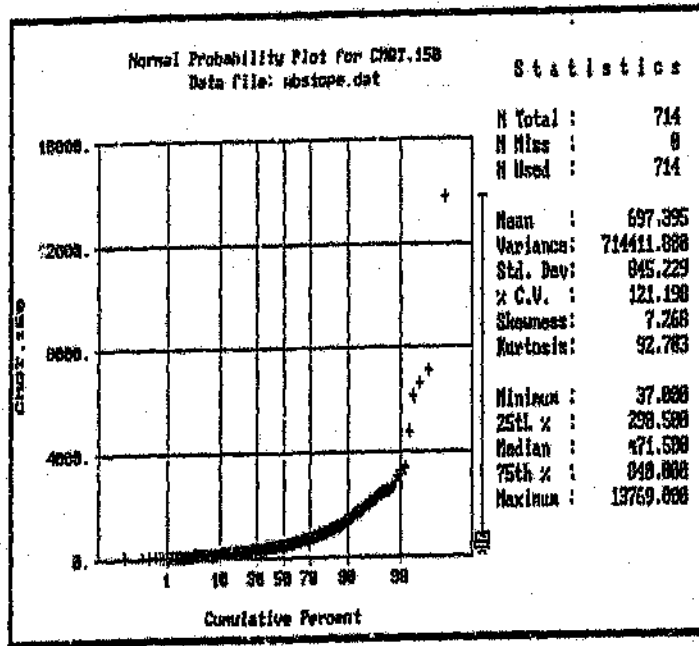


Figure D11: Probability Plot of the Stops Data Optimised to 150cm, Cmg/t Values.

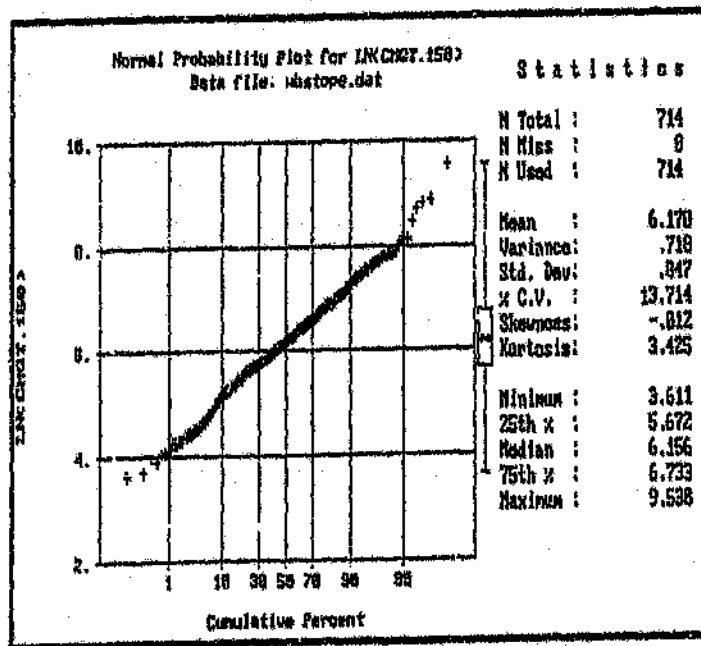


Figure D12: Probability Plot of the Stops Data Optimised to 150cm, Lk (cmg/t).

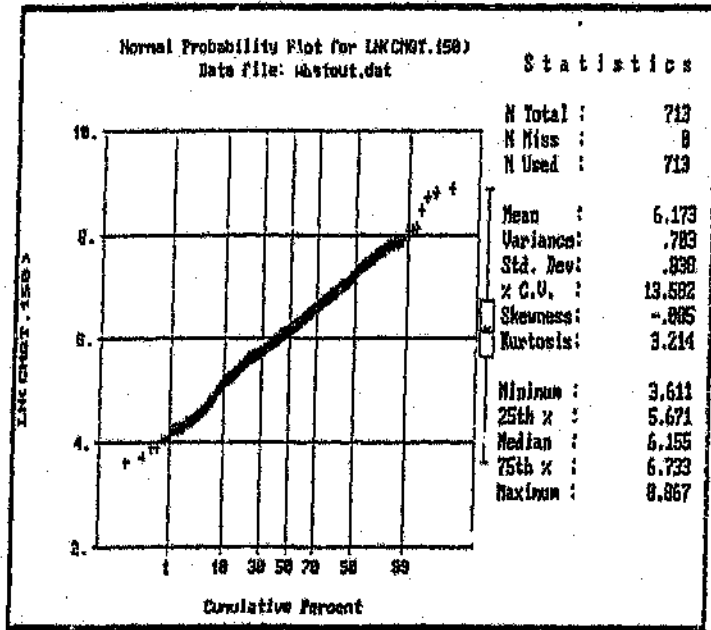


Figure D13: Probability Plot of the Slope Data Optimised to 150cm, ln (cmg/t) less the Outlier.

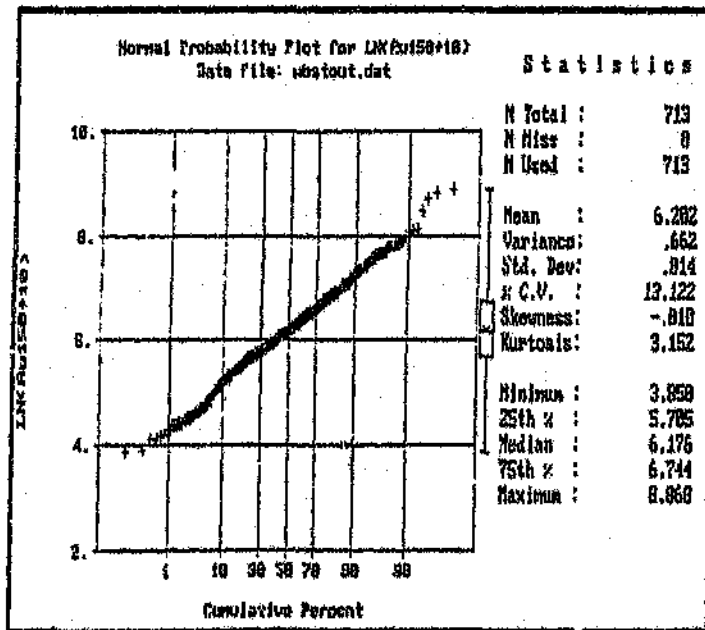


Figure D14: Probability Plot of the Slope Data Optimised to 150cm, ln (Cmg/t+β) less the Outlier.

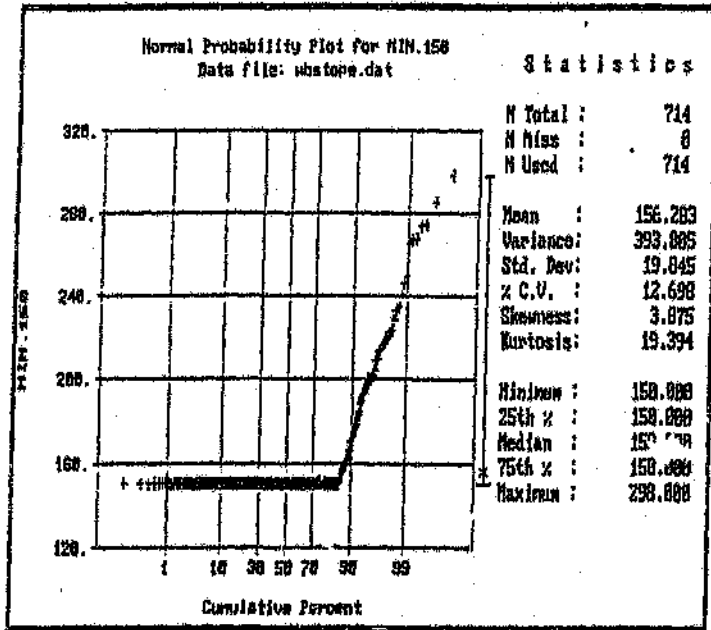


Figure D15: Probability Plot of the Slope Widths Optimised to 150cm.

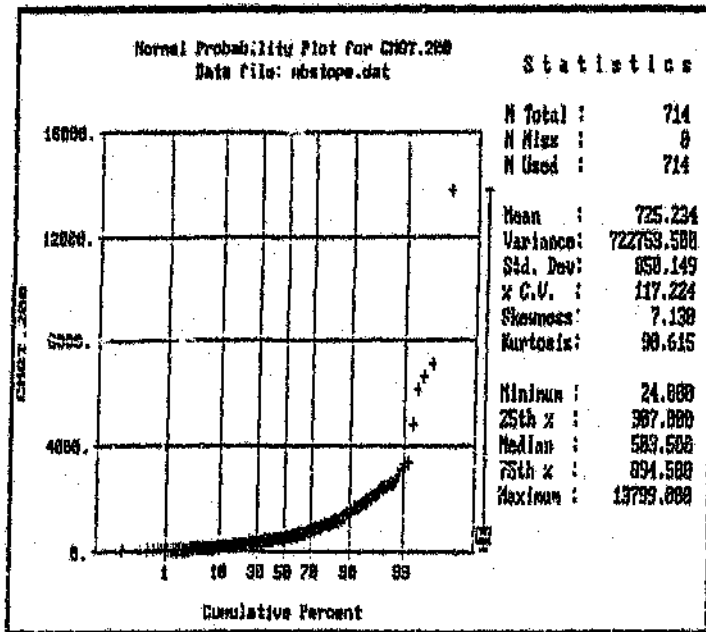


Figure D16: Probability Plot of the Slope Data Optimised to 200cm, Cmg/t Values.

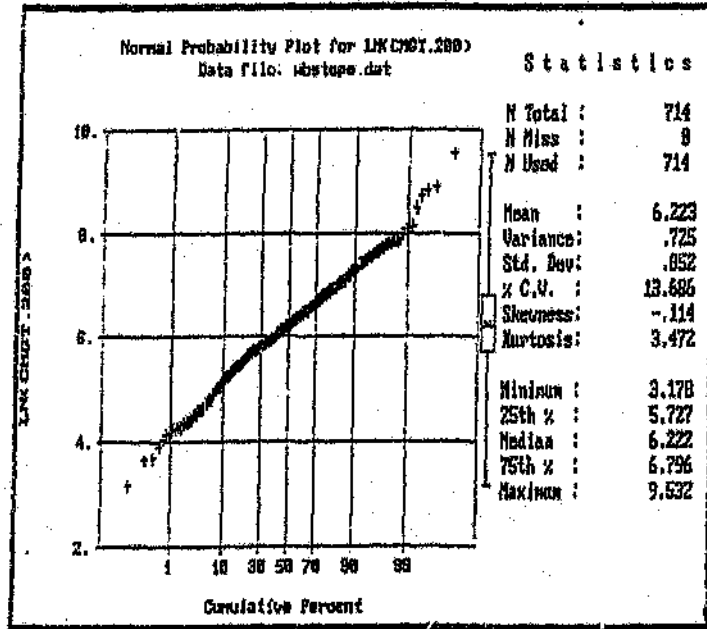


Figure D17: Probability Plot of the Stope Data Optimised to 200cm, ln (cmg/t).

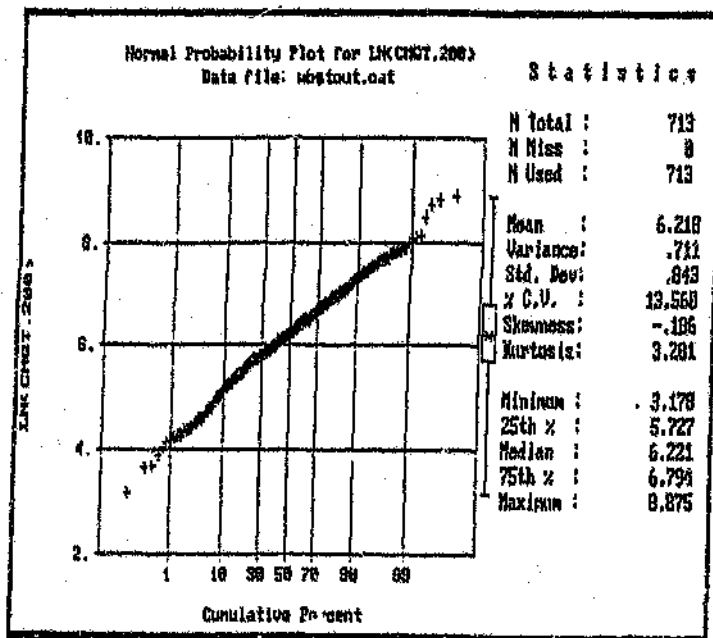


Figure D18: Probability Plot of the Stope Data Optimised to 200cm, ln (cmg/t) less the Outlier.

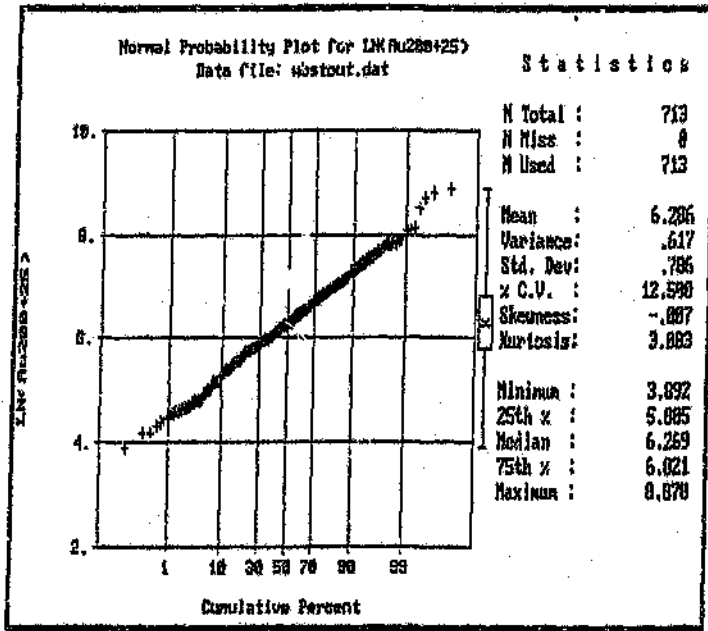


Figure D19: Probability Plot of the Slope Data Optimised to 200cm, In (mg/t+ β) less the Outlier.

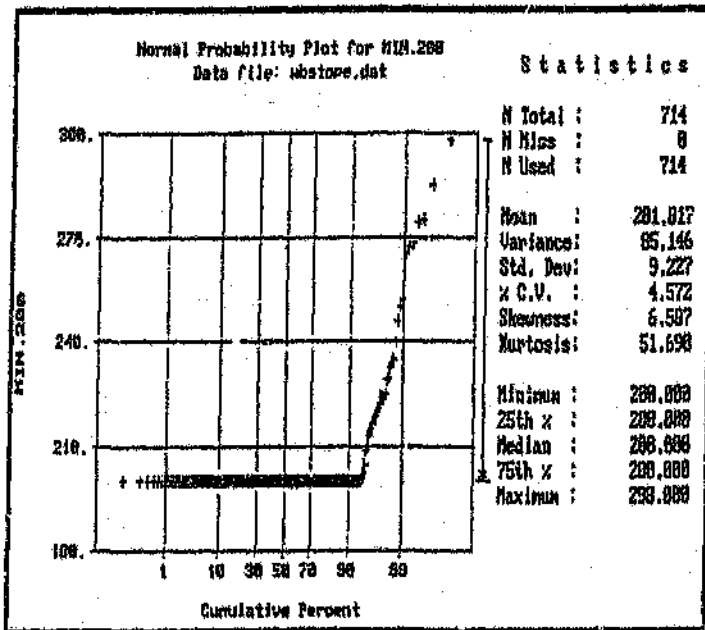


Figure D20: Probability Plot of the Slope Widths Optimised to 200cm.

APPENDIX E

Semivariogram Models Generated for the Evaluation

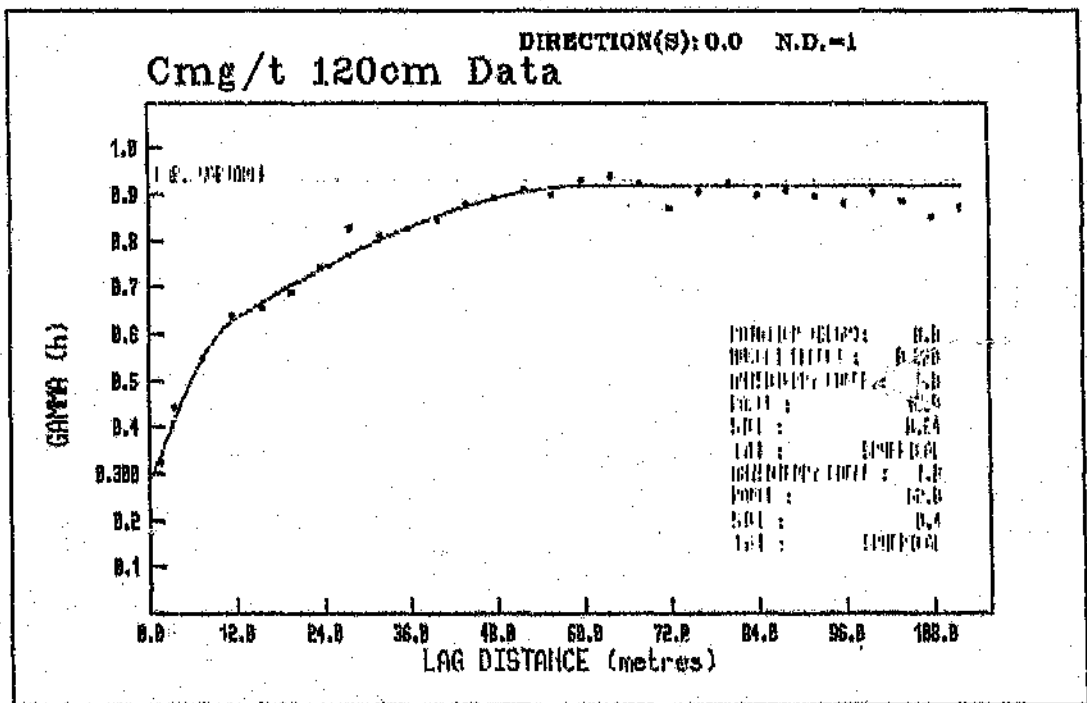


Figure H1: Semi-variogram for the $\ln(\text{cmg/t} + \beta)$ Values (120cm Optimisation), of all Development Data.

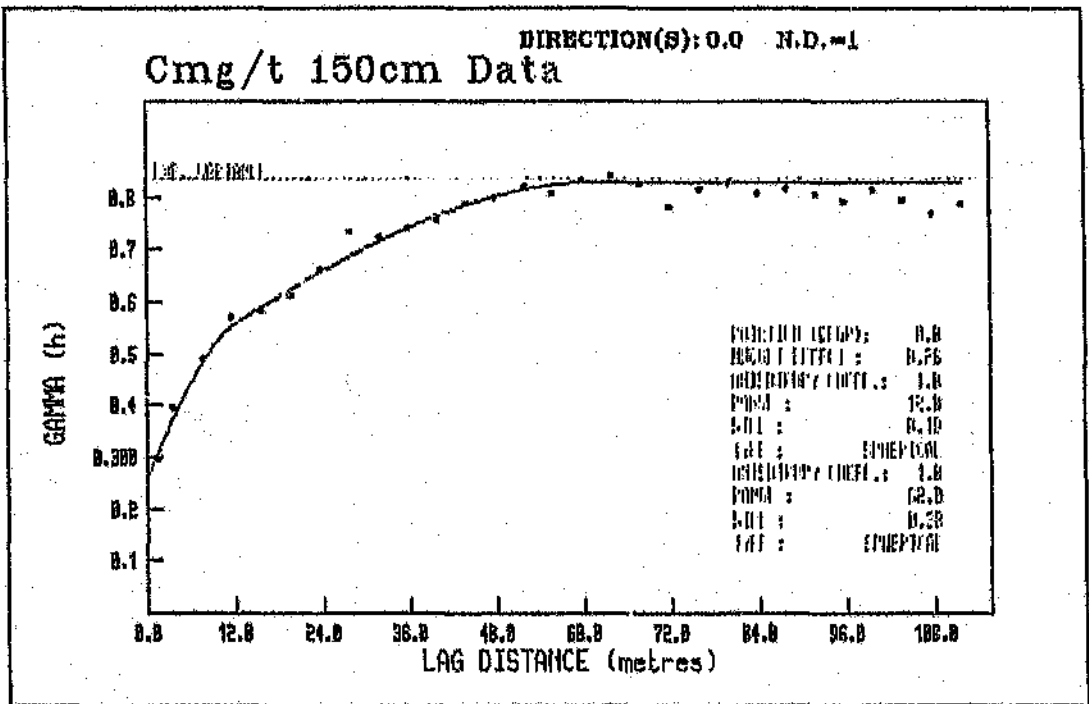


Figure E2: Semivariogram for the $\ln(\text{cmg/t} + \beta)$ Values (150cm Optimisation), of all Development Data.

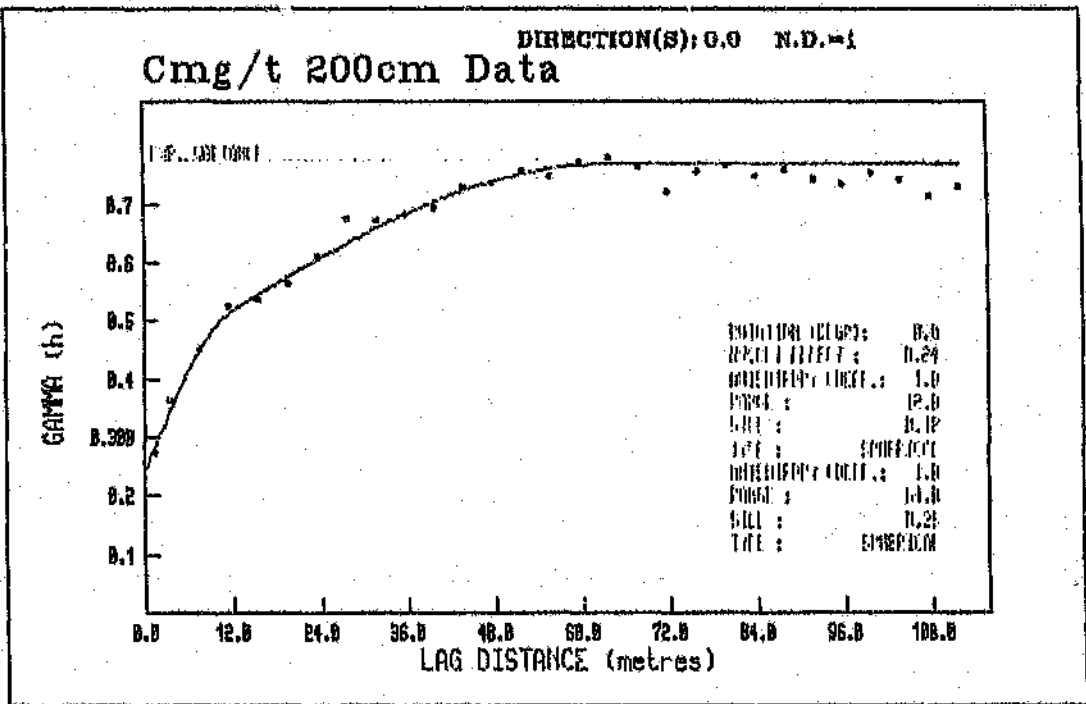


Figure E3: Semivariogram for the $\ln(\text{cmg/t} + \beta)$ Values (200cm Optimisation), of all Development Data.

DIRECTION(S): 0.0 N.D. = 1

Cmg/t 120cm Data

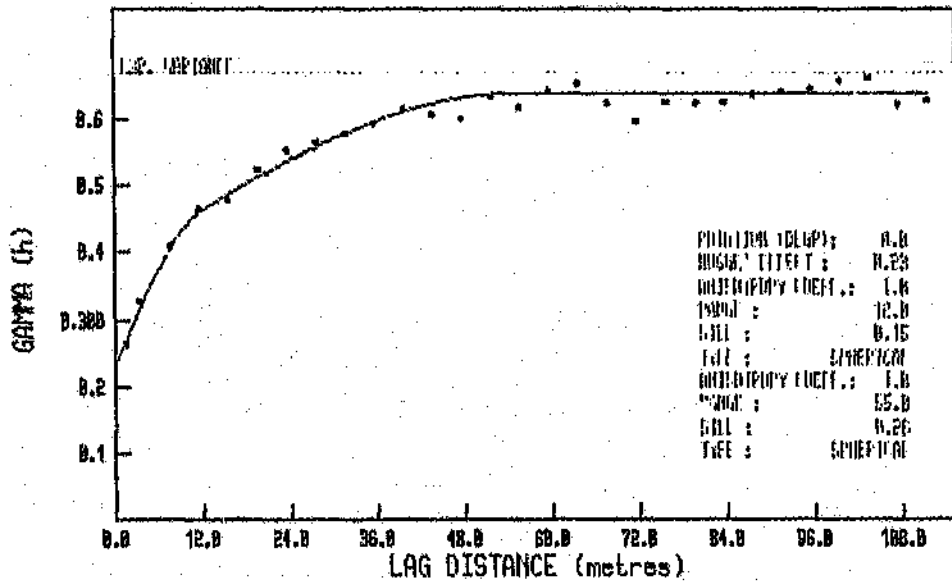


Figure E4: Semivariogram for the $\ln(\text{cmg/t} + \beta)$ Values (120cm Optimisation), less all Outliers.

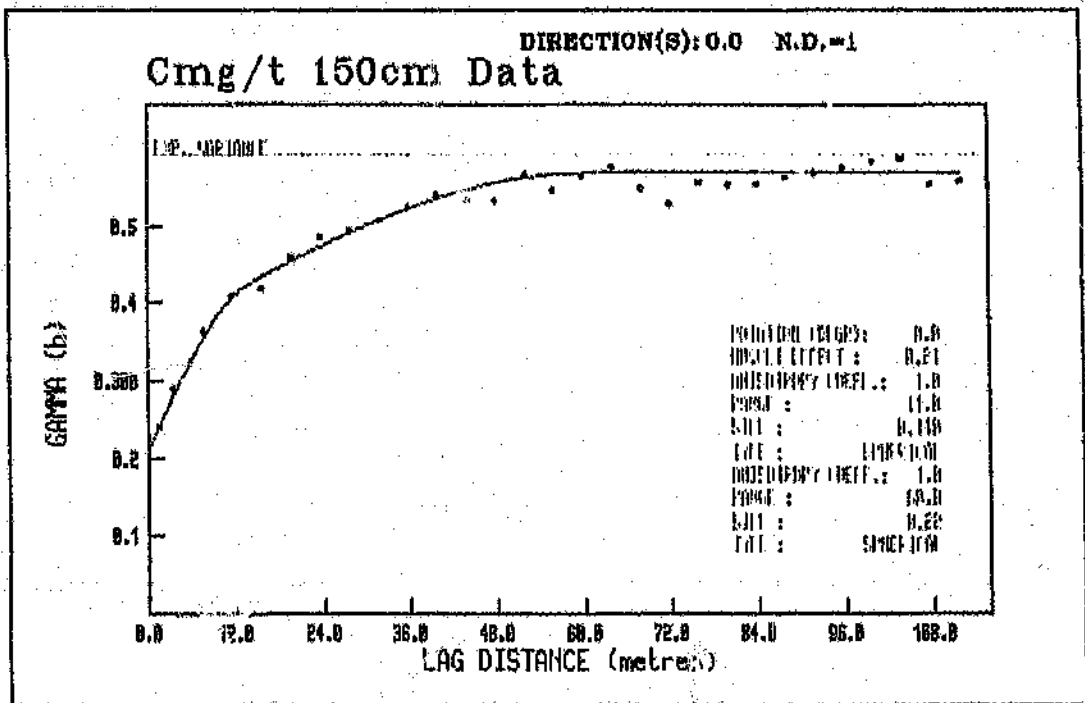


Figure E5: Semivariogram for the $\ln(\text{cmg/t} + \beta)$ Values (150cm Optimisation), less all Outliers.

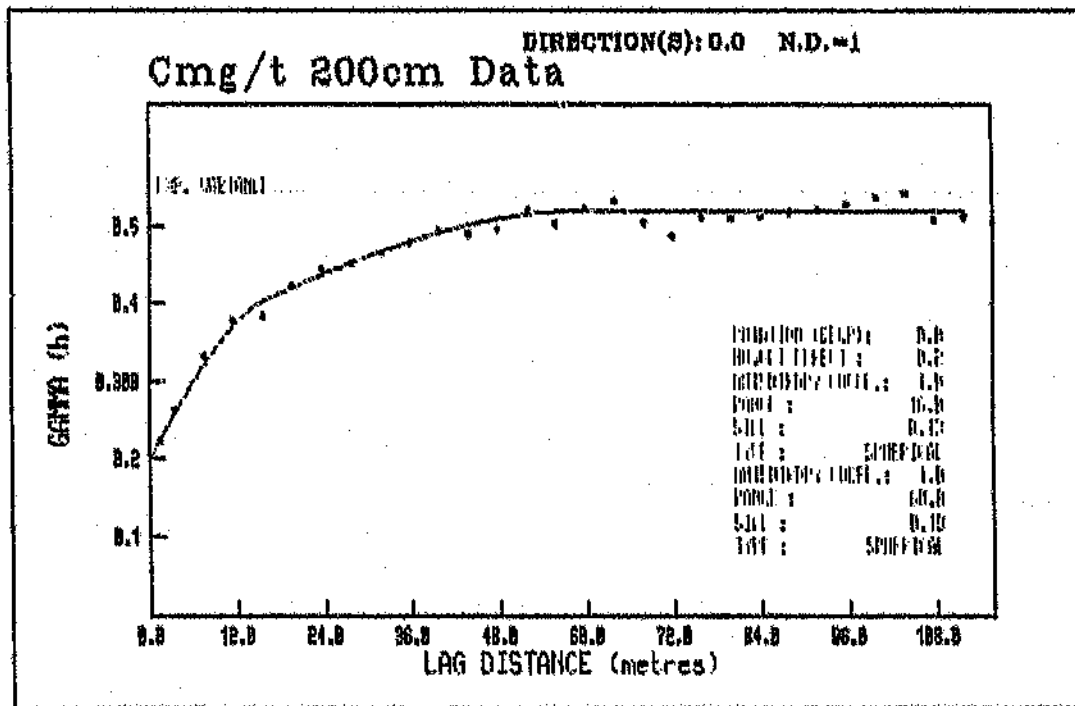


Figure E6: Semivariogram for the $\ln(\text{cmg/t} + \beta)$ Values (200cm Optimisation), less all Outliers.

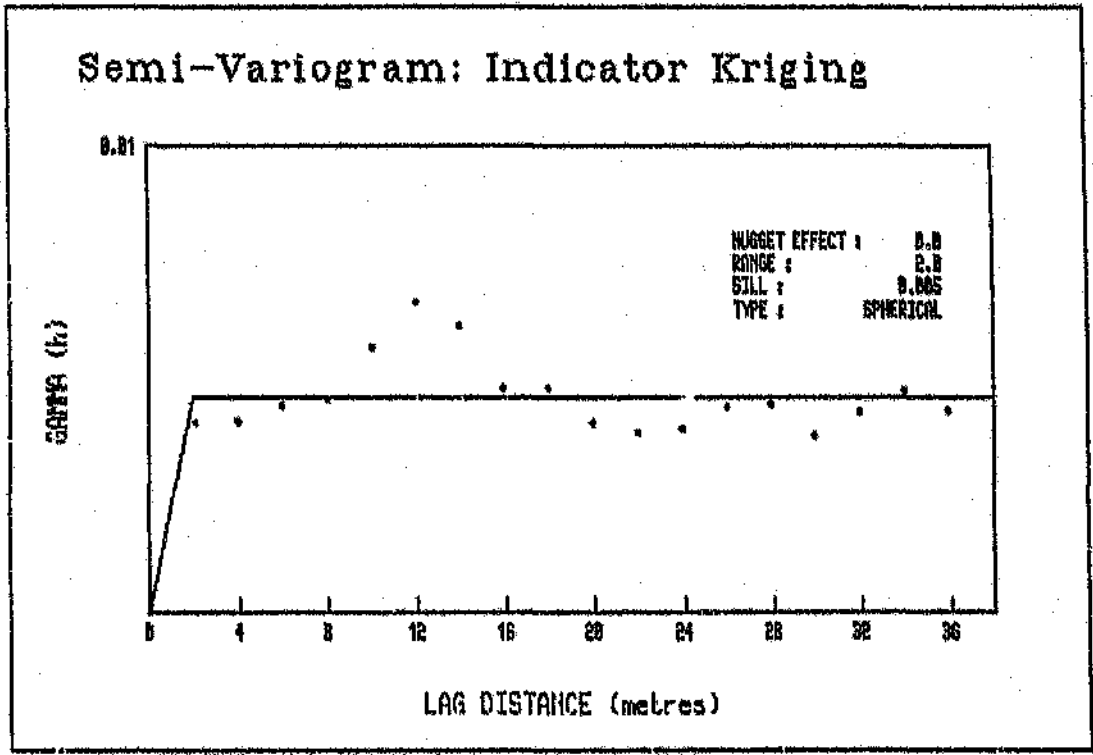


Figure B7: Semivariogram for the Indicators (High Values of all Optimisations).

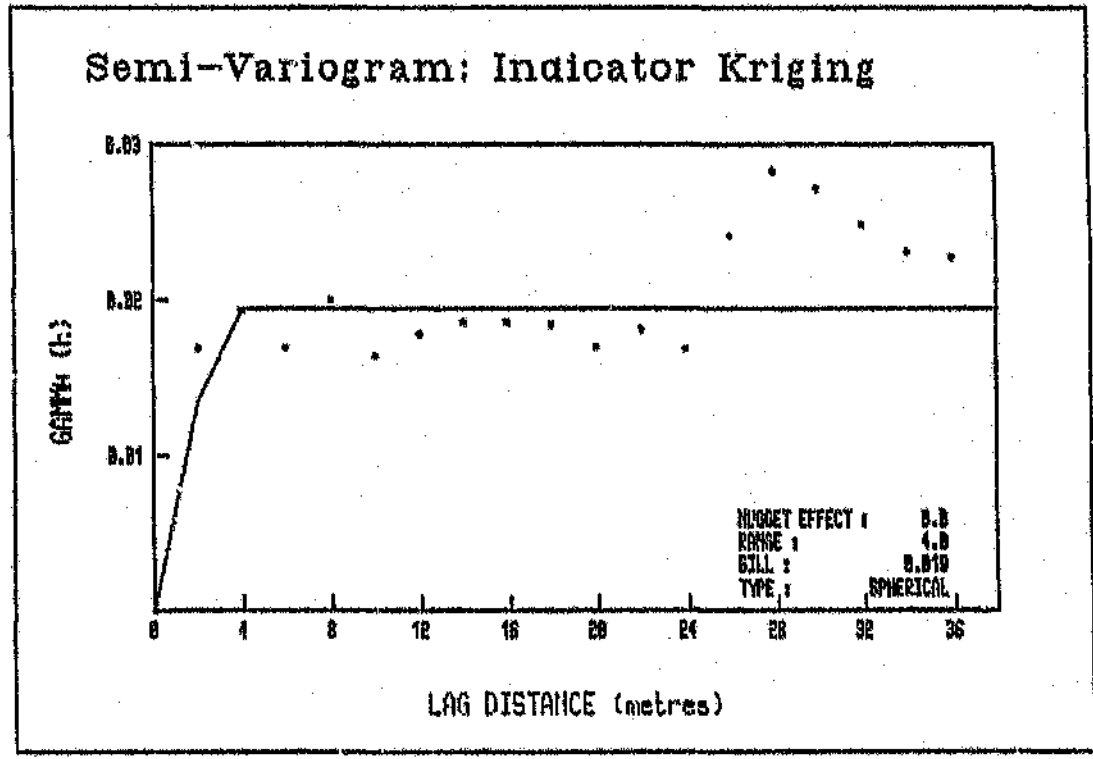


Figure B8: Semivariogram for the Indicators (Low Values of all Optimisations).

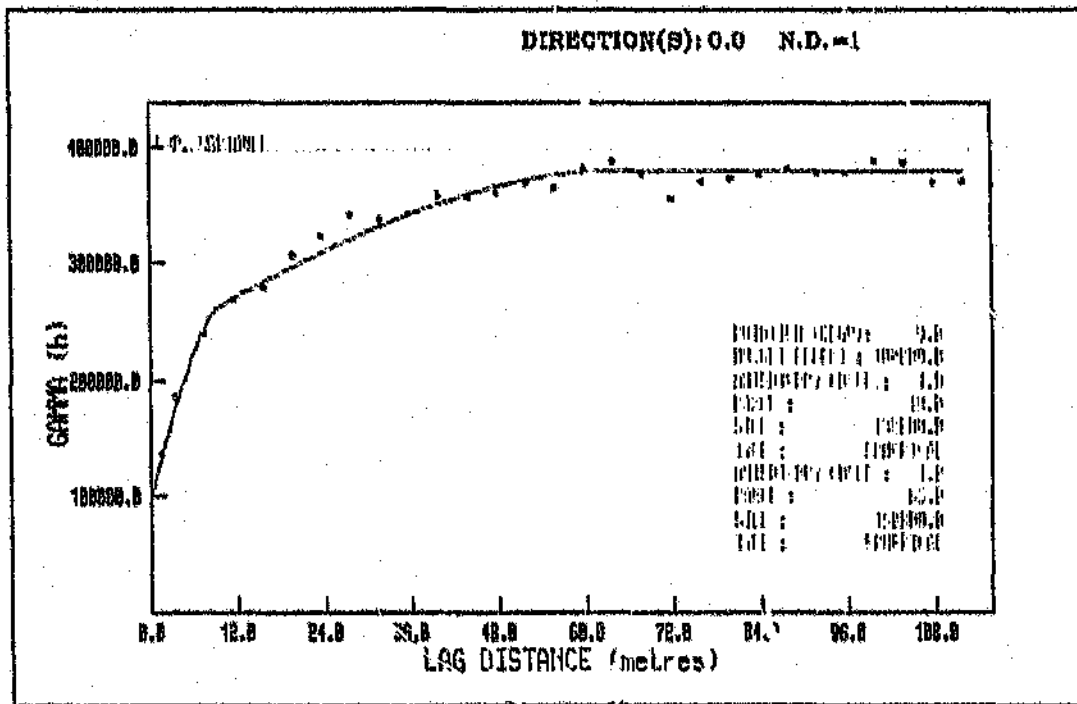


Figure B9: Semivariogram for the Transformed Values (applicable to all Optimisations).

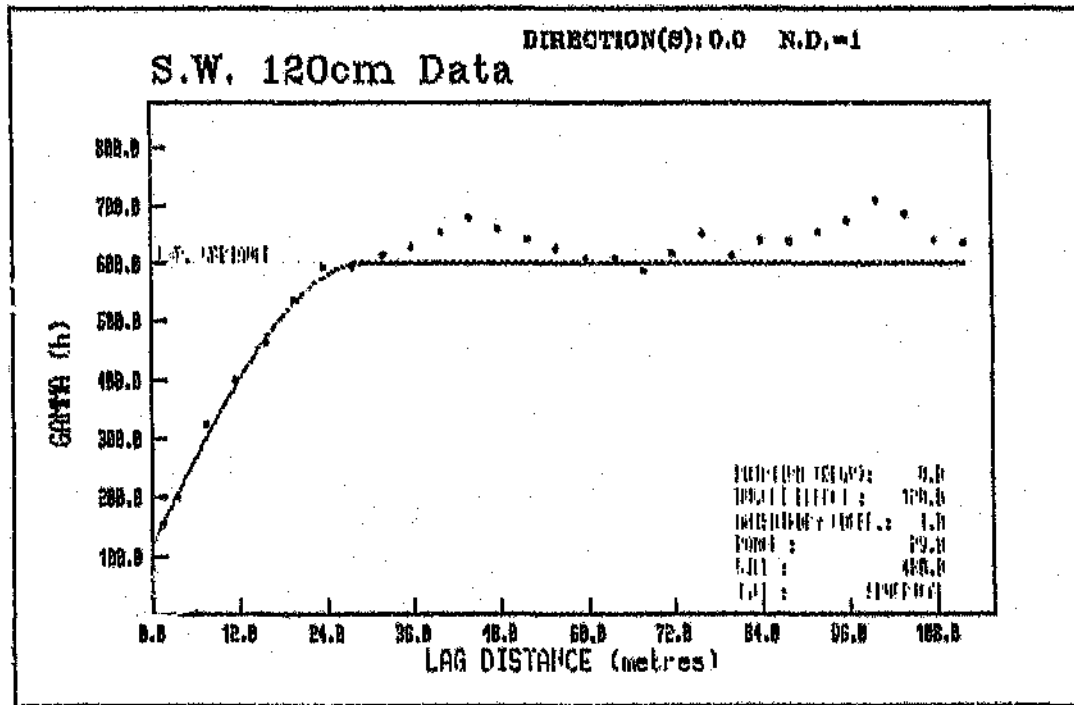


Figure H10: Semivariogram of the Optimised Slope Widths (120 cm).

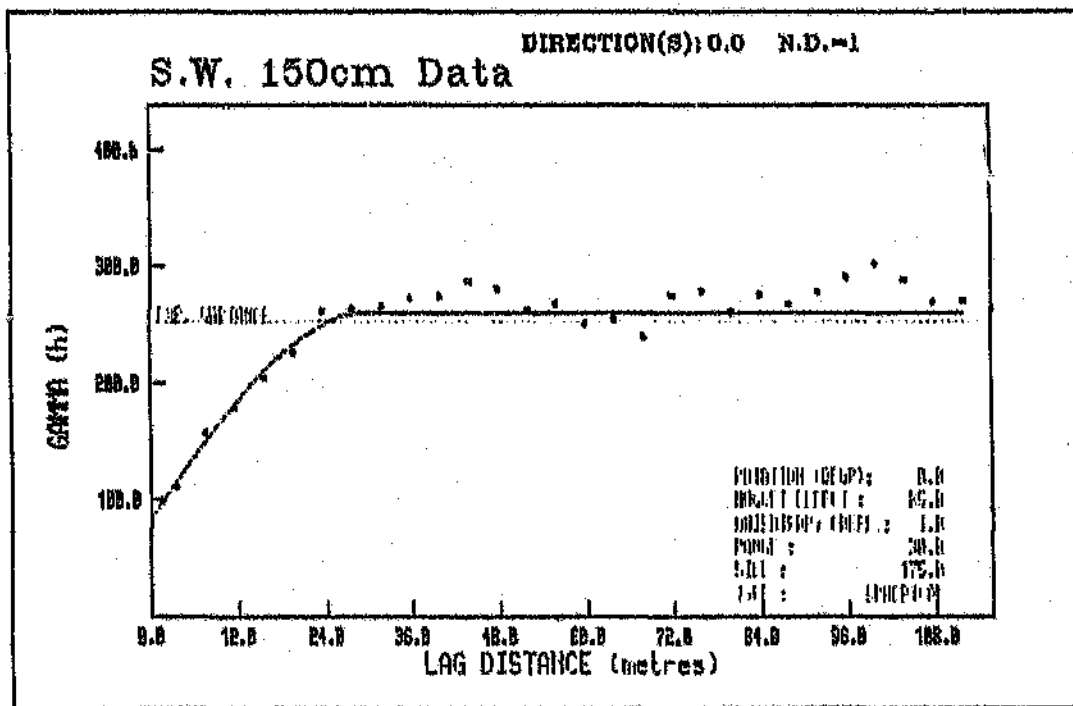


Figure B11: Semivariogram of the Optimised Slope Widths (150 cm).

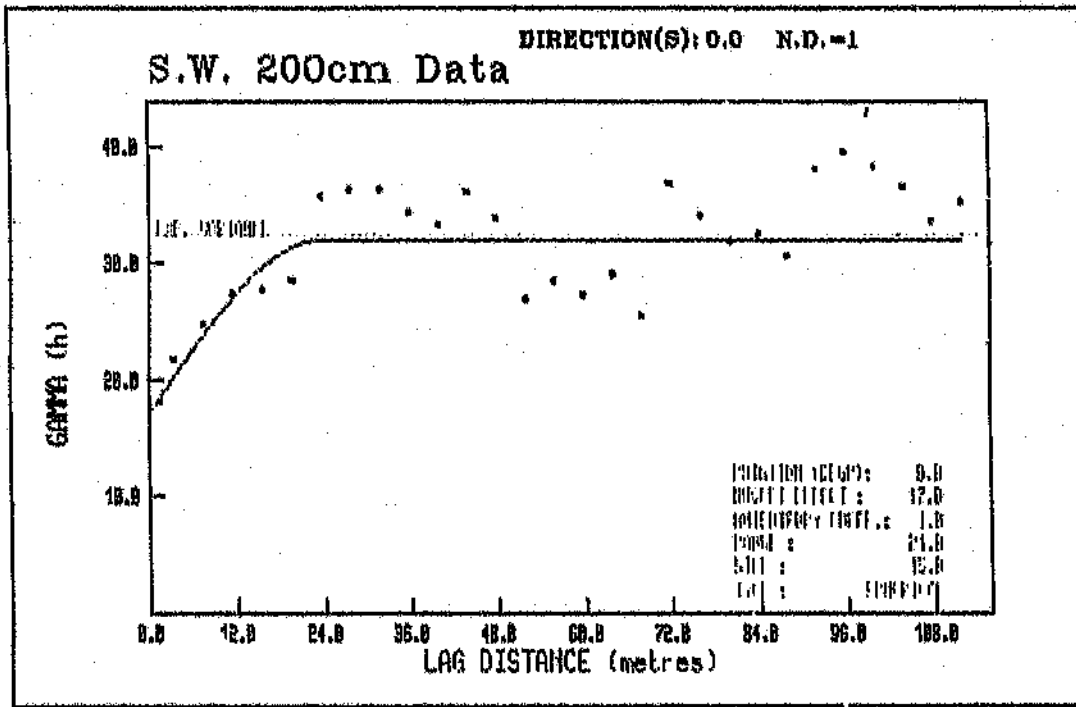


Figure B12: Semivariogram of the Optimised Slope Widths (200 cm).

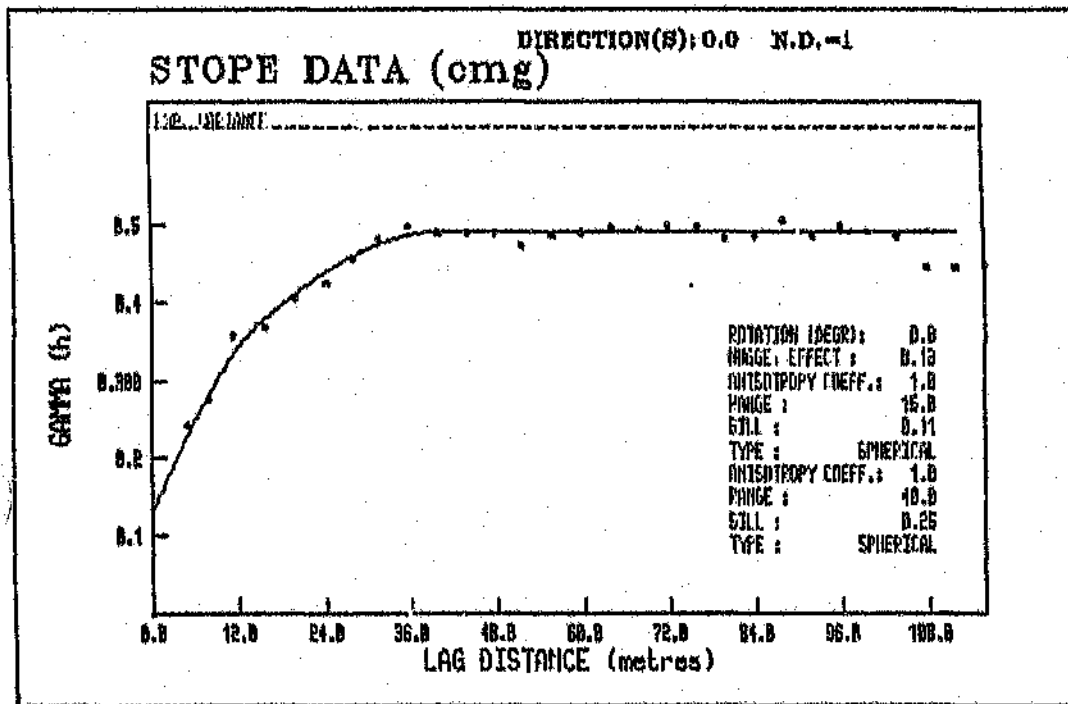


Figure E13: Semivariogram of the Actual Stope Cmg/t Values.

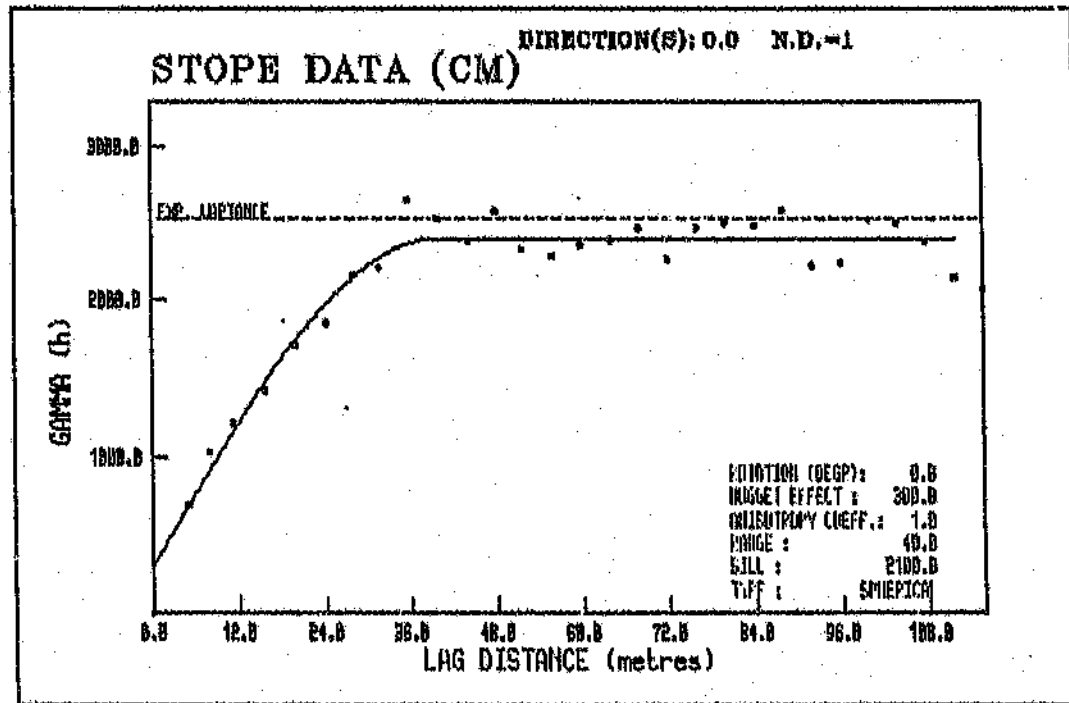


Figure E14: Semivariogram of the Actual Stope Widths.

APPENDIX F

The Error Statistics from the Cross Validation Exercises

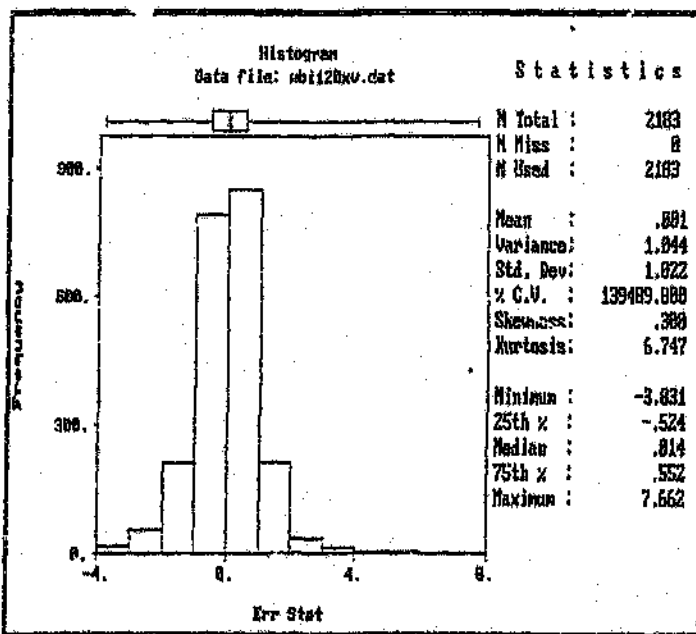


Figure F1 : Error Statistics from Case (a), 120cm Optimisation, Cross Validation of only Development Data.

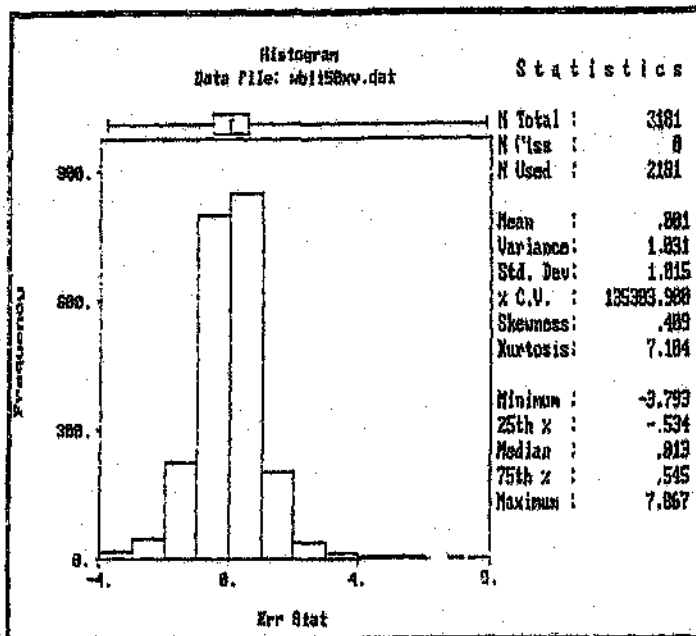


Figure F2 : Error Statistics from Case (a), 150cm Optimisation, Cross Validation of only Development Data.

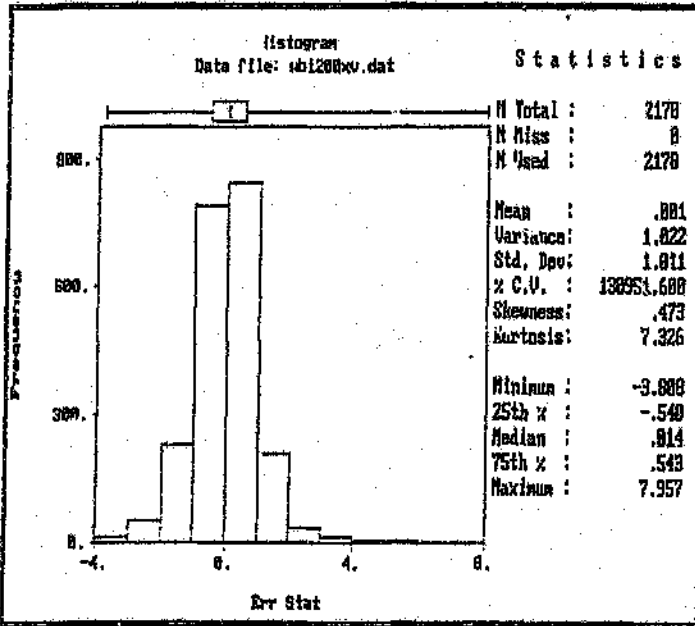


Figure F3 : Error Statistics from Case (a), 200cm Optimisation, Cross Validation of only Development Data.

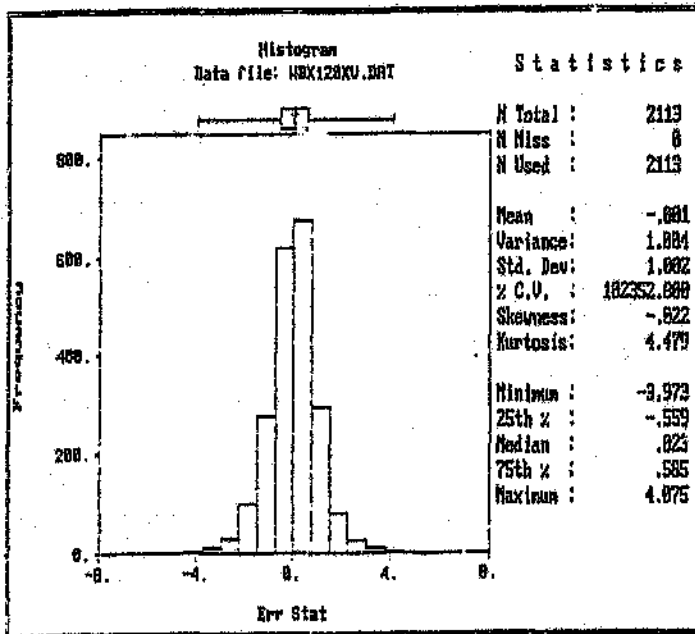


Figure F4 : Error Statistics from Case (b), 120cm Optimisation, Cross Validation of only Development Data.

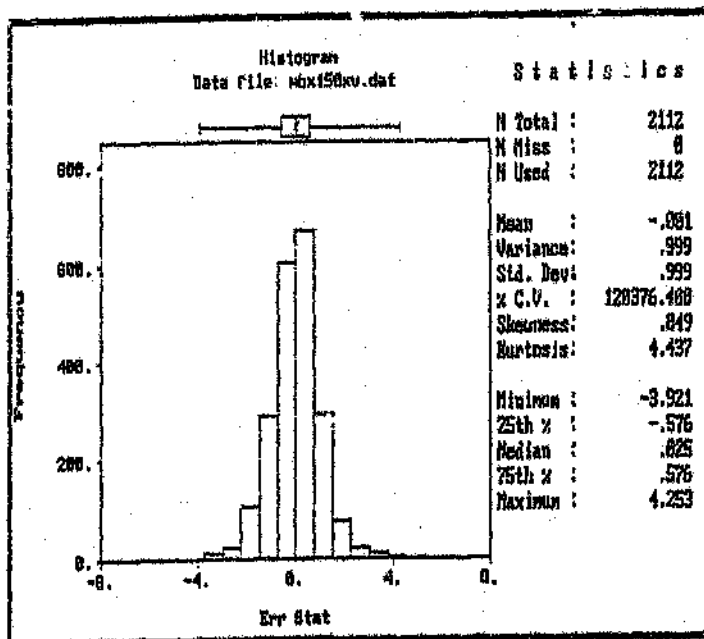


Figure F5 : Error Statistics from Case (b), 150cm Optimization, Cross Validation of only Development Data.

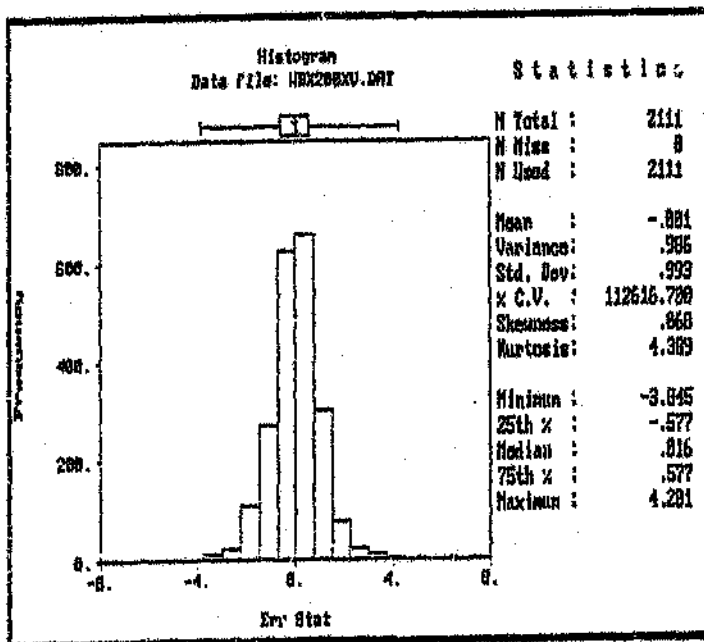


Figure F6 : Error Statistics from Case (b), 200cm Optimization, Cross Validation of only Development Data.

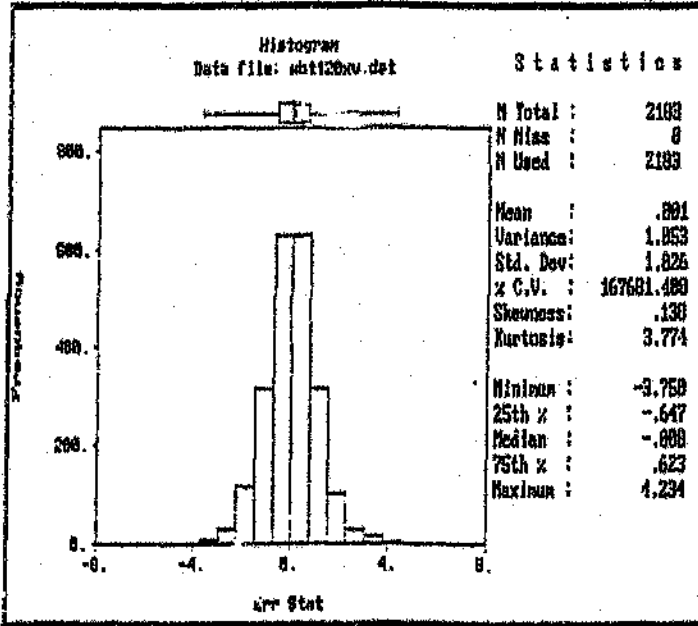


Figure F7 : Error Statistics from Case (c), 120cm Optimization, Cross Validation of only Development Data.

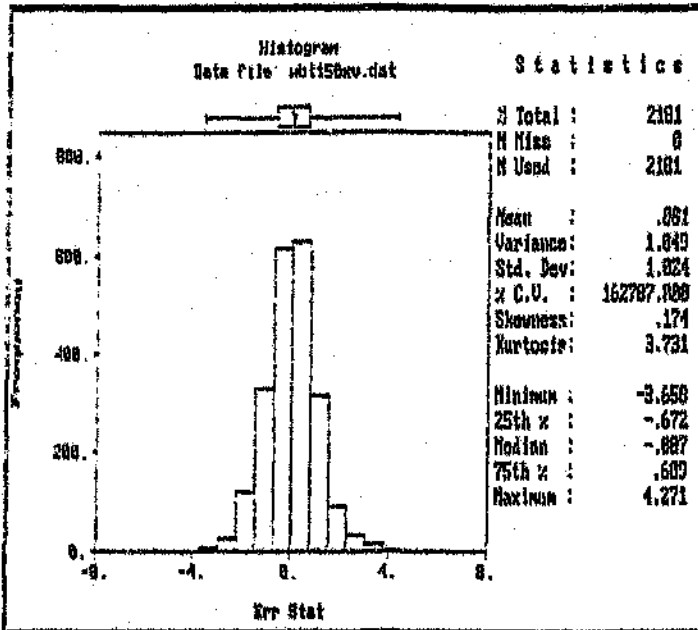


Figure F8 : Error Statistics from Case (c), 150cm Optimization, Cross Validation of only Development Data.

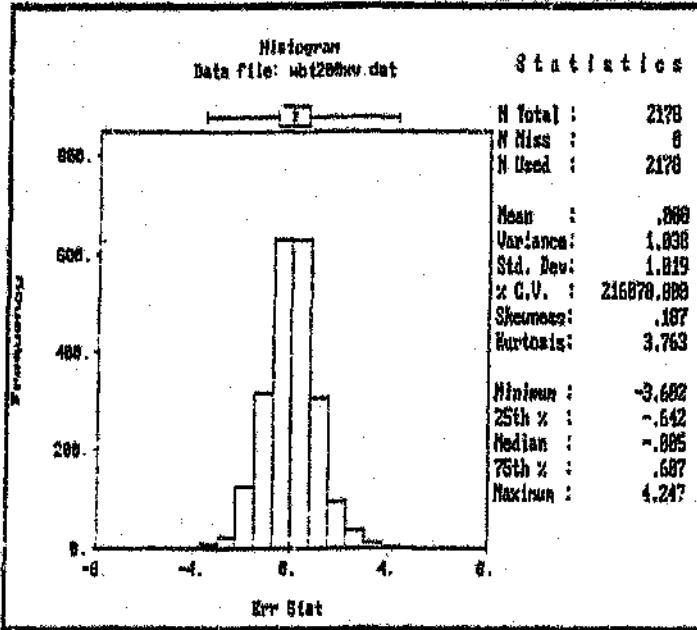


Figure F9: Error Statistics from Case (c), 200cm Optimization. Cross Validation of only Development Data.

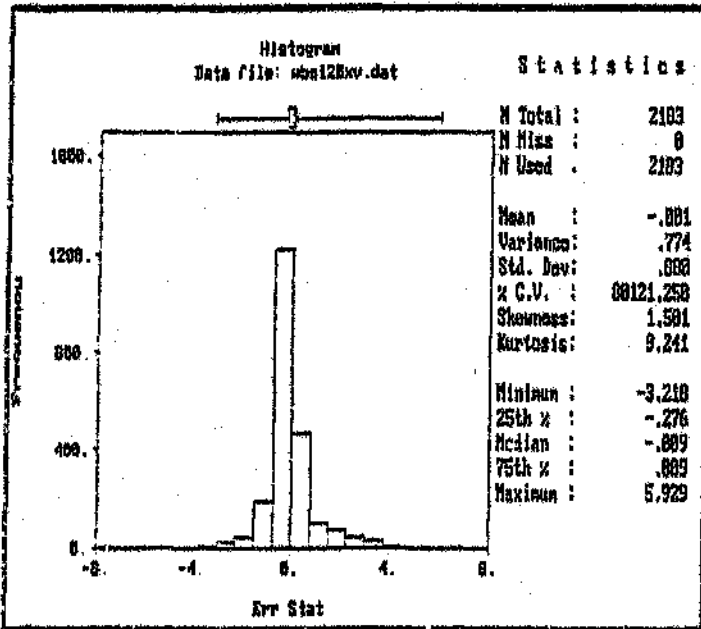


Figure F10: Error Statistics from Slope Widths Optimized to 120cm. Cross Validation of only Development Data.

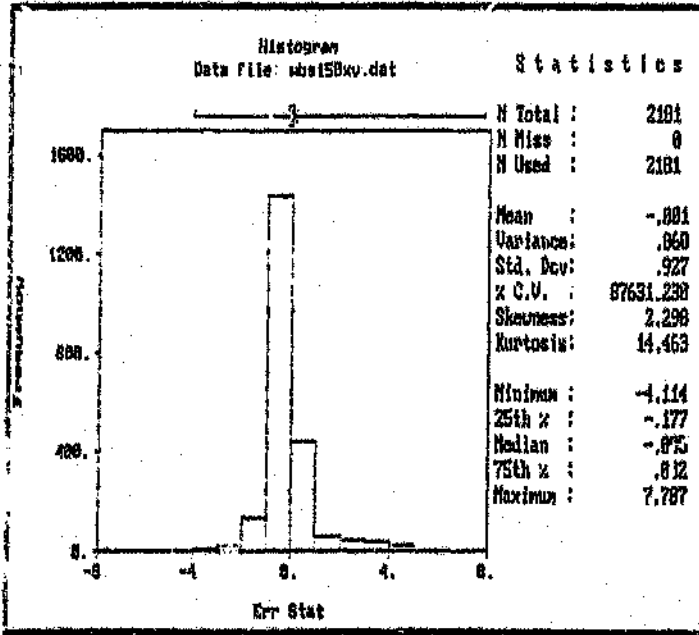


Figure F11: Error Statistics from Stops Widths Optimised to 150cm, Cross Validation of only Development Data.

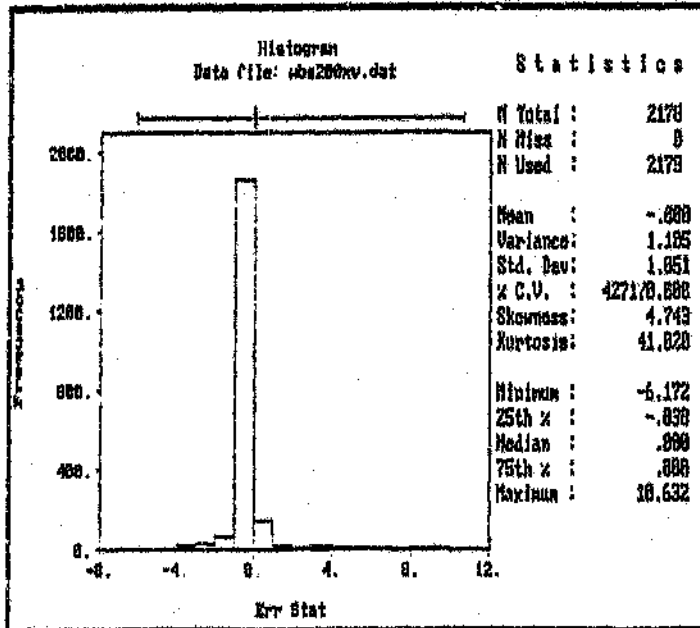


Figure F12: Error Statistics from Stops Widths Optimised to 200cm, Cross Validation of only Development Data.

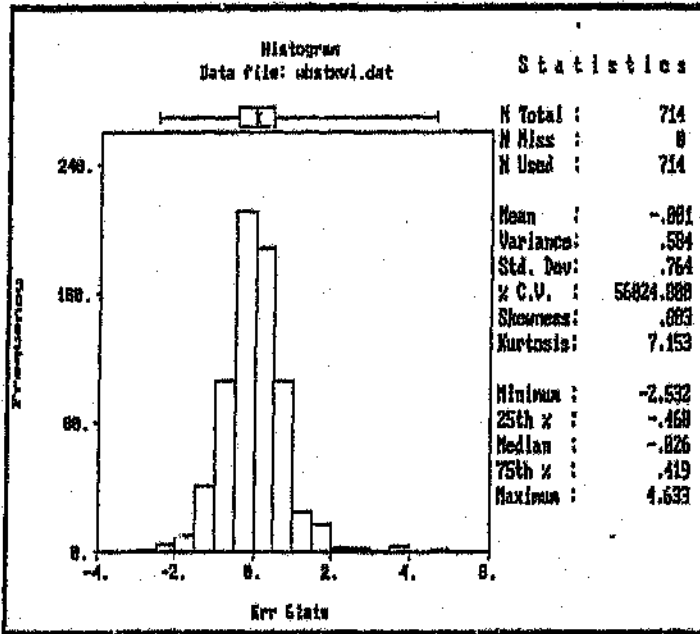


Figure F13: Error Statistics from Case (a), 120cm Optimisation, Cross Validation of only Slope Data.

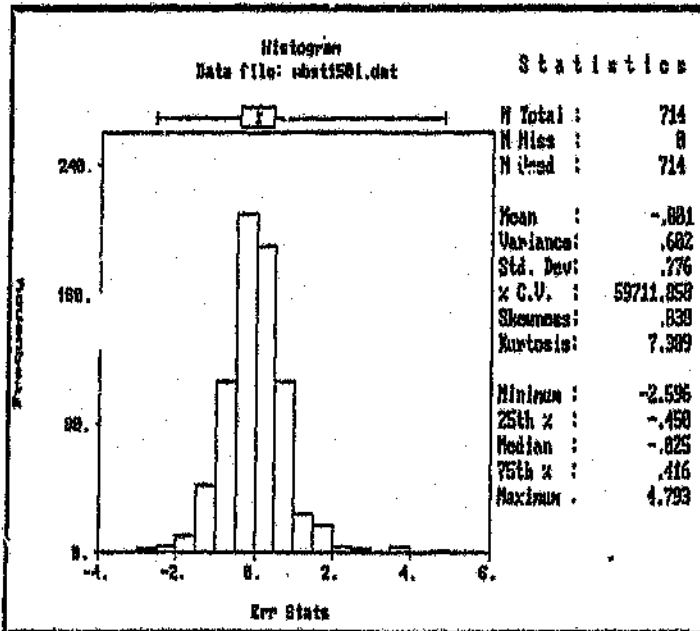


Figure F14: Error Statistics from Case (a), 150cm Optimisation, Cross Validation of only Slope Data.

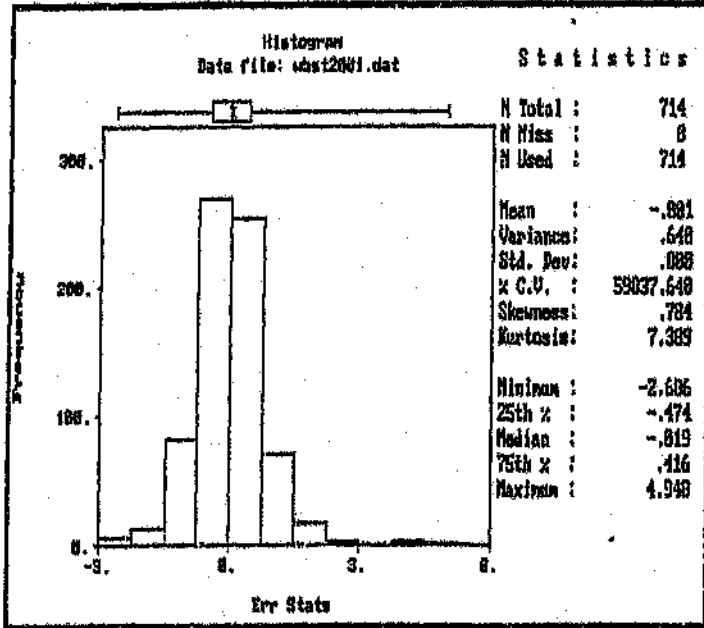


Figure F15: Error Statistics from Case (a), 200cm Optimization, Cross Validation of only Stops Data.

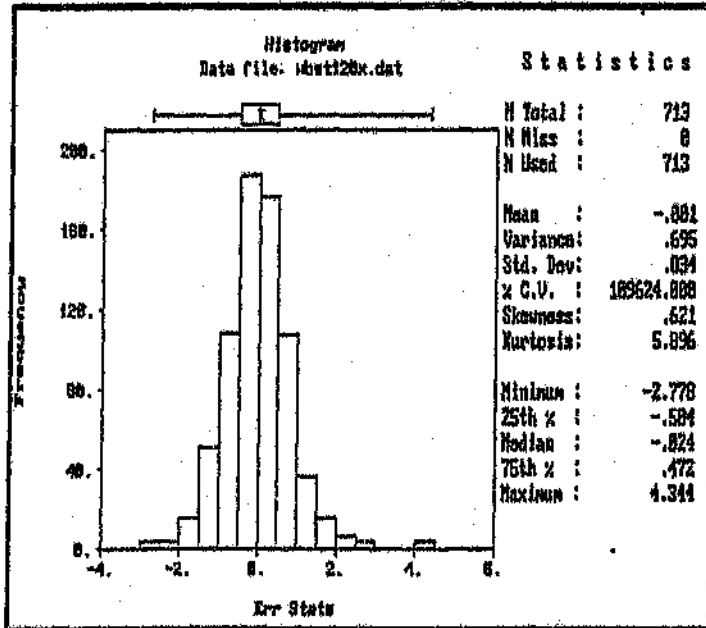


Figure F16: Error Statistics from Case (b), 120cm Optimization, Cross Validation of only Stops Data.

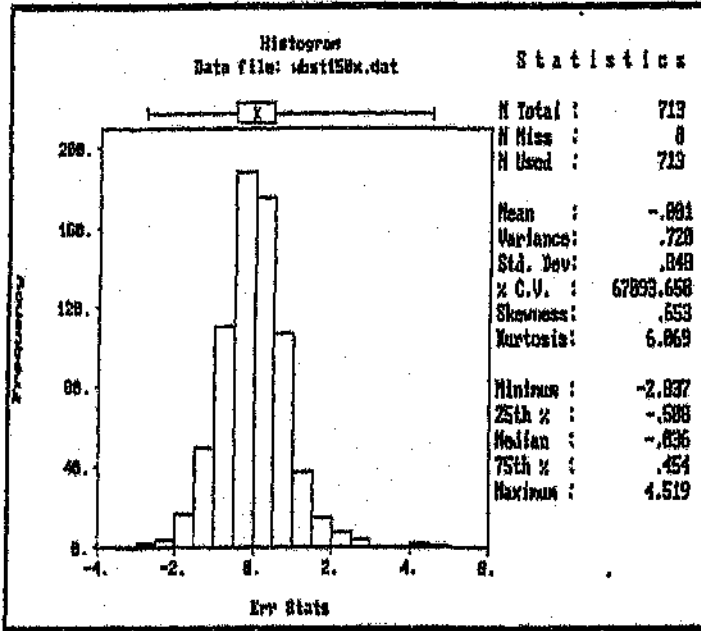


Figure F17: Error Statistics from Case (b), 150cm Optimization, Cross Validation of only Stop Data.

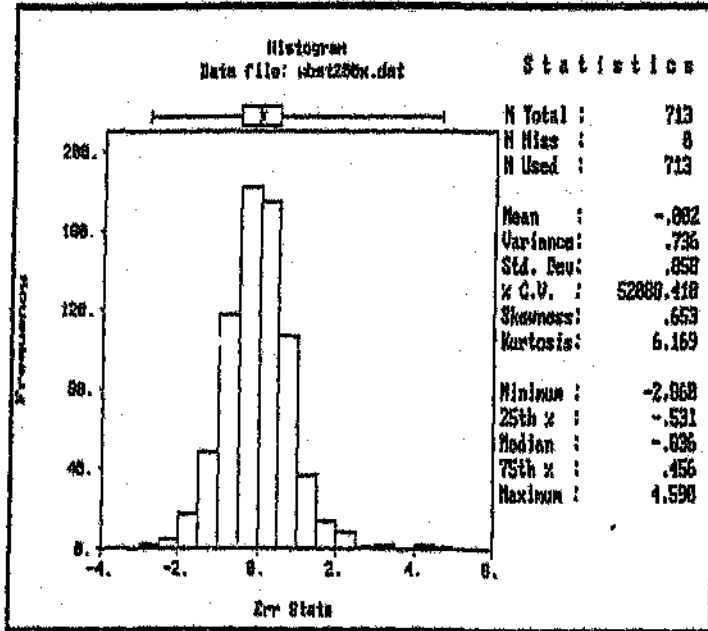


Figure F18: Error Statistics from Case (b), 200cm Optimization, Cross Validation of only Stop Data.

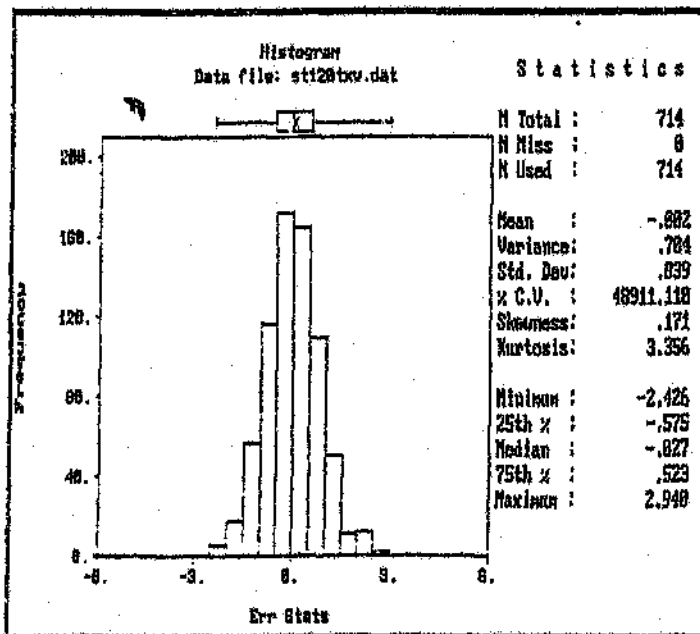


Figure F19: Error Statistics from Case (c), 120cm Optimization, Cross Validation of only Slope Data.

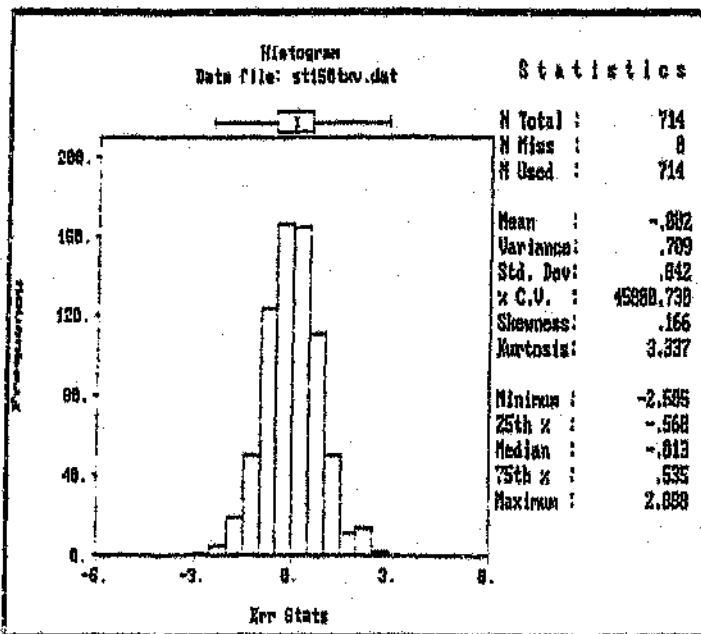


Figure F20: Error Statistics from Case (c), 150cm Optimization, Cross Validation of only Slope Data.

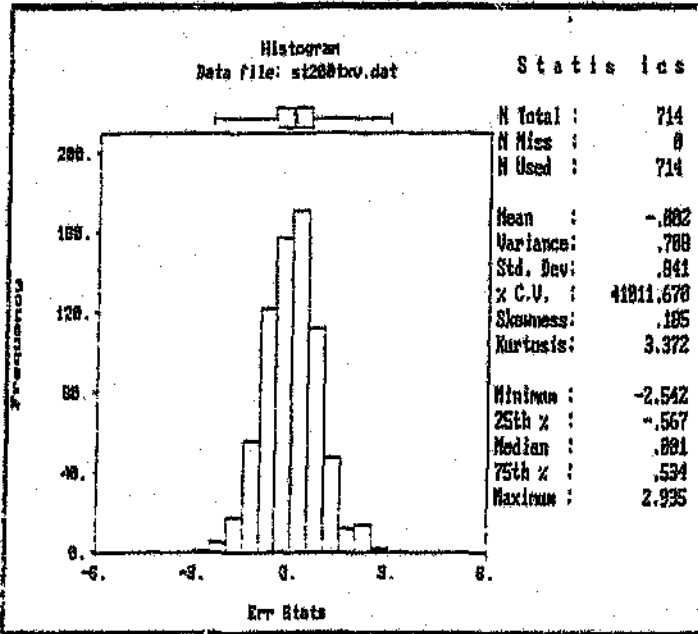


Figure F21: Error Statistics from Case (c), 200cm Optimisation, Cross Validation of only Stops Data.

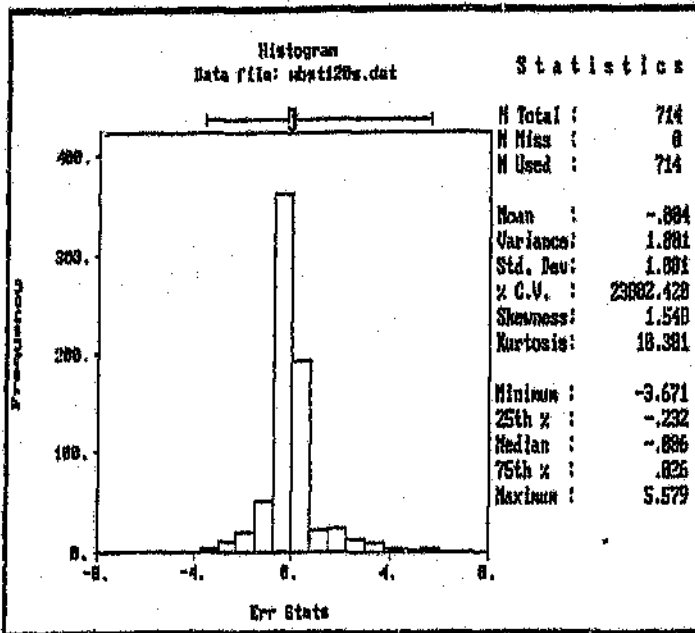


Figure F22: Error Statistics from Stops Widths Optimised to 120cm, Cross Validation of only Stops Data.

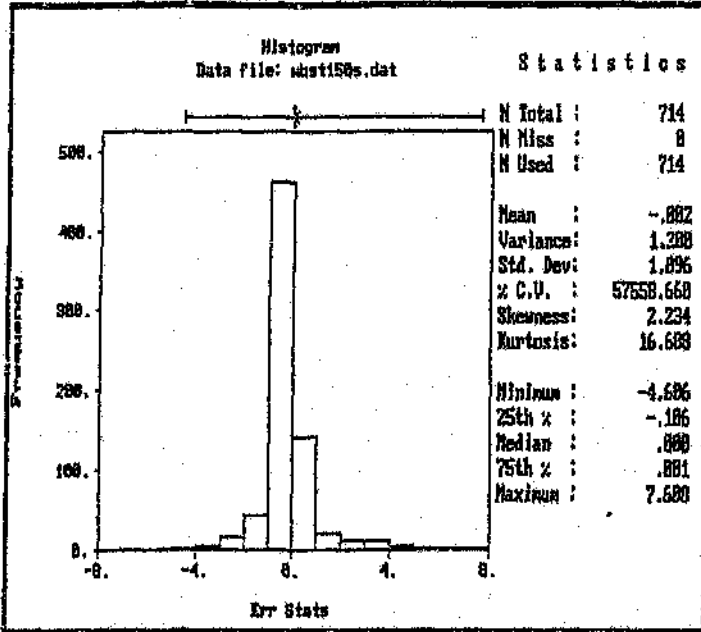


Figure F23: Error Statistics from Slope Widths Optimised to 150cm, Cross Validation of only Slope Data.

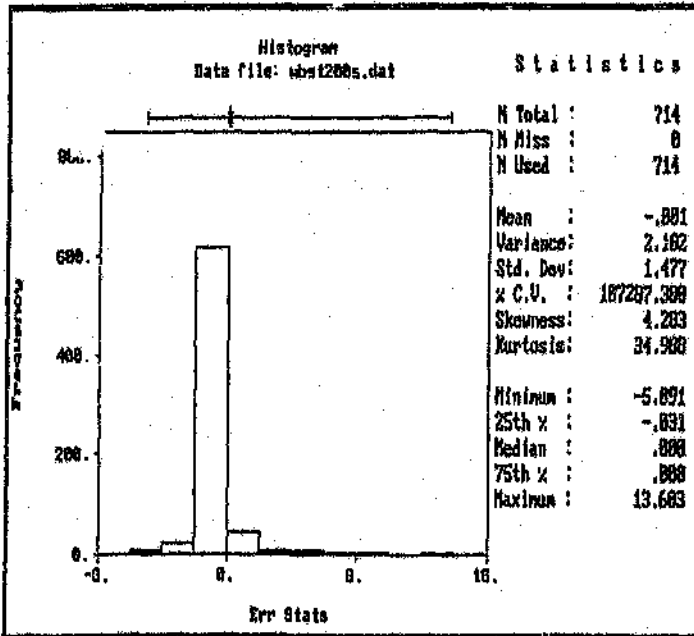


Figure F24: Error Statistics from Slope Widths Optimised to 200cm, Cross Validation of only Slope Data.

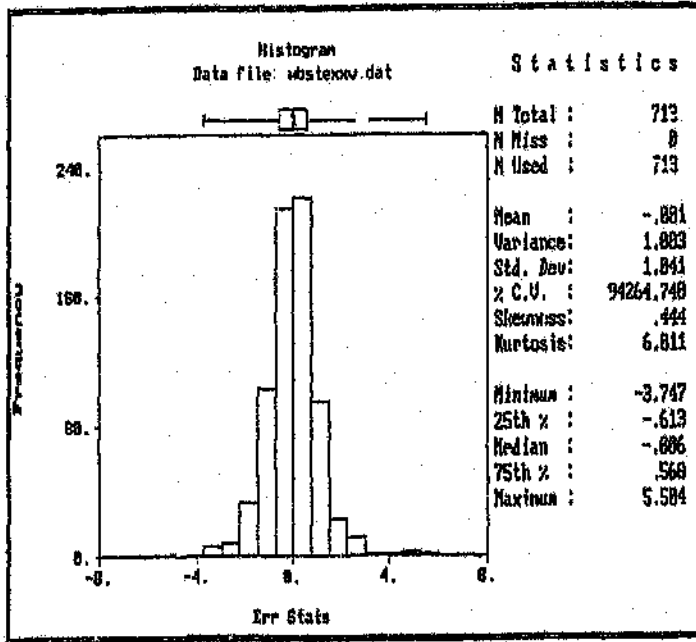


Figure F25: Error Statistics from the Actual Stop Value (cmg/t) Cross Validation.

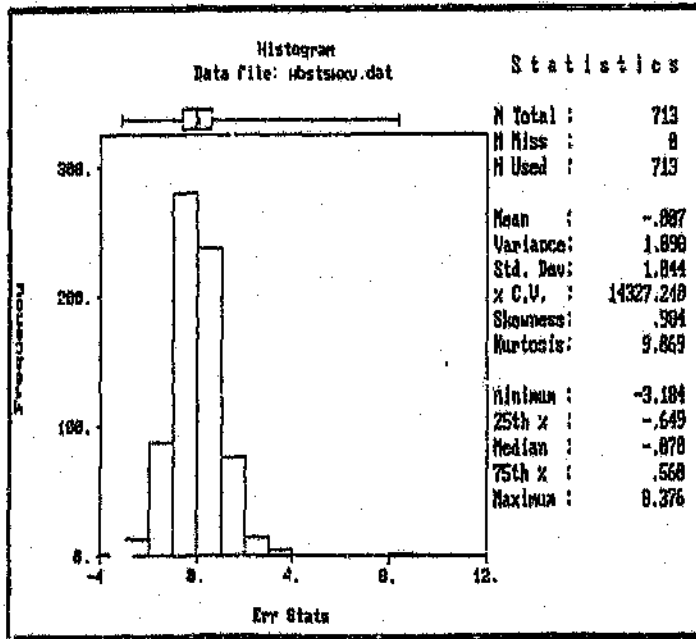


Figure F26: Error Statistics from the Actual Stop Width (cm) Cross Validation.

APPENDIX G

Grade-Stope Width Graphs for Case (a)

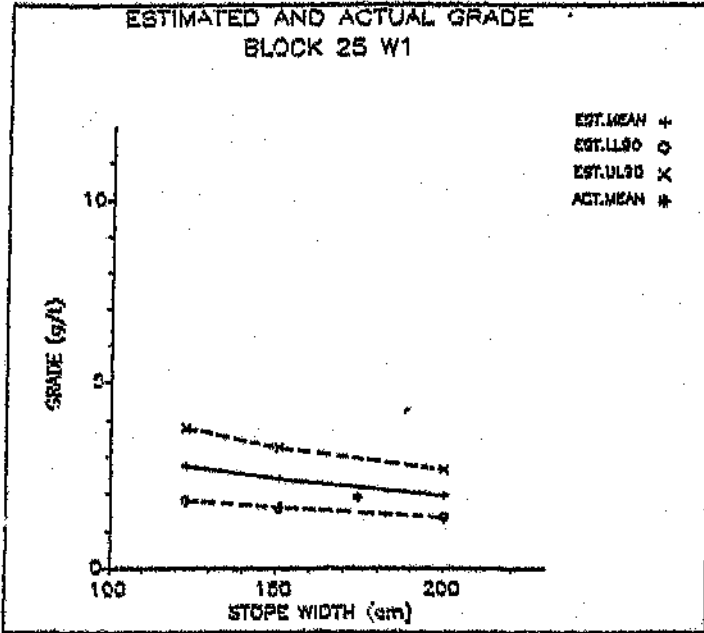


Figure G1 : Estimated and Actual Grades in Case (a) for Block 25 W1

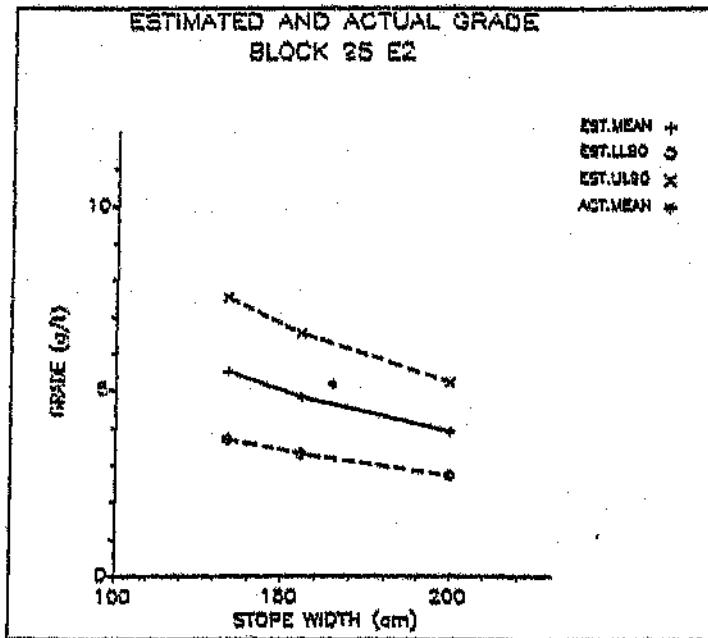


Figure G2 : Estimated and Actual Grades in Case (a) for Block 25 E2

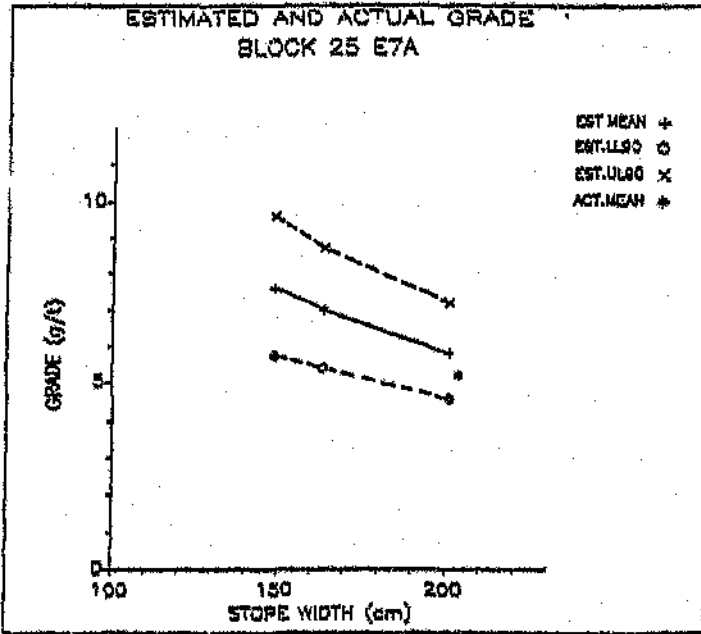


Figure G3 : Estimated and Actual Grades in Case (a) for Block 25 E7A

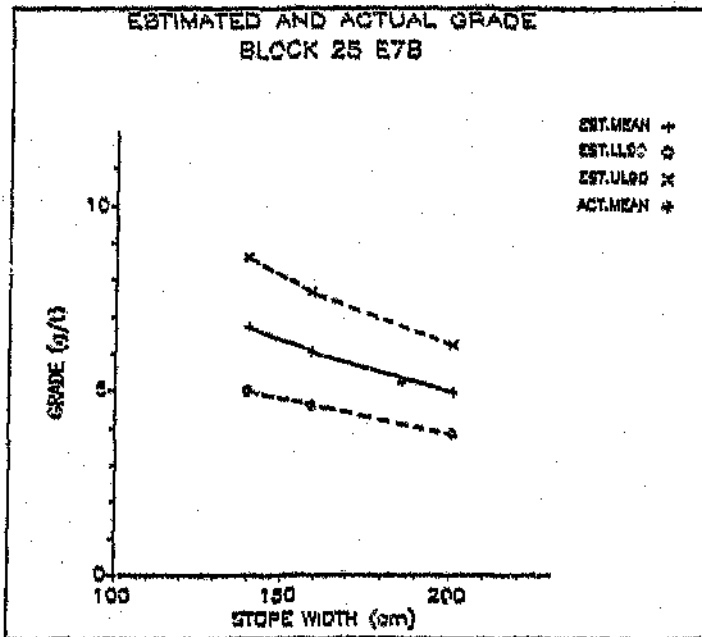


Figure G4 : Estimated and Actual Grades in Case (a) for Block 25 E7B

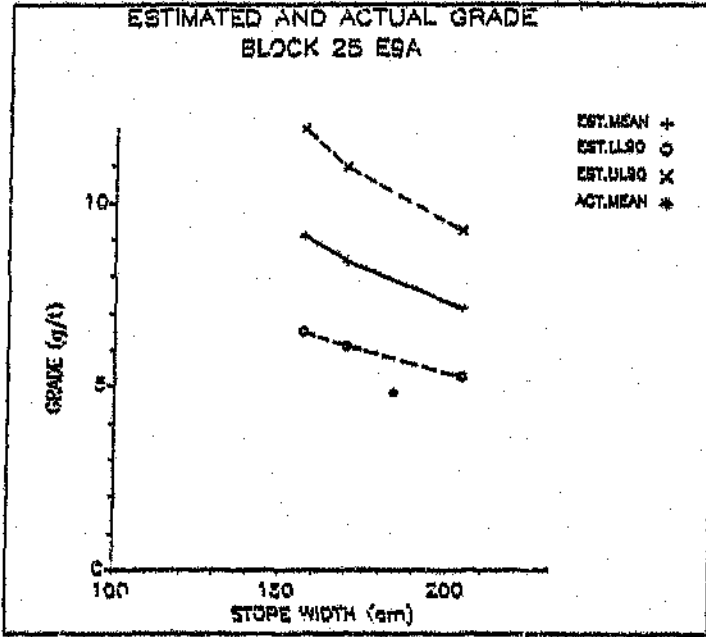


Figure G5 : Estimated and Actual Grades in Case (a) for Block 25 E9A

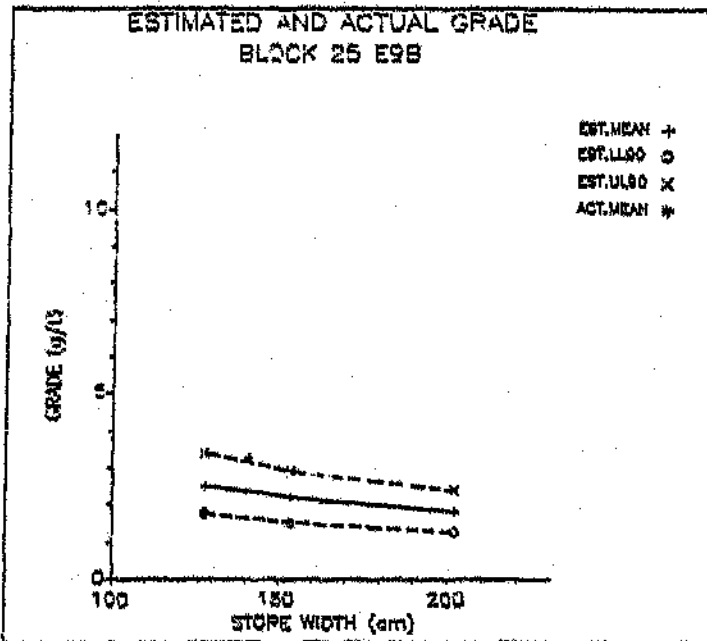


Figure G6 : Estimated and Actual Grades in Case (a) for Block 25 E9B

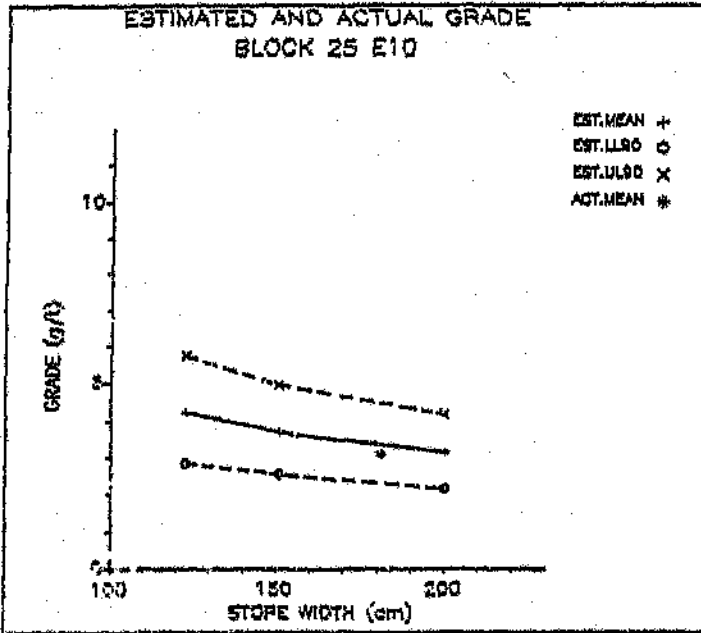


Figure 37 : Estimated and Actual Grades in Case (a) for Block 25 E10

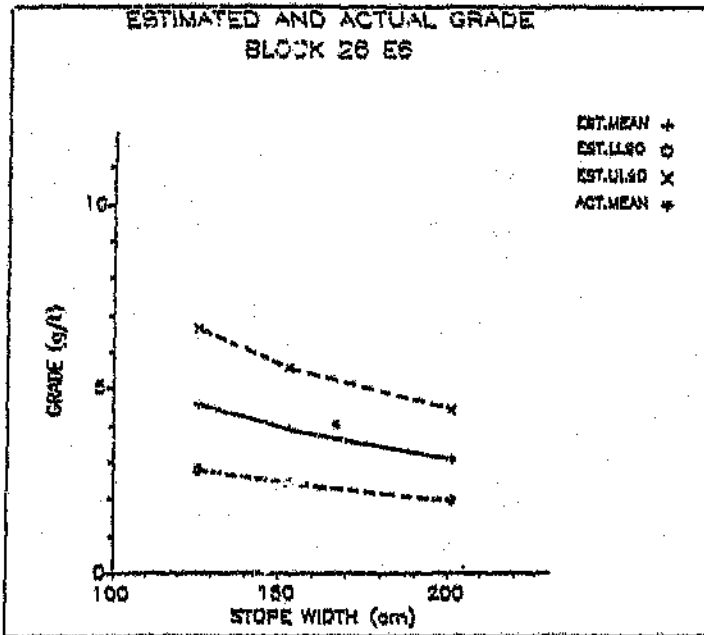


Figure 38 : Estimated and Actual Grades in Case (a) for Block 26 E6

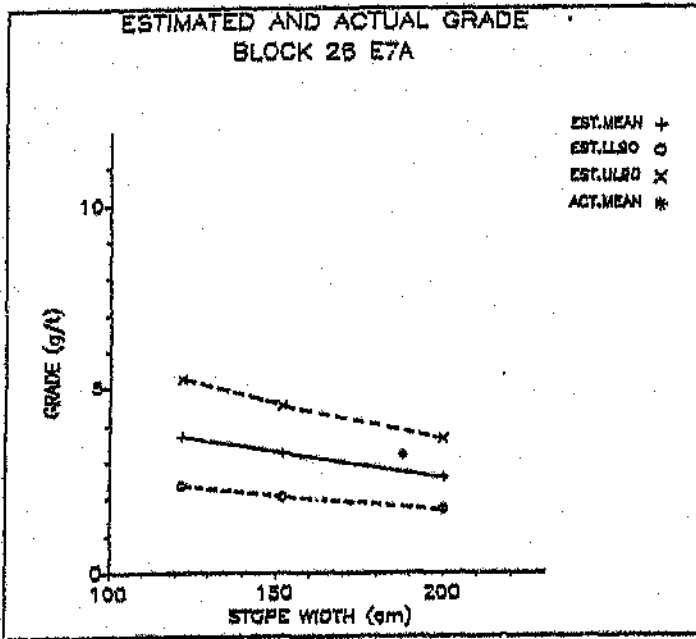


Figure G9 : Estimated and Actual Grades in Case (a) for Block 26 E7A

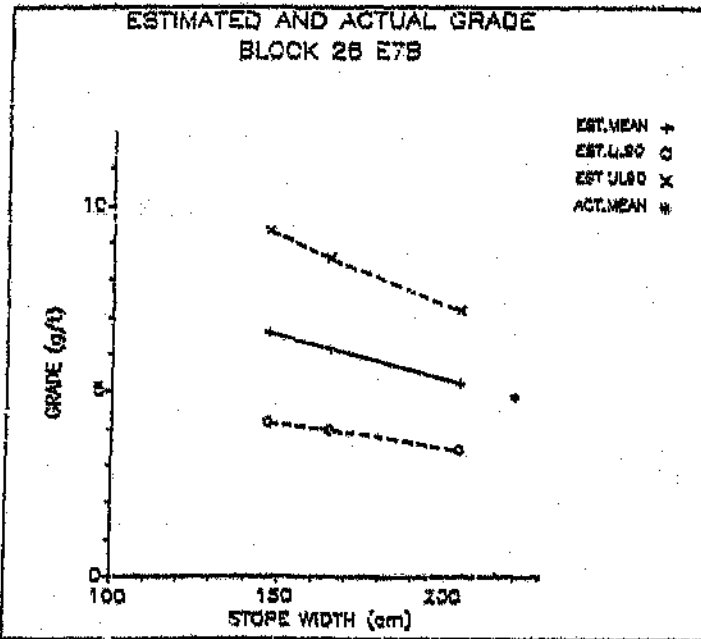


Figure G10 : Estimated and Actual Grades in Case (n) for Block 26 E7B

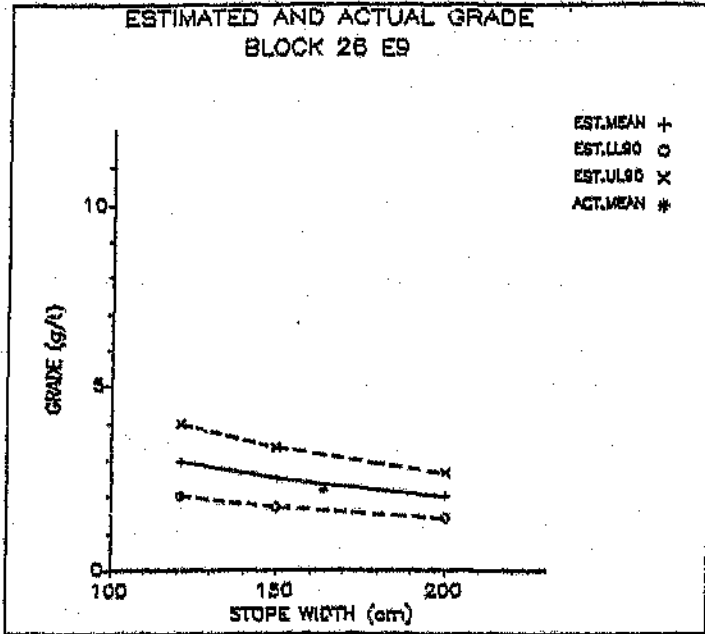


Figure G11 : Estimated and Actual Grades in Case (a) for Block 26 E9

APPENDIX H

Grade-Stope Width Graphs for Case (b)

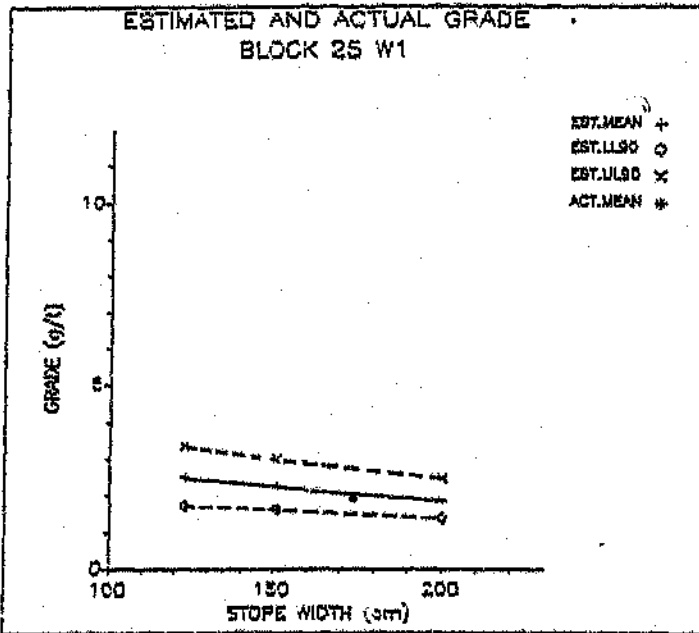


Figure H1 : Estimated and Actual Grades in Case (b) for Block 25 W1

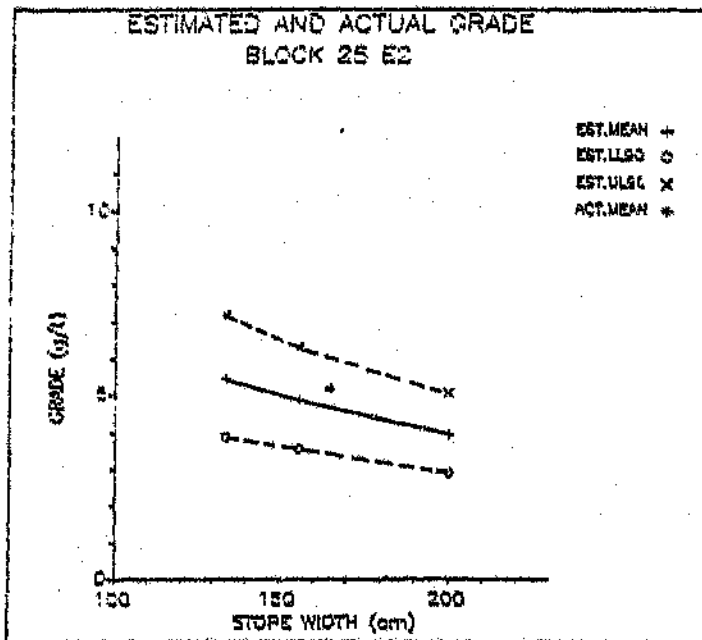


Figure H2 : Estimated and Actual Grades in Case (b) for Block 25 E2

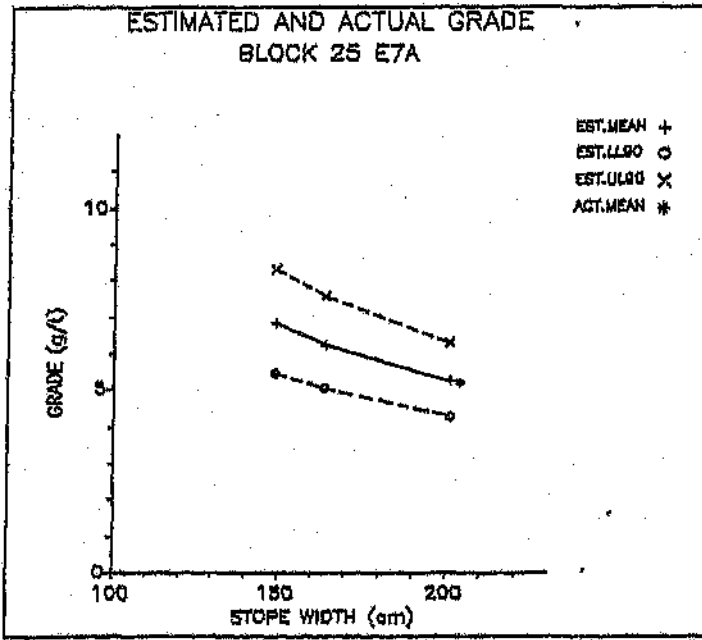


Figure H3 : Estimated and Actual Grades in Case (b) for Block 25 E7A

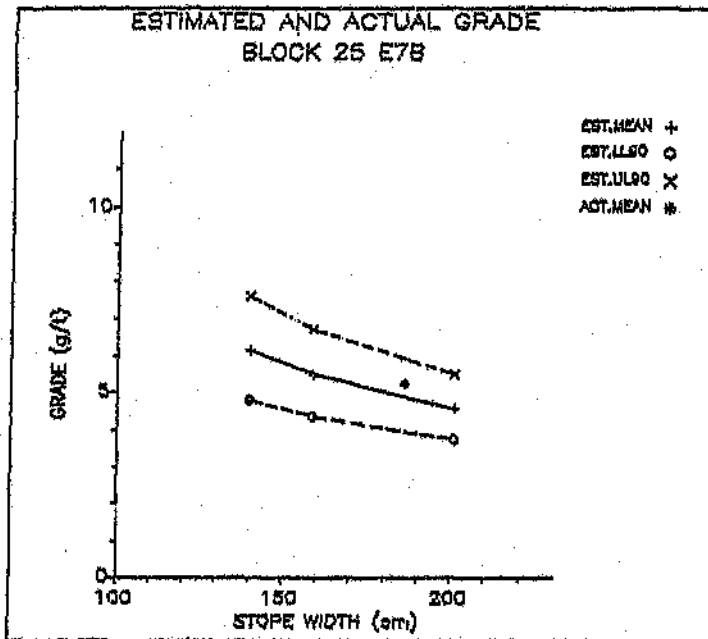


Figure H4 : Estimated and Actual Grades in Case (b) for Block 25 E7B

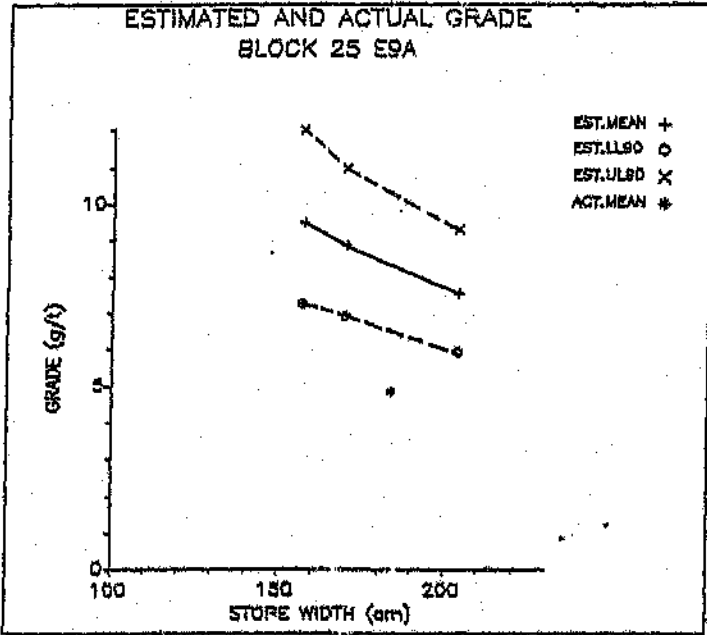


Figure H5 : Estimated and Actual Grades in Case (h) for Block 25 E9A

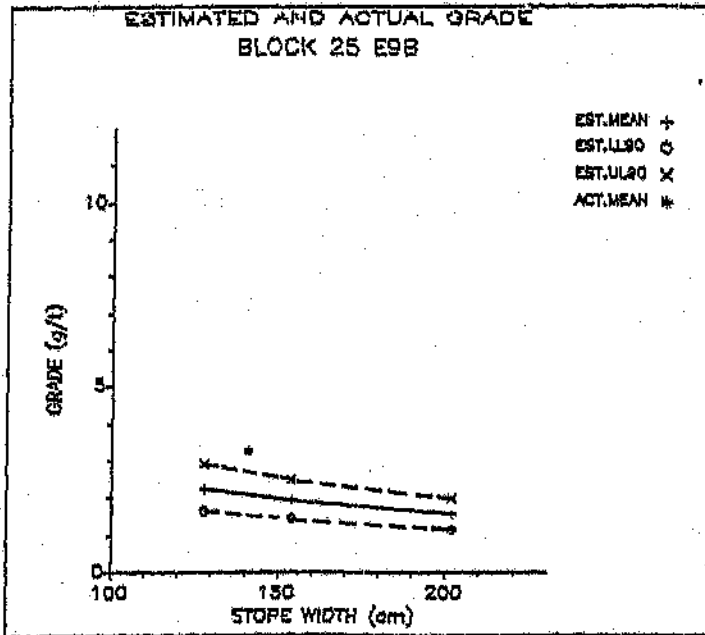


Figure H6 : Estimated and Actual Grades in Case (b) for Block 25 E9B

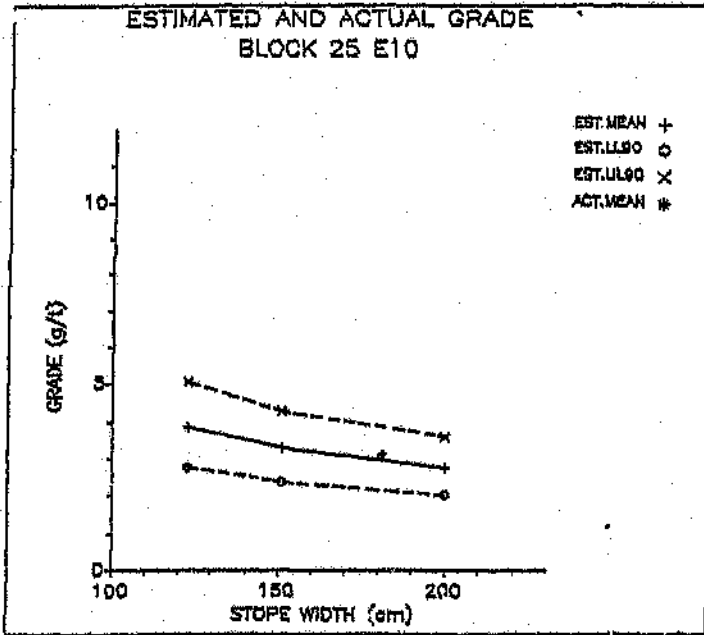


Figure H7 : Estimated and Actual Grades in Case (b) for Block 25 E10

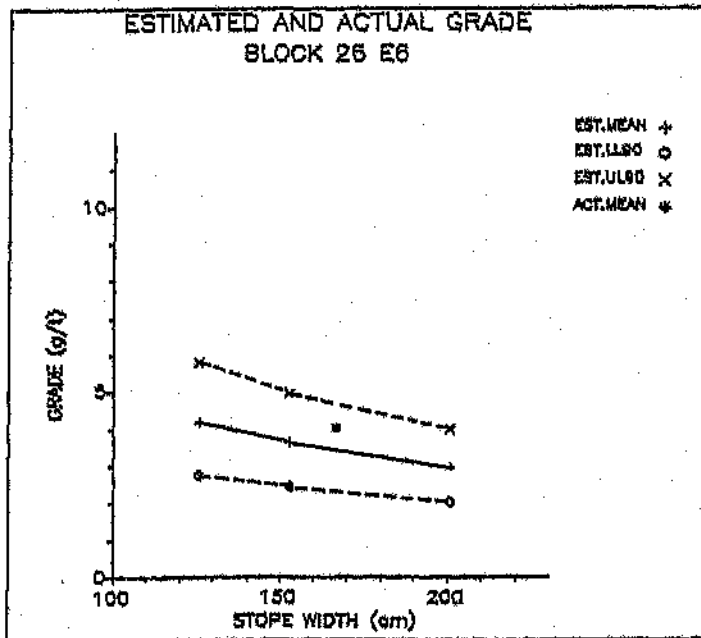


Figure H8 : Estimated and Actual Grades in Case (b) for Block 25 E6

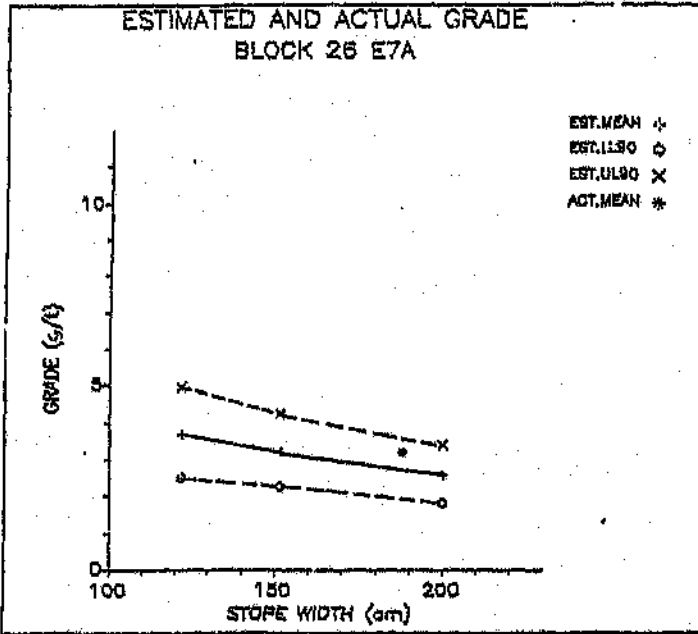


Figure H9 : Estimated and Actual Grades in Case (b) for Block 26 E7A

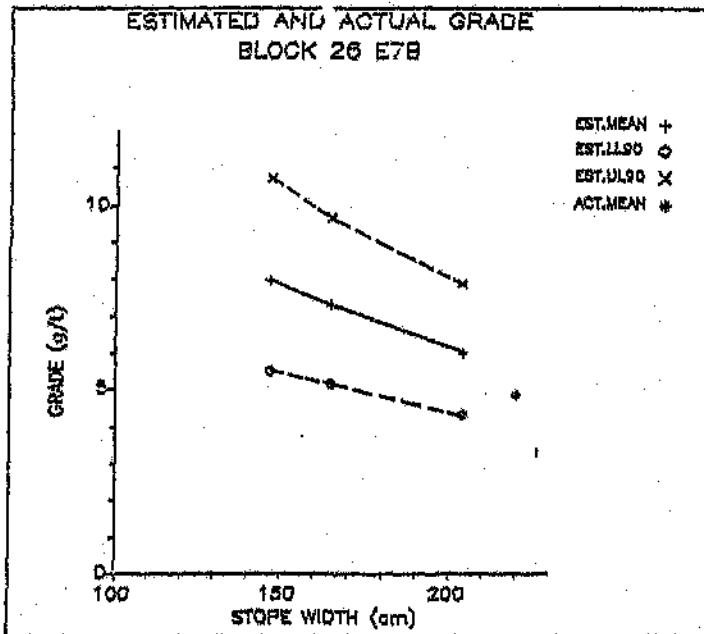


Figure H10 : Estimated and Actual Grades in Case (b) for Block 26 E7B

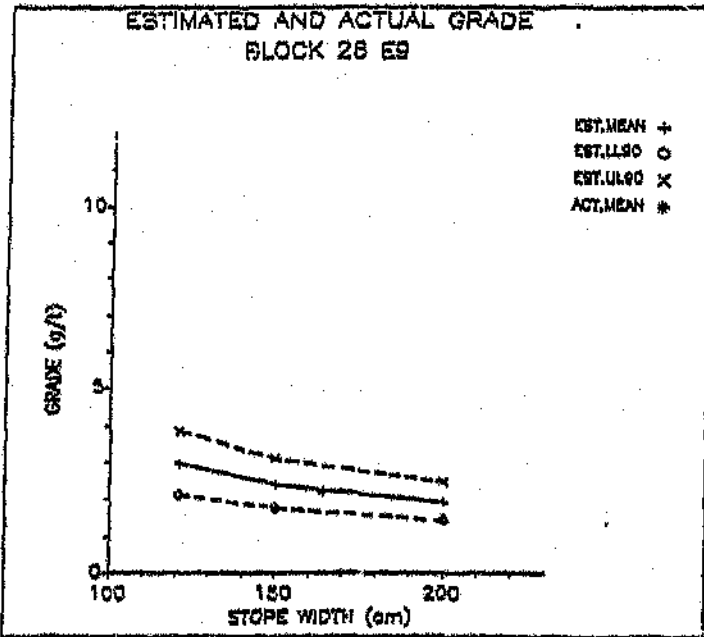


Figure III1 : Estimated and Actual Grades in Case (b) for Block 26 B9

APPENDIX I

Grade-Stop Width Graphs for Case (c)

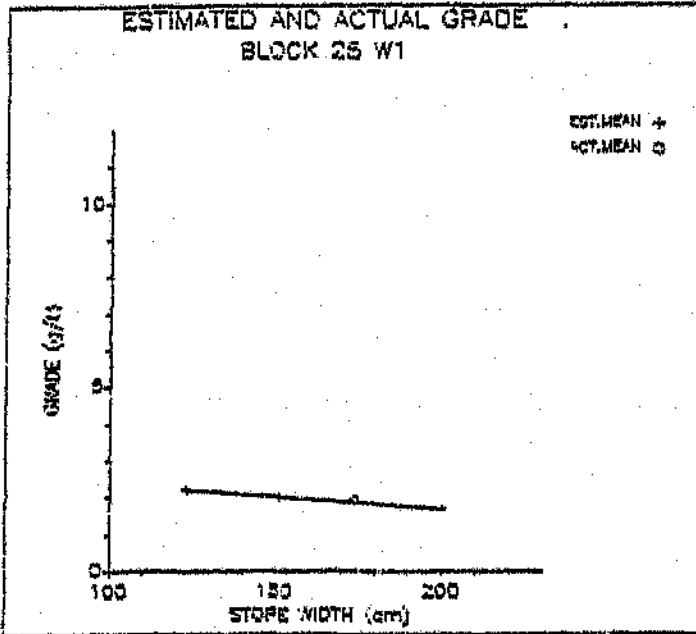


Figure 11 : Estimated and Actual Grades in Case (c) for Block 25 W1

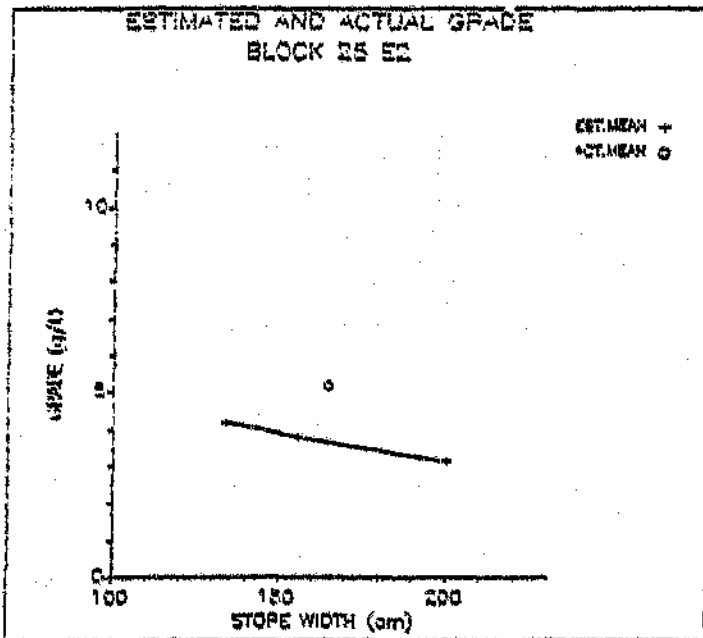


Figure 12 : Estimated and Actual Grades in Case (c) for Block 25 E2

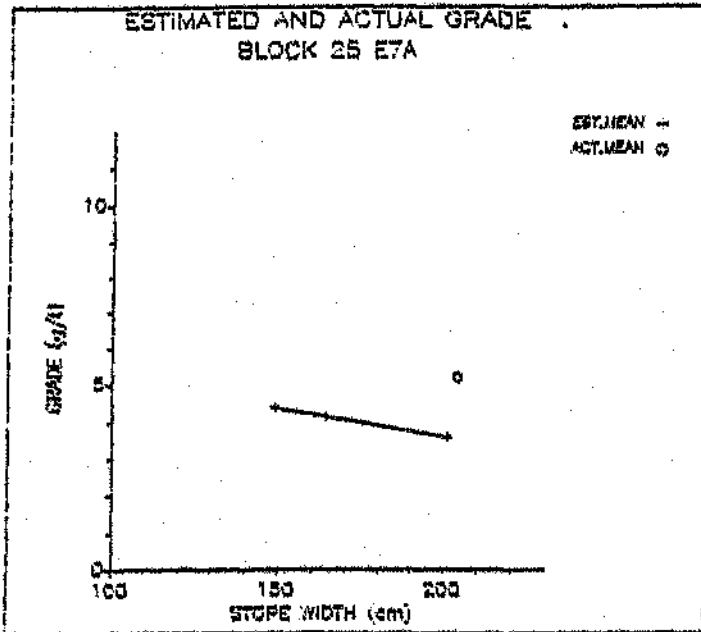


Figure 13 : Estimated and Actual Grades in Case (c) for Block 25 E7A

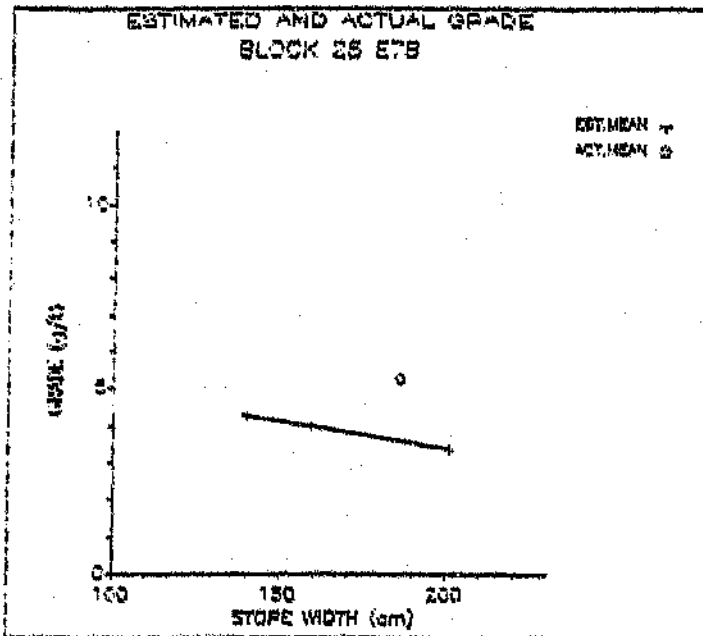


Figure 14 : Estimated and Actual Grades in Case (c) for Block 25 E7B

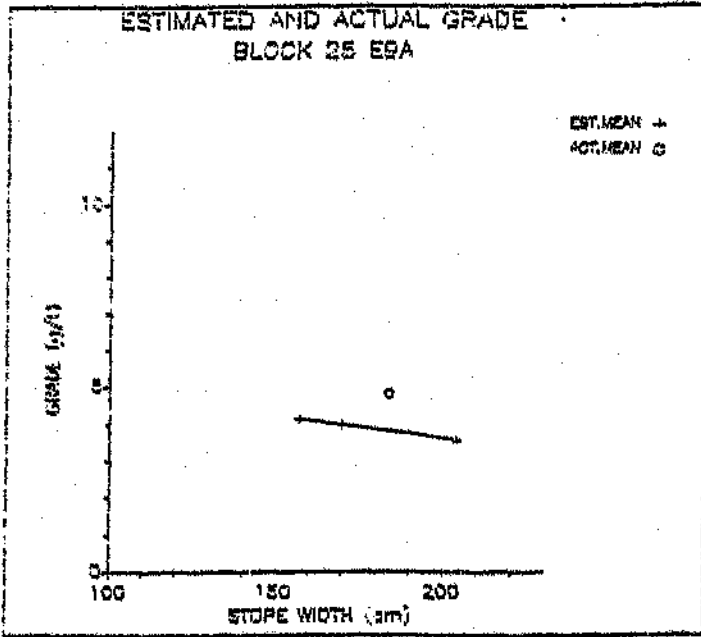


Figure 15 : Estimated and Actual Grades in Case (c) for Block 25 E9A

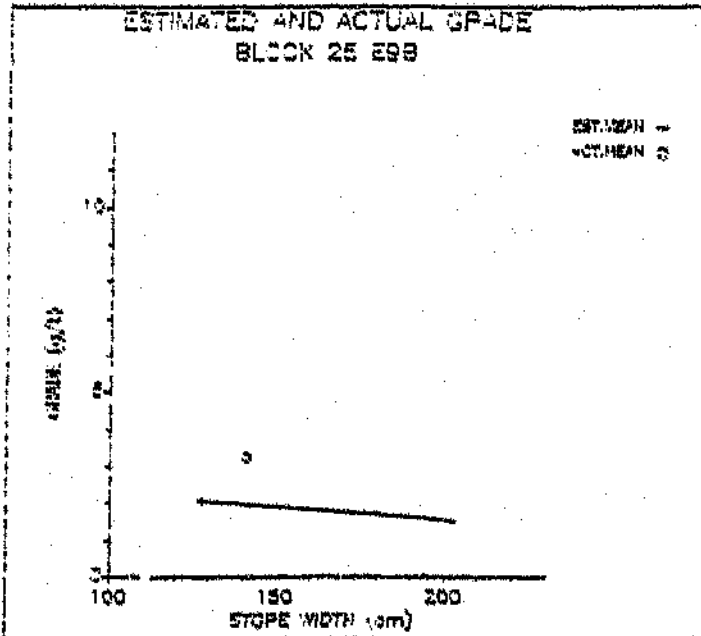


Figure 16 : Estimated and Actual Grades in Case (c) for Block 25 E9B

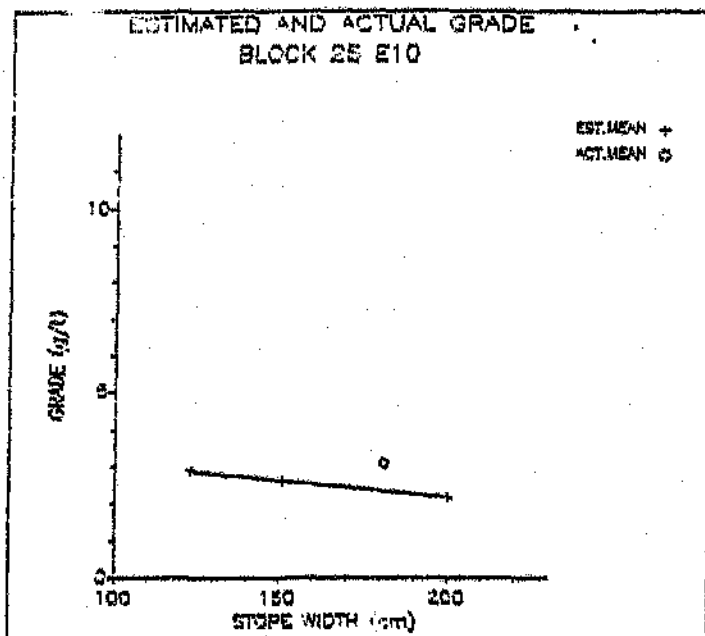


Figure 17 : Estimated and Actual Grades in Case (e) for Block 25 E10

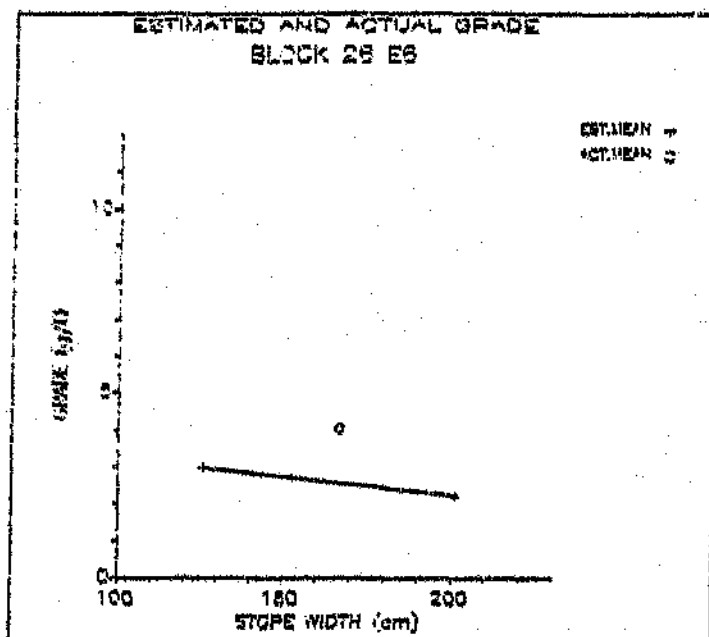


Figure 18 : Estimated and Actual Grades in Case (e) for Block 26 E6

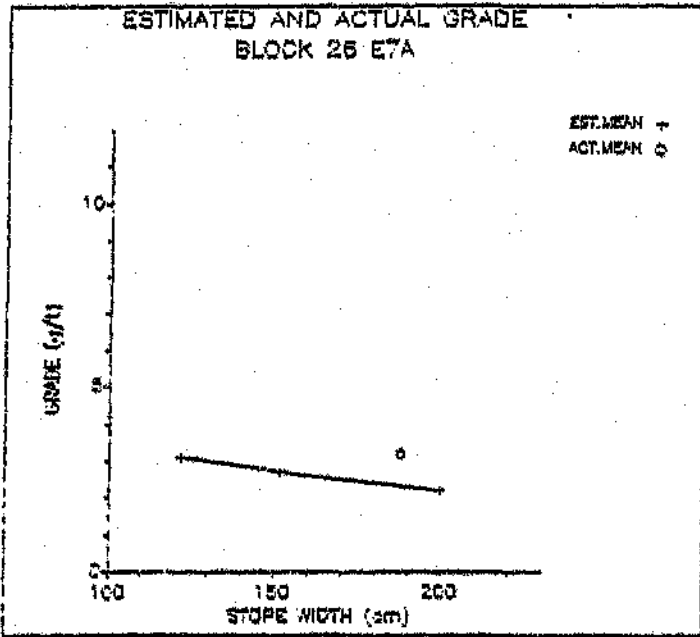


Figure 19 : Estimated and Actual Grades in Case (c) for Block 26 E7A

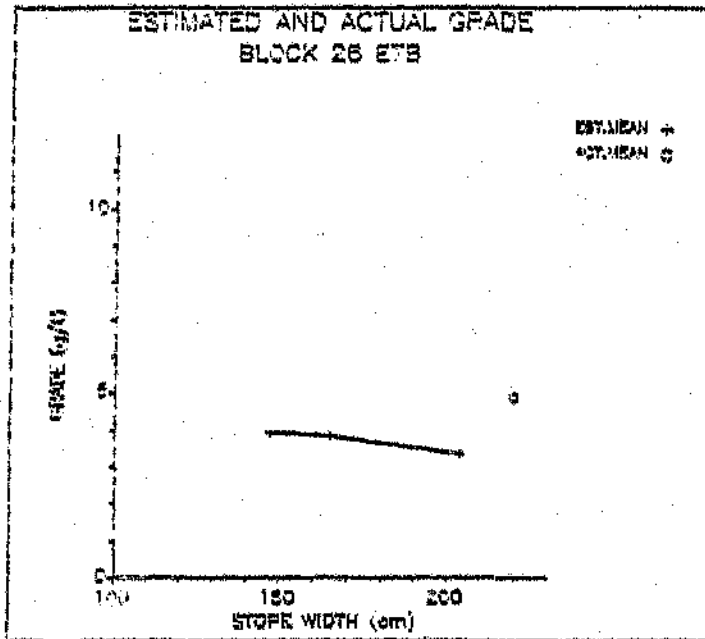


Figure 110 : Estimated and Actual Grades in Case (c) for Block 26 E7B

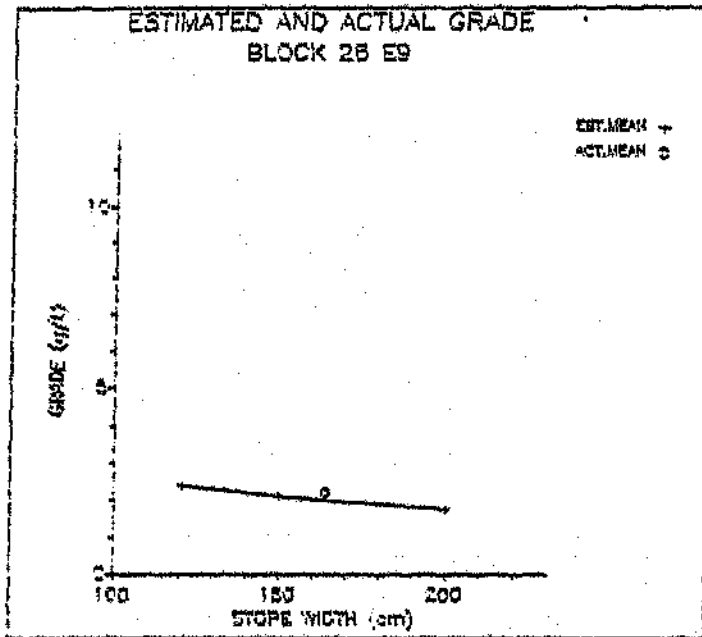


Figure 111 : Estimated and Actual Grades in Case (a) for Block 26 E9

BIBLIOGRAPHY:

- Anhaeusser, C.R. (1969). The Stratigraphy, Structure and Gold Mineralization of the Jamestown and Sheba Hills Area of the Barberton Mountain Land. Ph.D thesis (unpubl.), University of the Witwatersrand, Johannesburg.
- (1975), The Geological Evolution of the Primitive Earth: Evidence from the Barberton Mountain Land. Inf. Circ. Econ. Geol. Res. Unit, University of the Witwatersrand, Johannesburg, 98, 22pp.
- (1976), The Geology of the Sheba Hills Area of the Barberton Mountain Land, South Africa, with particular reference to the Eureka Syncline. Trans. geol. Soc. S. Afr., 79, 253-280.
- (1986), Archaean Gold Mineralisation in the Barberton Mountain Land, 113-154. In Anhaeusser, C.R. and Maske, S. (Eds)(1986), Mineral Deposits of Southern Africa Vol.I and II. Geol. Soc. S. Afr., Johannesburg.
- Barton, J.M., Jr., (1983). Isotopic Constraints on Possible Tectonic Models for Crustal Evolution in the Barberton Granite-Greenstone Terrane, Southern Africa, 73-79. In Anhaeusser, C.R. Ed.: Contributions to the Geology of the Barberton Mountain Land. Spec. Publ. geol. Soc. S. Afr., 9, 63-72.
- Bates, R.L. and Jackson, J.A. (1987), Glossary of Geology. Third Edition. American Geological Institute, Alexandria, Virginia.
- Brooker, A.J. (1991). Quality Control Techniques and the Management of the Ore Reserves. S. Afr. Inst. Min. Metall. School of Mine Valuation and Grade Control, June 1991.
- Clark, I. (1979). Practical Geostatistics. Elsevier Applied Science Publishers.
- Daneel, G.J. (1987). The Structural Controls of Gold Mineralization in the Moodies Hills Which Surround the Agnes Gold Mine, Barberton Greenstone Belt. M.Sc. thesis (unpubl.), University of Natal, Durban.
- Deutsch, C. (1989). Mineral Inventory Estimation in Vein Type Gold Deposits: Case Study on the Eastmain Deposit. CIM Bulletin, Volume 82, No. 930.
- Guertin, K. and Villeneuve, J.P. (1988), Estimation and Mapping of Rank Related Uniform Transforms of Ion Deposition from Acid Precipitation. Third International Geostatistical Congress, Avignon. Vol. III, 221-235.
- Hawkins, D.M. (1980). Identification of Outliers, Monograph on Applied Probability Statistics, Chapman and Hall.
- Himmerblau, D.M. (1970). Process Analysis by Statistical Methods. John Wiley and Sons Inc.
- Internal Report, Anglovaal (1977).

Internal Report, Anglovaal (1984).

Krige, D.G. (1978). Lognormal de-Wijsian Geostatistics for Ore Evaluation. S. Afr. Inst. Min. Metall. Monograph Series.

Pearlton, T.N, Murphy, R.D and Scott, W.D (1984). The Nature and Controls of Mineralization in the Agnes Gold Mine. Archaeon Gold: Barberton Centenary Symposium, Abstracts and Guide Book for Mine Visits and Field Excursions.

Poole, E.J. (1964). Structural Control of Mineralization in the Agnes Gold Mine, Barberton Mountain Land. Inf. Circ. Econ. Geol. Res. Unit, University of the Witwatersrand, Johannesburg, 22, 31pp.

Rendu, J.M. (1978). An Introduction to the Geostatistical Methods of Mineral Evaluation. S. Afr. Inst. Min. Metall. Monograph Series.

South African Committee for Stratigraphy (SACS, 1980). Stratigraphy of South Africa, Part 1 (Comp. L.E. Kent). Lithostratigraphy of the Republic of South Africa, South West Africa/Namibia and the Republics of Bophuthatswana, Transkei and Venda. Handbook geol. Surv. S. Afr., 8, 690pp.

Storrar, C.D. (1977). South African Mine Valuation. Chamber of Mines of South Africa, Johannesburg.

Viljoen, M.J., and Viljoen, R.P. (1969). An Introduction to the Geology of the Barberton granite-greenstone terraine. Spec. Publ. geol. Soc. S. Afr., 2, 9-28.

Wagener, J.H.F. (1986). The Agnes Gold Mine, Barberton Greenstone Belt, 181-185. In Anhaeusser, C.R. and Maske, S. (Eds)(1986), Mineral Deposits of Southern Africa Vol.I and II. Geol. Soc. S. Afr., Johannesburg.

Wuth, M. (1980). The Geology and Mineralization Potential of the Oorschot-Weltevreden Schist Belt south-west of Barberton, Eastern Transvaal. M.Sc. thesis (unpubl.), University of the Witwatersrand, Johannesburg.

Author: Brooker Andrew John.

Name of thesis: The application of geostatistical ore reserve evaluation methods in Archaean gold deposits- a case study of the Woodbine deposit, Agnes Mine in the Barberton Area.

PUBLISHER:

University of the Witwatersrand, Johannesburg

©2015

LEGALNOTICES:

Copyright Notice: All materials on the University of the Witwatersrand, Johannesburg Library website are protected by South African copyright law and may not be distributed, transmitted, displayed or otherwise published in any format, without the prior written permission of the copyright owner.

Disclaimer and Terms of Use: Provided that you maintain all copyright and other notices contained therein, you may download material (one machine readable copy and one print copy per page) for your personal and/or educational non-commercial use only.

The University of the Witwatersrand, Johannesburg, is not responsible for any errors or omissions and excludes any and all liability for any errors in or omissions from the information on the Library website.